EUROPEAN UNION
European Regional Development Fund

PROVINCIE FLEVOLAND

PowerParking

TU Delft

Offset Carbon Emission Accounting Methodology and Application to Solar Carport

Kaja Tegtmeier

Faculty of Mechanical, Maritime and Materials Engineering
Department of Process and Energy
Group of Energy Technology

Offset Carbon Emission Accounting Methodology and Application to Solar Carport

by

Kaja Tegtmeier

to obtain the degree of Master of Science in Sustainable Energy Technologies
at the Delft University of Technology,
to be defended publicly on Wednesday, the 8th of September 2021, at 10:00 AM.

Student number:	5153638	
Project duration:	November, 2020 – August, 2021	
Thesis committee:	Prof. dr. Ad van Wijk,	TU Delft, supervisor
	Prof. dr. ir. Zofia Lukszo,	TU Delft
	Dr. ir. Zian Qin,	TU Delft
	Karin Maatje,	Provinvcie Flevoland

This research was funded by the European Regional Development Fund under the Kansen voor West Program grant 00113 for the project PowerParking, as well as by the Province of Flevoland.

Acknowledgements

The completion of this project marks the ending of my academic career at TU Delft. The last two years of studying 'Sustainable Energy Technologies' have been an insightful and interesting but also challenging time. I am proud to say that I was able to master these challenges and achieve a steep learning curve.

This thesis has required an immense amount of work and time and would not have been possible without the help of many people.

I would like to give my thanks to all project partners of the PowerParking project. Thanks to Bart Doornbos from Solarpartners, Jasper Feuth from Eneco and Esger Schouten from PetaWatts for your cooperation and insights into the system design. A special thanks to the Provincie Flevoland for facilitating my thesis internship. To Karin Maatje from the Provincie Flevoland, thank you for your valuable feedback, time and continuous support.

Rishabh, thank you for your constructive feedback and suggestions, your patience, the constant support and discussions leading to steady progress. Your guidance throughout this project was invaluable. Thank you, Ad van Wijk, for teaching me to free myself from my own expectations and for chairing my defence committee. Also, I would like to thank Zofia Lukszo and Zian Qin for taking the time to join my defence committee.

I want to thank my parents for supporting me during this process and always believing in me. A special thanks goes to my sister, Svenja, for your valuable advice and being an endless source of motivation and inspiration to me. And, finally, a thank you to my friends for giving me perspective when everything seemed overwhelming and making the process of writing this thesis all the more enjoyable.

Kaja Tegtmeier
Delft, August 2021

Contents

List of Figures

List of Tables

List of Acronyms

AC Alternating current

AEF Annual (average) emission factor

Al-BSF Aluminium back surface field

BESS Battery energy storage system

BMS Battery Management System

CI Carbon intensity

c-Si Crystalline silicone

CO_2eq Carbon dioxide equivalents

CEC California Energy Commission

DC Direct current

EF Emission factor

EV Electric vehicle

ICE Internal Combustion Engine

IPCC Intergovernmental Panel on Climate Change

GWP Global warming potential

GHI Global horizontal irradiance

GHG Greenhouse gas

HEF Hourly (average) emission factor

ICEV Internal combustion engine vehicle

kWp Kilowatts Peak

KiBaM Kinetic Battery Model

LCA Life cycle assessment

MEF Marginal emission factor

MPP Maximum power point

MPPT Maximum power point tracker

NEI National Emission Inventory

NREL National Renewable Energy Laboratory

NiMH Nickel-metal hydride

OM Operating margin

PERC Passivated emitter and rear cell

PHEV Plug-in hybrid electric vehicle

PV Photo voltaic

PE Primary energy

REC Renewable energy certificates

RES Renewable energy sources

SoC State of charge

SAM System Advisor Model

UNFCCC Unites Nations Framework Convention on Climate Change

V2G Vehicle to grid

WTW Well-to-wheel

1

Introduction

Global awareness about the negative impact of anthropogenic greenhouse gas (GHG) emissions on the climate, mainly caused by the extensive combustion of fossil fuels, is increasing. Most nations have agreed to limit and budget GHG emissions and achieve carbon neutrality by mid-century within the Paris Agreement [1]. Domestic transportation contributed to 23.4 % of the total GHG emissions in the EU in 2019 and heavily relies on the direct combustion of fossil fuels. Electric vehicles (EVs) are seen as a way to reduce carbon emissions in the transport sector, as road transport contributed to 71 % of total transport emissions in 2019 in the European Union [2]. In order to achieve the emissions mitigating effect of EVs, they must be charged using zero to low emission electricity. Solar carports, consisting of a solar PV roof, EV chargers and energy storage, provide a possible solution for decarbonizing road transportation. To assess the actual climate change mitigation impact of solar carports, this research aims to determine the carbon emission offset achieved by such a system.

To accurately assess carbon emissions, an appropriate methodology to calculate carbon offset emissions has to be applied. However, there is considerable literature criticizing the existing methodologies and urging for more accurate methods [3–6]. Therefore, this research aims to gain an overview of current carbon emission accounting methods and potential deficits and develop an appropriate method to quantify carbon offsets. Assessing carbon offsets achieved through substitution of utility grid electricity requires the application of grid electricity emission factors and this report investigates the consequences of applying marginal, hourly average and annual average emission factors.

The developed carbon offset methodology is applied to a solar carport system containing a 465 kWp solar PV system, a 345 kWh nickel metal hydride (NiMH) battery and 16 EV charge points, located at the municipality building of Dronten in the Netherlands. To apply the developed methodology a computer simulation based on several sub-models is developed and various current and future scenarios are simulated. A major focus of this work is determining the effect of using different emission factors to carbon accounting assessments and selecting the most accurate approach. Next to the achieved carbon emission offset, the emission mitigation impact of the battery and the effect of variable EV demand are investigated in depth.

1.1. Research Motivation

An important tool in tackling the climate crisis is carbon emission accounting and budgeting. Quantifying the amount of GHG emissions is key in pursuing the goal of keeping the global temperature increase below 2°C, preferably 1.5°C, of pre-industrial levels, as agreed to within the Paris Agreement [1]. To reach this target, an emissions budget of 25 gigatons (GT) CO_2eq and 41 GT CO_2eq annual emissions, for the 1.5°C and 2°C targets respectively, has been defined for the year 2030 [7]. These targets are based on the assumption that every participating nation has the means to accurately estimate GHG emission reductions achieved through climate change mitigation projects. However, in reality there is debate about current emissions accounting methodologies and criticism on the standard framework for emissions accounting developed by the United Nations Framework Convention on Climate Change (UNFCCC) [8], especially for emissions related to the consumption of utility grid electricity [3].

Currently, the favored approach for carbon emission accounting of electricity consumption is to use annual average grid emission factors. This entails one static, averaged value for the whole year, lacking temporal

variability. However, this approach bears two major problems that are laid out in the following.

First, attributional carbon accounting gives a static overview of emissions that are attributed to a certain action. While this may be useful for managing emission budgets, it excludes consequential emissions in the system as a whole. It is crucial to chose the accounting methodology based on the question to be answered, which more often than not is give information about the overall environmental impact of an action for informed decision-making. The answer to such queries should include impacts on the whole system to provide decision-makers with the full picture. Hence, a standardized accounting methodology should differentiate between attributional and consequential accounting based on the question to be answered. The lack of an appropriate standardized GHG emissions assessment approach can lead to misallocation of emissions and distortion of realistic mitigation impact of emission reduction projects [4]. In turn, this can favor investments into mitigation projects that have lower emission reduction potential than their competing projects [5].

Second, emissions are often sold, or rather the lack of them is bought, in corporate carbon accounting which accounts for about 60 % of total electricity consumption (industrial and commercial sectors) [9]. This is done by trading contractual emissions which additionally distorts realistic emission accounting [5]. Companies buy contractual emissions from exclusively Renewable Energy Sources (RES), which allows them to allocate an emission factor of zero to their electricity consumption. However, due to heavy subsidisation of RES, there is an over-supply of certificates and their purchase does not increase RES capacity nor generation in the physical market [4]. A very simplistic example can illustrate this problem. Company A and company B are selling a similar product. Company A produces in Poland, with average emissions of 937 gCO_2/kWh, and company B produces in Sweden, emitting an average of 45 gCO_2eq for every kilowatt hour consumed [10]. Company A buys contractual emissions for RES and claims zero emissions for the energy used to make their product and markets it accordingly. Company B does not buy such contractual emissions and reports the low, but existent, emissions factor of its product while also investing the money that company A spent on the contractual emissions on efficiency improvements within its production process. On paper, the product from company A seems like it caused the least emissions and a consumer / decision-maker interested in emission mitigation is misguided into making the sub-optimal decision of buying the product from company A. This case highlights the importance of reporting accurate emission factors that reflect the systemic reality of the impact of any action.

From this, a need for a standardized methodology that considers the aims of the emission assessment and estimates the actual emissions *caused* by an action arises. The motivation of this work is to develop a methodology that can more accurately estimate carbon offsets related to local renewable energy, electric vehicle charging and energy storage projects and reflect the actual impact of an emission mitigation project to decision-makers. Additionally, application of the developed methodology aims at quantifying the carbon offset potential of the three major system components of the investigated solar carport system; the solar PV system, the battery storage system and the EV chargers.

1.2. Research Questions

The main research questions in this study are:

- **Research question I:**

  What is the recommended approach and emission factor selection to measure carbon emission offsets? And what is the annual cradle-to-grave carbon emission offset of the solar carport in Dronten?

- **Research question II:**

  What is the cradle-to-grave carbon emission offset potential of the battery system currently and with a higher share of RES in 2030?

With the following additional research questions:

- **Additional research question A:**

  How much carbon emissions occur by charging EVs directly from the grid, without installing a PV system and BESS, currently and 2030?

- **Additional research question B:**

  How is the system's carbon emission offset potential and total carbon emissions affected by installing a larger amount of EV charge points by 2030?

1.3. Report Structure

Chapter 2 presents some fundamental theory on carbon emissions accounting together with a comprehensive literature review on available carbon emission assessment methods.

Chapter 3 describes the technical configuration of the PowerParking system at the municipality building in Dronten. Furthermore, life cycle emission data on the major system components and utility grid electricity emission factor data used for the system simulation is described.

Chapter 4 explains the carbon emission assessment methodologies applied in this report. The simulation scope is laid out which presents various simulation scenarios of the solar carport system. This is followed by the developed methodology for estimating carbon offset emissions and carbon emissions. Additionally, the models used to simulate the behaviour of the solar array, EV demand profile, utility grid emissions and the battery operation are described.

Chapter 5 presents and analyses the results of the system simulations and emission calculations. This includes the results of the various sub-models employed to simulate the system operation. Also, the differences in calculated carbon emission offset using marginal and average emission factors are discussed. The results from the different simulation scenarios and life cycle carbon emissions caused by the system are presented and analysed as well. Additionally, limitations of the applied methodology are discussed.

Chapter 6 summarizes the conclusions drawn from this study, including some of the key findings of the system simulation regarding carbon offsets. In addition, suggestions for future research are proposed and recommendations to project stakeholders, policy-makers and solar carport designers are given.

2

Theory and Literature Review

This chapter lays out some important theory on carbon emissions accounting in section 2.1. Additionally, section 2.2 presents a comprehensive literature review of carbon accounting literature and assessment methods, including a conclusion on which emission factor is most suitable for carbon offset assessments.

2.1. Theory of Emissions Accounting

The three fundamental distinctions of emissions accounting are described in section 2.1.1. This is followed by definitions of GHG emissions and their scope in section 2.1.2.

2.1.1. Principles of Carbon Accounting

Various approaches to carbon accounting are found in literature and their choice can have a considerable impact on the result of an emissions study. The chosen approach depends on the purpose and scope of the study, the availability of data, the definition of system boundaries and other factors. This section presents the most important distinctions in the fundamental approach to accounting for carbon emissions of electricity.

Production versus Consumption Based

Emission factors (EFs) can be determined based on electricity production or consumption. In centralized energy systems, electricity is produced in large power plants and then transmitted to the place of the consumer. Carbon emissions can be allocated to either the production facility or the end consumer of electricity. Reporting of National Emission Inventories (NEI), as required by the UNFCCC, are currently based on production of electricity without including (international) trade volumes. However, there is discussion on the accuracy of this approach [11, 12]. The production based approach quantifies the amount of carbon emissions released per unit of energy generated by a specific generation facility. This is straightforward and easy to calculate from the known power plant efficiency and fuel / resource consumption. The carbon intensity (CI) of the major primary energies (PE) is well researched and agreed upon [13].

The allocation of emissions to the consumption of electricity is more complex because the flow of electricity cannot be traced back to a single generation facility. Additionally, losses during transmission and interregional and international trade must be included [11]. Therefore, estimating the consumption based CI of electricity relies on assumptions and in any case yields some inaccuracies. Nevertheless, consumption based allocation allows the consumer to establish a more realistic estimation of carbon emissions from their electricity consumption and (some of) the responsibility of emissions should be allocated to the consumers as production would not exist without them. Peters [11] argues that consumption based methods give better insight into environmental evaluations, however, they acknowledge the obstacles in applying production based approaches and its inaccuracies. Lenzen et al. [12] argue that the responsibility for carbon emissions should be shared between producer and consumer to give incentive of improving all stages of the supply chain. An analysis by Larsen and Hertwich [14] found the consumption based approach to yield better applicability for assessing the performance of carbon emission mitigation efforts.

A study by Tranberg et al. [15] asserts the discrepancy of production and consumption based carbon accounting for European countries. Figure 2.1 shows the hourly production and consumption carbon intensities per country. Some countries (LT, AT, LV, HU, SK, ME) show very large differences in production and

consumption based carbon intensities and almost all countries show some deviation. The results shown in figure 2.1 emphasize the importance of including electricity imports in order to accurately report consumption based carbon emissions.

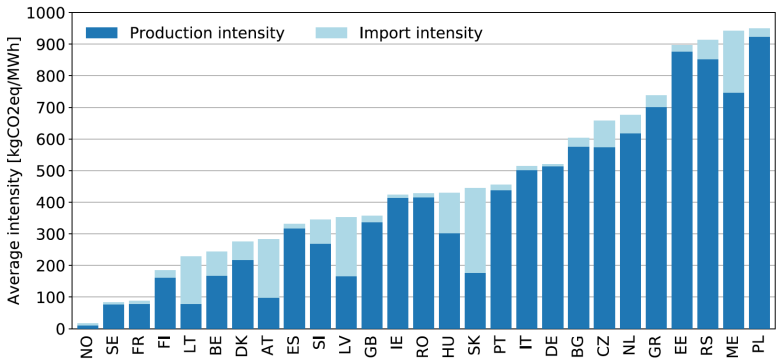

Figure 2.1: Hourly average electricity production and consumption carbon intensity by country (EU) [15]

To conclude, for the scope of this project it is conceptually more correct to use emission factors that are based on the actual consumption of electricity in the Netherlands because physical flows of electricity, and its emissions, are reflected more accurately.

Market versus Location Based Carbon Accounting

Carbon emissions can be traded on the energy market in the form of renewable energy certificates (RECs), power purchase agreements (PPAs), guarantees of origin (GOs), utility green tariffs and similar. Even though these agreements differ slightly in their details, generally, they allow a reporting entity to purchase the right to apply emission factors of a specific technology type. This type of emission allocation is called market based. Companies are able to report zero emissions from electricity consumption by contractually purchasing exclusively renewable electricity. However, the market based approach yields two major problems; it does not give incentive for additional RES capacity and it does not reflect the physical flows of electricity (and emissions), as investigations by Brander et al. [4] show. The first problem stems from the fact that contractually purchased EFs trade energy from already installed RES and as renewable capacity exceeds the contractually purchased volume it does not elicit additional investment in RES. Hence, buying contractual emissions induces neither direct nor indirect emission reductions. The second problem results in a limited decision-usefulness of the market based approach for consumers and planners as they do not represent physical occurrence of carbon emissions.

The contrary approach is a locational method which defines the average emissions related to electricity generation for a defined geographic area, *location*. Here, the total emissions of all generators are averaged over the total electricity produced for that location. These EFs reflect significant variations in regional or national generation portfolios and give a more realistic idea of carbon emissions occurring from producing one unit of electricity. The regional and temporal granularity are important considerations in application of the locational approach. Generally, the shorter the temporal resolution the more accurate the EF. Geographic boundaries must be chosen so that im- and exports can be traced well, i.e. national or state levels (in bigger countries) yield good accuracy. Accuracy of results and decision-usefulness are of high importance in this study, which is why it is chosen to apply a locational approach.

Distinction of Attributional and Consequential Carbon Accounting

Another crucial distinction in carbon accounting methods, originating from life cycle assessment (LCA) studies, is that of attributional and consequential approaches. In attributional methods a fixed amount of CO_2 emissions is allocated to a specific project or action [5, 16, 17]. These emissions occur along the project's life cycle stages and lie within the defined system boundaries without taking into account effects on a larger system scale. Such assessments make use of average emission data, i.e. annual average emission factors, for evaluation of environmental performance. Averaged EFs quantify the mean environmental impact (in terms of CO_2 emissions) of producing a unit of electricity.

Consequential methods describe a change in the system as a consequence of the project or action investigated. More specifically to electricity systems, consequential methods quantify the change in emissions caused by the consumption or generation of one unit of electricity. Consequential analyses use marginal emission factors for grid electricity as this represents the change in a emissions caused by additional demand or generation [5]. Plevin et al. [18] argue that the consequential approach is the "conceptually superior approach" as it yields better decision-usefulness, because it quantifies real-world changes. The difference in results between the two approaches can be significant [5] and is, therefore, investigated in this study.

2.1.2. Definitions and Scope of GHG Emissions

This study investigates the difference in offset emissions and occurring emissions which are defined as follows.

Offset Emissions are "units of carbon dioxide-equivalent (CO_2eq) that [are] reduced, avoided, or sequestered to compensate for emissions occurring elsewhere" [19]. Offset emissions are utilized to achieve emission compensation for unavoidable GHG emissions and can be traded in cap-and-trade systems in order to achieve emission targets [20]. Specific to an emission mitigation project, such as the PowerParking system in Dronten, offset emissions are greenhouse gases that are mitigated as a consequence of installation of said system. These entail occurring GHG emissions from manufacturing, installing, operating and disposing of the system as well as emissions caused by electricity imports from the grid. Additionally, avoided emissions, which are the emissions related to reduction in consumption of grid electricity are taken into account. Estimating offset emissions follows the offset carbon emissions approach defined in section 4.2.1.

Emissions encompass the total mass of GHG emissions caused directly and/or indirectly by a system, an organisation or a person measured in mass of CO_2eq, and are often referred to as a carbon footprint [20]. The total emissions associated with a project or system occur in the various life cycle and supply chain stages of the investigated system. Applying the concept of carbon emissions to the PowerParking system results in accounting emissions from manufacturing, installing, operating and disposal of the system and consumption of utility grid electricity. Emissions are calculated through following the carbon emissions accounting methodology, as presented in section 4.2.2.

Reporting of GHG emissions is classified into three scopes by the World Resources Institute [20], each representing emissions from certain life cycle stages and activities. The scheme in figure 2.2 explains the definitions of scope 1, 2 and 3 emissions. Scope one emissions include direct emissions from project owned and

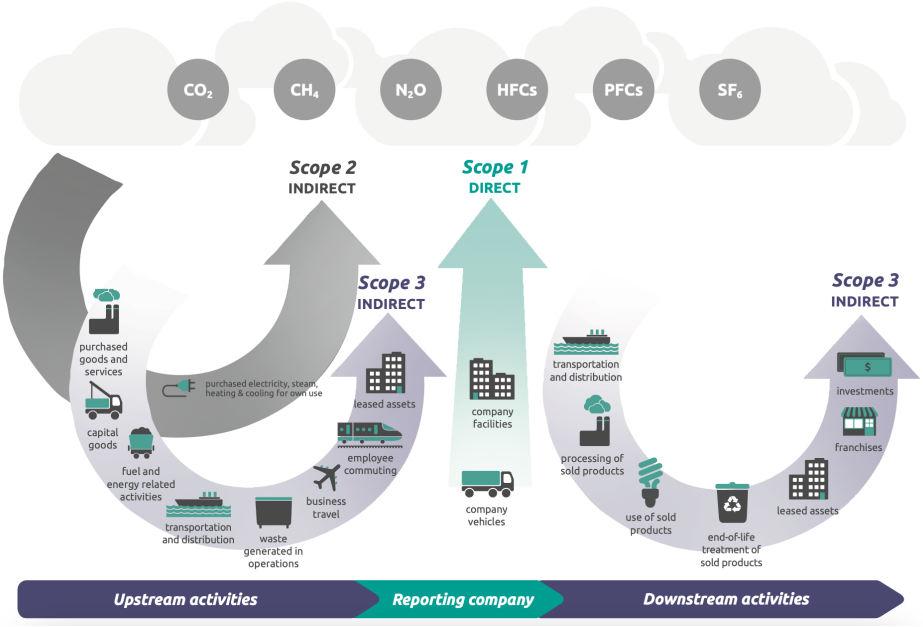

Figure 2.2: Description of GHG emissions scopes along supply chain [21]

controlled processes. In this study, scope 1 emissions entail all life cycle emissions (manufacture, operation, recycling/disposal) of the PV and battery system. Scope 2 encompasses emissions from purchased energy

(electricity, heat, cooling, etc.), for which emissions occur at the location of generation (power plant, boiler, etc.), hence they are labelled "indirect". In this project, all imports of electricity from the grid fall into the scope 2 category. All other indirect emissions are grouped within scope 3, which the company/project does not own or control. Reporting of scope 1 and 2 emissions is mandatory, while scope 3 are voluntary [20]. This study considers scope 1 and 2 emissions.

The GHGs included in this study are all gases as defined by the *Intergovernmental Panel on Climate Change* (IPCCC) [22] with a global warming potential (GWP) relative to CO_2 for a 100-year time horizon. Their respective GWPs can be found in table A.1 in appendix A.1.1.

2.2. Literature Review

This section contains a comprehensive literature review on carbon emission factor assessment methods. First, the methods used for the literature review are explained in section 2.2.1. Second, literature using and presenting three different carbon emission factor methodologies are reviewed in section 2.2.2. Third, papers reviewing and comparing multiple approaches are discussed in section 2.2.3. Finally, section 2.2.4 gives a conclusion of the literature review and implications for this study.

2.2.1. Literature Review Methods

The literature review was conducted as the first phase of this research study. The aim of the literature research was to gain an overview of state-of-the-art carbon emission assessment methods and, based on these, either to select or develop a suitable carbon offset approach for the investigated system.

To find relevant literature several digital libraries and search engines, consisting of IEEExplore, Science Direct, ResearchGate, Mendeley and Google Scholar, were used. A combination of the following keywords was used to preselect relevant studies on the aforementioned platforms: "carbon emissions", "grid/electricity carbon intensity", "average annual emissions", "average hourly emissions", "marginal emission factor", "emission offset", "grid intervention", "renewable energy technologies", "life cycle analysis", "electric vehicle", "environmental impact" and "decentral energy system". From key papers found through this initial search, more literature was found through the backward snowball method.

2.2.2. Carbon Emission Factor Assessment Methods

Many studies have been conducted with the aim of estimating GHG emissions caused by or offset through emission mitigation projects. There is no commonly agreed upon methodology for carbon emission assessment of utility grid electricity amongst researchers and most studies apply different approaches [3] which rely on the conceptual distinctions as laid out in section 2.1.1.

There are three main approaches in assessment of carbon emission factors: Annual average emissions, hourly average emissions and marginal emissions factors. This section explains the three approaches in more detail and presents papers that review several carbon emission assessment methods and that propose or apply these methods.

Annual Average Emission Factor

The most commonly applied emission accounting approach across studies, mainly due to its simplicity, is the annual average emission factor (AEF). The AEF is calculated from the carbon intensity (CI) of all power plants in the electricity grid in a region or country. The accumulated carbon emissions of all power plants over a year are divided by the total annual energy generation to find the AEF, as seen in equation 2.1.

$$\text{AEF}\left[\frac{gCO_2eq}{kWh}\right] = \frac{\text{Total annual } CO_2\text{eq emissions}\left[\frac{gCO_2eq}{yr}\right]}{\text{Total annual energy generation}\left[\frac{kWh}{yr}\right]} \tag{2.1}$$

The research conducted by Hawkins et al. [23] offers an extensive comparative LCA of EVs and internal combustion engine vehicles (ICEVs) using AEFs for determining use phase emissions of EVs. The study identifies the high sensitivity of life cycle emissions towards the assumed CI of electricity [23]. This emphasizes the need to accurately determine emission factors and choose an appropriate approach. The main disadvantage of the approach is that AEFs do not provide any temporal variability, as they only give one average value for the whole year. However, increasing penetrations of RES in the grid mix cause the grid emissions to exhibit higher variability over time. For example, an EV could charge at times with a 60 % share of RES in the grid mix or when the RES share is below 10 %, both yielding very different life cycle emissions for the EV, which is not reflected in AEFs. Therefore, utilising AEFs in emission assessment studies on time-variable loads or generators results in highly simplified results compared to applying time variable emission factors.

Nealer et al. [24] use AEFs to compare the environmental impact of ICEVs and EVs in the Unites States. The study conducts a LCA, including an analysis on environmental impacts of resource extraction, manufacturing, use phase and recycling or decommissioning. The use of AEFs becomes relevant in assessing emissions in the use phase of EVs from charging the vehicle and has a large impact on the study outcome. Grid emissions were disaggregated for 26 regions in the US, thereby, providing geographic granularity to the analysis. However, in addition to the lack of temporal granularity, AEFs assume that generation of all power plants is affected equally by an increased load, neglecting realistic interactions of an additional load and the electricity

Table 2.1: Overview of literature using or presenting annual average emission factors

Literature	Data	Geography	Objective
Hawkins et al. [23]	Annual energy generation and CI of each plant/fuel type	Europe	Comparison of life cycle environmental impact of EVs and ICEVs in Europe across various categories.
Nealer et al. [24]	Annual energy generation and CI of each plant/fuel type	26 grid regions in U.S.	Comparison of life cycle emissions (from extraction of raw materials, manufacturing, driving, and disposal or recycling) of modern BEVs and ICEVs in the Unites States.
Moro and Lonza [10]	Annual energy generation and production (EIA) and CI of each plant/fuel type	EU member states	Calculation of well-to-wheels emissions of EVs taking into account international trade.

grid. Nealer et al. recognize these inaccuracies, but argue that their aim is to find typical EV emissions for a particular grid region and to compare long-term developments of carbon emissions from EV charging, which, they find, is reflected in AEFs. In contrast to [23], the approach presented in [24] allows for spatial variability, but similarly lacks temporal variability and both do not take into account the effect of marginal power plant dispatch caused by an added load. Utilising AEFs for analyses such as in [23] or [24] can be justified by the fact that they aim to quantify emissions over the vehicle's lifetime and do not aim to analyse the system change (and offset emissions) caused by large-scale EV introduction. However, the possibility of estimating imprecise emission factors can lead to a limited validity of conclusions drawn and give incentive for unfavorable policy decisions.

Moro and Lonza [10] present a well-to-wheel (WTW) analysis of modern EVs in EU member states using AEFs including international trade data, i.e. a consumption based approach. Importing electricity with a high CI results in a higher national AEF and electricity imports with low CI lowers the AEF. Even though this approach presents the physical flows of electricity and its CI more realistically, the approach still bears the deficits of the methods in [23] and [24] with regards to the application considered in this study. Table 2.1 summarizes the presented literature using AEFs and the advantages and disadvantages of the approach are summarized in table 2.2.

Table 2.2: Advantages and disadvantages of annual average emission factors

Advantages	Disadvantages
• Simple approach • Availability of data • Allows comparison of past, present and future grid mix • Electricity trade can be included	• No temporal variability • No (or little) geographical variability • Neglects interactions between variable loads and the power grid

Hourly Average Emission Factor

A similar approach to annual averages is the method of hourly average emission factors (HEFs). As its name suggests, the differentiating aspect is that HEFs entail the carbon emissions of all power plants in the system with hourly temporal granularity. Here, the total carbon emissions from all power plants in one hour are divided by the total amount of electricity generated in that hour to determine the hourly average emissions (see equation 2.2). The details in the approach as to which power plants are included, whether international trade is included and the time step vary depending on the approach.

$$\text{HEF}\left[\frac{gCO_2eq}{kWh}\right] = \frac{\text{Total } CO_2\text{eq emissions in one hour}\left[\frac{gCO_2eq}{h}\right]}{\text{Total hourly energy generation}\left[\frac{kWh}{h}\right]} \tag{2.2}$$

Schram et al. [25] criticize the lack of temporal variability in AEF and calculate HEF for their analysis on the GHG emission reduction potential of various carbon reduction measures or technologies in eight EU countries. They find significant variations (above 10 %) in the emissions reduction potential of EVs in four of the eight analysed countries when using HEFs instead of AEFs [25]. When comparing emissions caused by the operation of a BESS using an AEF and HEFs, a decrease of over 110 % (Germany) is found when applying HEFs instead of AEFs. This is because HEFs are lower during the day due to higher shares in RES, which is

Table 2.3: Overview of literature presenting or using hourly average carbon emission factors

Research study	Data requirements	Geography	Objective
Schram et al. [25]	Electricity generation data (from ENTSO-E) and fuel CI (from ecoinvent v3 database)	Austria, Belgium, France, Germany, Italy, the Netherlands, Portugal and Spain	Estimating the GHG emission reduction potential of EVs, heat pumps, PV and batteries and compare the impact of communal energy sharing on GHG emissions.
Khan et al. [26]	Half-hour national electricity generation and consumption data (Electricity Authority), GHG emissions from electricity generation (NZ Ministry for the Environment)	New Zealand	Analysis of time-dependent CI of New Zealand's electricity grid.
Khan [27]	Half-hourly electricity generation and consumption data (Power Grid Company of Bangladesh Ltd), Generation emission data	Bangladesh	Assessment of GHG emissions in Bangladesh using a time-varying carbon accounting approach to study impacts on capacity planning.
Tranberg et al. [15]	Hourly grid carbon intensity data (e.g. from TSO) and national consumption data	EU	Proposal of a new real-time and consumption-based approach in carbon accounting based on flow tracing.
Ghotge et al. [28]	Hourly grid carbon intensity data	Netherlands	Quantification of the effect of EV smart charging on the mean carbon intensity of the used/charged electricity.
Baumgärtner et al. [29]	15 min electricity generation data and hourly trading data and merit order model	Germany	Investigation on time-dependent grid mix emissions in a low-carbon electricity grid using a MILP model.

when the BESS is usually charged. In six of the eight countries BESS emissions are substantially lower using the hourly values. This discrepancy highlights the inaccuracy of AEFs when applied to time-varible loads. Further, Schram et al. [25] recommend to consider the use of marginal emission factors.

An analysis by Khan et al. [26] showed large (up to 40 %) inter-seasonal variation in grid CI and up to 10% variation in daily CI using half-hourly emissions data in New Zealand [26]. They conclude that hourly, or "time-varying", emissions should be used for decision-making in demand side management instead of annual averages. Furthermore, Khan et al. [26] suggest that investigations on the carbon emission reduction potential of demand side management measures based on marginal emissions would yield more detail. In an assessment of grid carbon emissions in Bangladesh, Khan [27] confirms the importance of temporal variation in carbon emissions regarding accuracy of results.

Tranberg et al. [15] propose a method for determining hourly grid emission factors based on electricity trade data within Europe. Their approach considers not only the production of electricity, but traces the flow of electricity across borders to the country of consumption with hourly granularity. They calculate HEFs by determining the average emissions of consumed electricity, rather than produced electricity, for every country. The difference in electricity production and consumption volumes is found to be significant and highlights the importance of including trade in determining accurate national emission factors [15]. As mentioned, for the application in this study it is conceptually correct to use consumption based emission factors as the electricity being substituted by the investigated system includes international trade and cannot be attributed to a specific generator.

Ghotge et al. [28] use HEFs for their analysis of the effect of price-optimized charging on EV emissions based on the method proposed in [15]. They choose this approach because it reflects the fluctuating CI of electricity mixes with a high share of RES and, therefore, yields increased accuracy compared to annual averages. They mention the lack of accuracy stemming from not using marginal emissions, however, HEFs are evaluated to be suitable due to the small size of the analysed system [28]. Additionally, they acknowledge the difficulty in determining marginal emission factors, as it requires either a complex model or is very data-intensive. This is because a very accurate model of the energy system is required to model realistic marginal emission factors, else the results have high uncertainty and may be misleading.

Baumgärtner et al. [29] present a power system optimization model (mixed integer linear programming, MILP) and assess the implications of using hourly average and marginal emission factors on power system emissions. They find that by utilizing HEFs to optimize the system operation and planning emissions can be reduced by 6 %, while up to 60 % of emissions can be saved when using marginal emissions [29]. The large reduction when using marginal values stems mainly from optimizing the (temporal) operation of the system based on the high volatility of marginal emissions through demand side management. This underlines the importance in considering accurate emission factors for system operation. Baumgärtner et al. [29]

Table 2.4: Advantages and disadvantages hourly average emission factors

Advantages	Disadvantages
• Does not require detailed model of the energy system • Takes into account daily and seasonal variation, which is especially significant with a high share of RES • Can include cross-border trade, as seen in [15]	• Does not account for the specific emissions associated with the marginal plant due to the increased load • No suitable for emission offset studies

recommend to use grid average emissions for *attributional* emission studies and marginal emissions for *consequential* studies, as explained in section 2.1.1.

Overall the six presented approaches are all rather similar in the way they calculate emissions, with the exception of including trade data. The different papers applying and presenting HEF approaches are summarized in table 2.3 and advantages and disadvantages of HEFs are outlined in table 2.4.

Marginal Emission Factor

Marginal emission factors (MEF) are the emissions caused by the marginal plant, i.e. the cheapest plant that can still increase its generation at a given moment in time. This approach considers the fact that an additional load will not cause all power plants to increase their production. Low-cost and must-run plants are the first plants to be dispatched and run close to continuously; they are not affected by an added load. Nonetheless, an increase in demand inevitably causes an increase of generation on the particular plant that is on the operating margin. This is shown in the simplified merit order seen in figure 2.3 where a shift of the demand curve to the right causes a larger amount of electricity produced from plant 3. Plant 1 and 2, with lower variable costs, do not change their generation. Hence, the emissions caused by the added demand are effectively only the emissions from the marginal plant (plant 3 in figure 2.3), rather than an average of all operational plants as AEFs and HEFs assume.

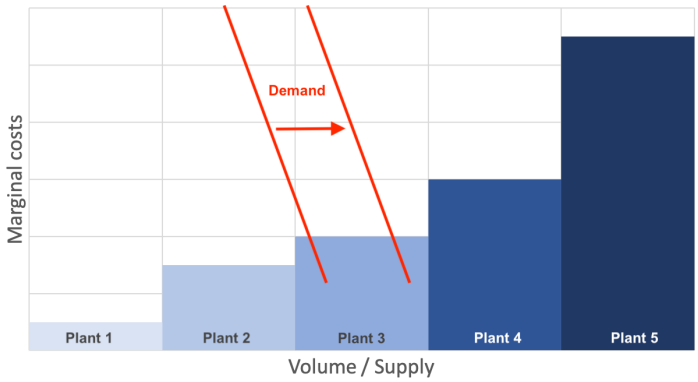

Figure 2.3: Simplified merit order of plants and effect of increased load on marginal power plant 3

Hawkes [30] presents a methodology to estimate MEFs which is using historical power plant dispatch and electricity demand data to conduct a linear regression. This approach does not assume an underlying structure of power plants and naturally reflects ramping constraints and market mechanisms. However, these advantages are especially apparent when using historic data but the regression model approach is not advantageous for future scenarios and, therefore, not suitable for this study. Hawkes [31] extends his MEF approach in [30] to reflect the long-term structural change of an electricity system caused by an additional load. This approach models the future electricity generation using the TIMES model [32] and compares a base demand scenario to different increased marginal demand scenarios. So called, Long-run MEFs, are then found by dividing the additional emissions by the added load [31]. This approach directly includes emissions from new power plants that satisfy additional demand or avoided emissions from decommissioned plants due to additional RES production. However, the long-run MEFs are averaged over future years and do not yield hourly emissions values needed to model inter-daily fluctuations in RES and EV charging load in this research.

Graff Zivin et al. [33] define a regression model which allocates MEFs to electricity consumption based on the relationship of aggregated emission changes and load changes on an hourly time-step for historic data.

Table 2.5: Advantages and disadvantages of the two main approaches to estimate marginal emission factors

Approach	Description	Advantages	Disadvantages
Regression model	Determines correlation of increased demand and generation and attributes incremental generation to a marginal demand through linear regression.	• Does not force the merit order structure on observed data	• Time-interval often large, as modelling effort is high when regression is done for every hour • Not suitable for hourly analysis in future studies
Merit order model	Construction of merit order based on operating costs of each plant and identification of marginal plant from recorded electricity price or generation volume.	• Realistic representation of electricity system • Applicable for future studies	• Requires very detailed model for viable emission estimates • Does not include other market mechanisms

A potential risk of this approach is that non-causal changes in production, such as uncontrollable RES, are included in the regression model, thereby, distorting the MEF.

Tamayao et al. [34] calculate typical regional carbon emissions of plug-in hybrid electric vehicles (PHEV) and EVs for varying emission factors, including an AEF and consumption- and production-based MEFs. They argue that consumption-based MEF are conceptually the most appropriate approach. These can be determined by identifying the marginal plant (mix) through a merit order model or by use of a regression model. The study by Tamayao et al. [34] employs the regression model of [33] to quantify MEFs from the correlation of changing demand and changes in emissions from power production in a regression model on historic data. As mentioned, this approach can result in error from non-causal emission allocation, however, conceptually it is accurate.

Hadley and Tsvetkova [35] construct three future load duration curves (for varying seasons) and add projected PHEV demand onto them to identify the type of marginal plant used to satisfy this additional demand for preset charging times and schedules. Thomas [36] bases their MEF calculations on the predictions on the prospective marginal plants in 2020 and 2030 identified in [35]. Thomas [36] then determines the CI of the marginal plant (fuel) to estimate typical emissions of EVs. The main downside of this approach is that EV demand is accumulated for a predefined charging time in which all cars are charged, which does not reflect realistic EV charging schedules nor allows for including controlled EV charging. This might be suitable when examining the predicted impact of large-scale EV introduction on the electricity system as a whole but does not yield sufficient insight for the scenario-based study presented in this research.

McCarthy and Yang [37] develop a merit order model based method to determine MEFs. The merit order of plants is constructed from structuring all power plants from lowest to highest variable (operating) costs (as seen in figure 2.3). The MEF is then estimated from matching the merit order with the hourly electricity prices and identifying the plant with operating costs closest to the market price under the assumption that the marginal plant is the price-setting plant. McCarthy and Yang [37] point out that their model does not account for complex or difficult to predict market mechanisms, however they find the merit order model to predict the power plant type and, therefore, emissions well.

Verzijlbergh and Lukszo [38] argue that AEFs are faulty for calculating EV emissions and present a merit order based approach for finding Dutch MEFs. The method is similar to [37] and constructs MEFs from determining the price-setting plant in the merit order. Nonetheless, they stress the sensitivity of their results towards EV charging times, generation portfolio and other market factors, which can lead to inaccurate future predictions and calculations of MEFs.

Harmsen and Graus [39] assess the use of average and marginal emission factors with regards to electricity abating grid interventions. They find marginal emissions suitable for "scenario-based" and/or future studies yielding a large electricity abatement [39]. Moreover, Harmsen and Graus [39] hold AEFs to be faulty for aforementioned cases. They present a merit order based approach to determining future MEF including the effect of avoided loads on capacity building.

Schram et al. [40] advocate for the use of MEFs instead of an AEF for accurate evaluation of the environmental impact of time-variable GHG reduction measures and propose a method to determine them. Their method involves the construction of a merit order of plants (as in [37–39]) from which the marginal emissions profile is built from either the emissions of the most expensive (price-setting) plant in every hour or from finding the plant with operating costs closest to the actual market clearing price. Schram et al. [40]

recommend the former for future studies and the latter for historic studies.

The methodology presented in [40] is applied in Schram et al. [41] to investigate an optimized control algorithm of an energy storage system. MEFs are chosen because the studied system contains local PV generation which displaces generation (and emissions) of the marginal plant. Choosing temporal-variable EFs is especially important when determining the system operation, i.e. deciding when the BESS is charged from the grid or PV, as the study finds that emissions can be reduced by up to 57.2 % compared to not optimizing based on marginal emission factors [41].

As mentioned, Baumgärtner et al. [29] use the merit order approach for estimating MEFs in their comparative study finding that 60 % of emissions can be saved when applying MEFs in their MILP optimization model. The two main approaches in finding MEFs are compared in table 2.5 and all studies proposing or using an approach to determine MEFs are collected in table 2.6.

Table 2.6: Overview of literature presenting or using marginal carbon emission factors

Research study	Approach	Data requirements	Geography	Objective
Hawkes [30]	Linear regression model	Hourly power generation (Elexon), fuel consumption data (DUKES)	United Kingdom	Presents an approach for estimating marginal emission factors based on empirical power plant behaviour observations to determine carbon reduction potential of demand-side interventions.
Hawkes [31]	Construction of future load duration curve	Future energy mix and demand profiles and carbon emissions of each plant	United Kingdom	Presents method to estimate long-run MEF that take into account structural change of electricity system due to the investigated intervention.
Graff Zivin et al. [33]	Regression model	Hourly generation and emissions data of each plant (EIA and EPA), electricity consumption data (FERC)	United States	Methodology development to determine marginal CO_2 emissions of variable loads considering interconnected electricity systems.
Tamayao et al. [34]	1. AEF ; 2. MEF based on regression models	1. NERC regional AEF; 2. MEF data from [33] and [42]	Unites States	Assessment of typical, regional carbon emissions of PHEV and EVs for varying grid emission factors, regional boundaries and charging control algorithms.
Thomas [36]	Construction of future load duration curve	Supply, general demand and (PH)EV demand predictions	United States	Calculation of average GHG emissions from EVs based on the marginal grid mix emissions for various regions in the United States.
McCarthy and Yang [37]	Merit order model	EDGE-CA model, EV demand profile	United States	Simulation of added EV load to the Californian electricity grid using an hourly electricity dispatch model.
Verzijlbergh and Lukszo [38]	Merit order model	Marginal costs (calculated from capacity, efficiency, variable operation, maintenance costs and fuel costs)	Netherlands	Analysis of GHG emissions from EV charging considering interactions of electricity grid and EV load.
Harmsen and Graus [39]	(Future) merit order model and effect on capacity planning	Future grid mix, marginal operating costs and annual power production	Netherlands	Evaluation of AEF and MEF to determine the CO_2 emissions related to certain electricity savings interventions.
Schram et al. [40]	Merit order model	Dutch generation capacity profile (ENTSO-E) and each plant's marginal costs and emissions	Netherlands	Proposal of method to determine marginal emission factors for evaluating the environmental impact of RES integration and demand-side management interventions and application in the Netherlands.
Schram et al. [41]	Merit order model	Model from [40]	Netherlands	Assessment of multi-objective optimization approach for operation of a BESS with local RES to determine trade-off between costs and CO_2 emission minimization using marginal emission profiles.
Baumgärtner et al. [29]	Merit order model	Hourly electricity production (ENTSO-E) and emissions per type of plant	Germany	Investigation on time-dependent grid mix emissions in a low-carbon electricity grid using a MILP models.

2.2.3. Review and Comparative Papers

The review paper by Hacker et al. [43] examines six different approaches to determine the environmental impact of carbon emissions through large-scale introduction of EVs in the European market. The study finds

that life cycle GHG emissions of EVs highly depend on the estimated CI of the electricity grid, emphasizing the sensitivity of results to the choice of assessment method and that simplified methods can be misleading. Hacker et al. [43] come to the result that average emission factors are a "simplifying approach" and to correctly account for EV emissions the emissions from the marginal plant must be considered.

Jochem et al. [44] assess EV carbon emissions in Germany in 2030 using four different methods, consisting of average annual, average hourly, marginal and balancing zero emissions, to underline the dependence of the outcome on the method used. They find emissions between 0 and 550 g CO_2eq/kWh, differing significantly amongst applied accounting methods [44]. The study concludes that marginal emissions yield the most suitable approach in accounting emissions from EVs, however, the high uncertainty in calculating marginal emission factors are considered a disadvantage.

Ryan et al. [3] compare 32 existing methodologies for determining carbon emissions caused by a particular load on the electricity grid. Additionally, the paper applies ten of these methods to calculate emission factors of EVs in the United States. The results differ by up to 68 % in the mean value of the emission factor among marginal and average EFs, emphasizing the need to choose an appropriate method to achieve realistic results [3]. Finally, the paper recommends to use MEFs for accurately assessing the emissions caused from an increased load or injection of renewable energy because the output change will stem from the marginal plant.

The United Nations Framework Convention on Climate Change (UNFCCC) [8] have developed the *Tool to calculate the emission factor for an electricity system*, defining a framework that is widely used as a standard in emissions accounting. The approach is based on, first, calculating an operating margin (OM) emission factor and, second, determining the build margin emission factor and, finally, finding the combined margin emission factor. The tool defines four different methods to find the OM emission factor: Simple OM, simple adjusted OM, dispatch-analysis OM, and average OM. Simple and simple adjusted OMs are similar to average annual emissions, but excluding (simple OM) and separating (simple adjusted OMs) emissions from low-cost and must-run power plants. This differentiation is made because grid interventions do not have influence on the operation of these power plants. The average OM-EFs are equivalent to annual average emissions and the dispatch data analysis OM correspond to marginal emissions. The latter determines the marginal mix from the merit order of plants (sourced from the national dispatch center) and the associated hourly emissions are calculated from hourly production, fuel consumption and type of the marginal mix. The tool includes a decision framework for the choice of OM emission factors, which is mainly based on the availability and level of detail of power plant data. This is one of the downsides of [8], as the choice of approach should not be dependent on the available data, instead the most accurate approach for the application should be chosen. This is underlined by the result that emission factors can vary by up to 68 % across different approaches, as found in [3], leading to critically inaccurate results. The tool does not explicitly state the preferred or most accurate method, however, due to the high data intensity and hourly temporal resolution the dispatch data analysis OM are concluded to be the most accurate method presented.

2.2.4. Literature Review Conclusion

For the objective of this emissions study, it is concluded that MEFs are conceptually the most accurate approach in order to estimate the offset carbon emissions through the BESS in relation to the local PV system and EV charging demand. A major disadvantage of the reviewed MEF approaches is the necessity for a highly detailed model to produce viable MEF estimates and, in return, the inaccuracy of emissions factors found through a simplified merit order model. Therefore, it is chosen to use MEFs that are estimated from a large data collection of observed power system behaviour for the current (2019) carbon emission assessment (see section 3.7 for the methodology). All previous studies that have been found estimate MEFs either from a regression model ([30, 31, 33, 34]) or a merit order model ([29, 37–41]). No study was found that uses observed power plant dispatch data to determine MEFs, which presents the novelty of the emissions assessment approach in this analysis. This solves the concerns about high inaccuracy of MEF estimation raised by Jochem et al. [44]. Additionally, the availability of such database addresses the problem of high modelling effort mentioned by Ghotge et al. [28].

The real-time MEF database does not include future (prediction) data for 2030, hence the problem of inaccuracy and need for a very detailed model are not solved for the future model. Moreover, a very complex merit order or regression model still yields large uncertainty with regards to determining the marginal plant in the future. This could lead to gross misestimates of MEFs, as emissions of individual power plants can vary significantly. Consequently, it is chosen to use HEFs for the future system simulation, due to the fact that these are averaged and give a better estimate of offset grid CI without the risk of large misestimates.

3

System Description & Emissions Data

This chapter describes the investigated solar carport system in detail. The physical system boundaries with regards to the model in this study are defined in section 3.1. Section 3.2 gives a general overview of the PowerParking system. Detailed information on system design and LCA emissions of the PV system are given in section 3.3. The technical details of the BESS, including the battery management system, and LCA emissions of the NiMH batteries are presented in section 3.4. The EV charge points are described in section 3.5 and the structure of the carport and corresponding LCA emissions are presented in section 3.6. The emission factor data on MEFs and HEFs is presented in section 3.7.

3.1. System Boundaries

For the modelling of energy flows in the investigated system and the resulting emissions it is crucial to establish well defined system boundaries. For the purpose of this study, the included components of the system are the PV system and the battery energy storage system. The EVs charging at the solar carport are outside of the physical system boundaries and are treated as a load to the system.

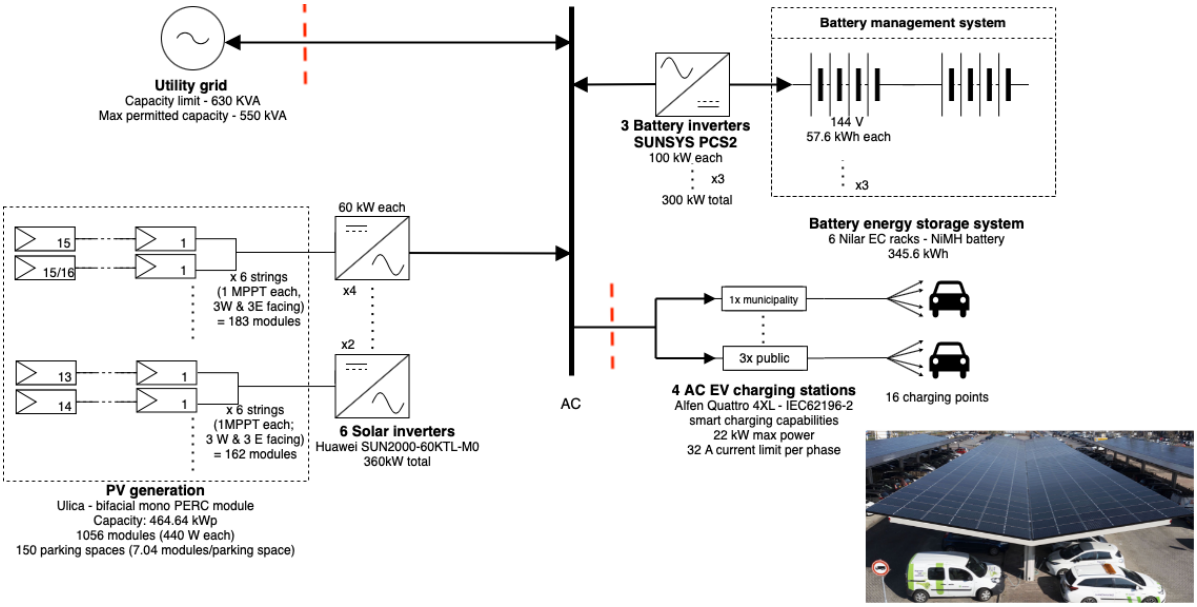

Figure 3.1: Single line diagram of the car park, including PV system, BESS, EV charging and utility grid connection. Physical system boundaries are marked in red.

Electricity delivered to the municipality building from the BESS is not included in the simulations in this study. The reasoning for this is that the building's energy demand would occur regardless of implementation

of the carport system. Accordingly, consumption occurring from the office building is treated as grid exports. Figure 3.1 shows the system and its physical boundaries marked by the red lines.

3.2. System Overview

The investigated system is the solar car park of the municipality building in the city Dronten, the Netherlands, at 52°31' N, 5°42' E. The system has been designed in the effort of achieving energy-neutrality of the municipality building. The roof area of the building alone is able to support installation of a 116 kWp solar system, which is not sufficient to achieve energy neutrality on an annual basis. Hence, the area of 150 parking spaces is additionally covered by a solar PV system. The parking lot consists of three parallel carport installations, each providing parking to either side, thereby covering 6 parking rows. The first two rows (rows one and two in figure 3.2) cover 26 parking spots each on either side, totalling to 52 spots each. The last parking row is slightly shorter at 23 parking spots and one side is used for a cycling path underneath (row three in figure 3.2). The general layout of the system can be seen in figure 3.2, showing the numbering of the rows.

The PV modules are mounted on a steel carport structure. The parking lot provides parking for ICEVs and EVs and 16 parking spots are reserved for only EVs, since they are equipped with a charge point each. Four charge points are reserved for the municipality's EV fleet while the remaining twelve are available to visitors. A battery stores excess energy from solar production and supplies it to the building and EV charging at times of lower solar generation, thereby increasing the self-sufficiency of the town hall. The battery system is located in two shipping containers underneath the carport roof.

Figure 3.2: Layout of the solar car park with row numbering, Source: Fotostudio Wierd

The car port system makes use of building-integrated PV by replacing a conventional roof structure with bifacial PV modules, which can be seen in figure 3.3.

The single line diagram of the car park is shown in figure 3.1. There are three main components of the system connected to the main AC bus (shown in the center):

- The PV system is shown in the lower left corner.
- The BESS is displayed on the top right side to the AC bus.
- The four AC (alternating current) EV charging stations are shown in the bottom right corner. Each charging station possesses 4 charge points, allowing a total of 16 EVs to charge simultaneously.

All of these system components are described in further detail in the next sections. Additionally, the utility grid connection with a capacity limit of 630 kVA and a max permitted capacity of 550 kVA is shown in the single line diagram. This connection supplies both the car park and the town hall building.

3.3. PV System

The PV system is mounted on a steel T-frame carport structure (described further in section 3.6) on the area of 150 parking spaces, of which 119 are actual parking spots. The remaining spots are used for a walking path,

Figure 3.3: Street view of car park and charging station, Source: Fotostudio Wierd (edited)

a biking path and the BESS. A total of 1056 PV modules are installed, amounting to a ratio of 7.04 modules per parking space and an installed capacity of 464.64 kWp. The installed modules are the mono half-cut bifacial modules of the type UL-440M-144BDG by the manufacturer *Ulica solar* [45]. The specifications of the modules can be found in table 3.1 and the installed modules are seen in figures 3.2 and 3.3. The modules are bifacial and can generate electricity from irradiation on its rear side at an efficiency of at least 70% of the front side efficiency.

Table 3.1: Ulica solar UL-440M-144BDG PV module specifications [45]

Parameter	Value
Power, P_{max}	440 W
Efficiency, η	19.92 %
Voltage at MPP, V_{MPP}	40.8 V
Current at MPP, I_{MPP}	10.78 A
Open circuit voltage, V_{OC}	49.6 V
Short circuit current, I_{SC}	11.34 A
Bifaciality factor	> 70 %
Temperature coefficient of P_{max}	-0.360 %/°C
Temperature coefficient of V_{OC}	- 0.330 %/°C
Temperature coefficient of I_{SC}	+0.049 %/°C
Dimensions module (L/W/H)	2131/1052/30 mm
Cell dimensions (LxW / No cells)	166x83 mm / 144

Table 3.2: Huawei SUN2000-60KTL-M0 inverter specifications [46]

Parameter	Value
Max input voltage	1100 V
MPPT operating voltage range	200 - 1000 V
Rated input voltage	600 V
Rated AC power	60 kW
Max current per MPPT	22 A
Max short circuit current	30 A
Max number of inputs	12
Number of MPPT trackers	6
European efficiency	98.5 %

The PV system consists of six arrays in total, that each consist of six times two strings in parallel with a maximum power point tracker (MPP) each (6 MPPs and 12 strings per array). Four of the six arrays have 183 modules (rows 1 & 2) and the remaining two have 162 modules (row 3). Half of the modules are facing east and the other half west, both at a 10° tilt. The string configuration is shown in figure 3.4.

Each array has its own solar inverter with a capacity of 60 kW, resulting in a total of 360 kW. The used solar inverter is the SUN2000-60KTL-M0 inverter by *Huawei*, with some of its specifications summarized in table 3.2.

The resulting system V_{OC} is between 642.2 - 790.4 V (strings have between 13 and 16 modules), which is within the 1100 V max input voltage limit of the inverter. The approximate working voltage, which is 40.6 V for each individual module, of each string will be between 527.8 - 649.6 V. This lies within the operating voltage range of the inverter between 200 to 1000 V. The DC/AC ratio is 464.64 kWp / 360 kW = 1.29.

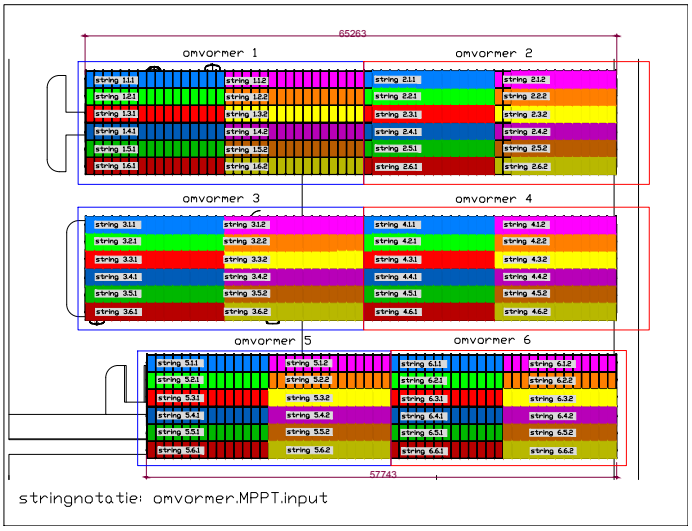

Figure 3.4: String configuration of PV System, in correspondence with site developer

3.3.1. LCA Emissions PV System

The PV system does not emit GHG emissions during its operation. However, for the cradle-to-grave emissions analysis all life cycle stages must be considered which are not all zero. Around 75 % of PV emissions occur during upstream and downstream processes, including the extraction of resources, manufacturing, installation, maintenance, decommissioning and disposal of the plant [47]. Most LCA studies on PV modules determine GWP for one kilowatt hour of generated electricity, which is dependent on location (solar irradiation), module life time, efficiency and other parameters that can all have significant impacts on GWP. In this study it is chosen to use GWP found per PV module for better transparency and decreased dependence on the above mentioned parameters.

While there are many LCA studies on standard aluminium back surface field (Al-BSF) crystalline silicon (c-Si) PV modules [48] there are only few LCA studies on PERC PV modules [49–51]. Luo et al. [51] conduct a cradle-to-grave analysis on three different PV system configurations and technologies, including PERC modules. The configuration most similar to the Ulica modules is a double-glass PERC module without frame. The study estimates GHG emissions of 198.9 kg CO_2eq for one 60-cell double-glass PERC module. Since the Ulica modules have 144 half-cut cells (72 full cells), this value is adjusted to 238.68 kg CO_2eq. This is found to be considerably lower than the more traditional Al-BSF modules, which emit 215.9 (259.1 for 72-cells) kg CO_2eq over their lifetime. The study also determines per kWh emissions, which amount to 20.9 g CO_2eq/kWh for operation in Singapore (1580 kWh/m_2/year) for the PERC double-glass module.

M. Lunardi et al. [50] use one kWh as functional unit and find a GWP of 26 g CO_2eq/kWh generated in Southern Europe with a solar irradiation of 1700 kWh/m_2/year for PERC modules (they do not disclose per module values). Similarly, Jia et al. [49] find emissions of 20 g CO_2eq/kWh for a 410 W PERC module operating in Beijing, China (1573 kWh/m_2/year). The results of the three studies are very comparable and can verify the per module result found in [51]. Additionally, Hsu et al. [48] screen almost 400 LCA studies on PVs and harmonized results of 13 selected studies, finding a mean of 52 ± a standard deviation of 29 g CO_2eq/kWh for standard Al-BSF modules. Al-BSF modules have lower efficiency and hence, the CO_2 emissions per kWh are expected to be higher compared to PERC modules [49, 50]. De Wild-Scholten and Huld [52] publish carbon emissions per kWp of installed PV system, which gives 370 kg CO_2eq for the 440 W modules assuming mono c-Si and accounting for a technology share of 30.9 %. This study is not specific to PERC modules, however it validates the magnitude of the per module values of [51]. The increased value can be explained by the carbon footprint of PERC modules being lower than Al-BSF modules [49, 50] and the fact that the study by De Wild-Scholten and Huld [52] was conducted for 2011 and emissions from PV module manufacturing are still decreasing with production optimization [53] while power ratings of modules have increased.

There are 1056 modules installed, therefore, the total LCA emissions from the PV modules are 252 tons CO_2eq, referred to as C_{PV} in the following. The LCA emissions from the PV system are summarized in table 3.7.

3.4. NiMH Battery Energy Storage System

The battery system has multiple components. It consists of the battery racks, a battery inverter and a battery management system (BMS) which are described in this section.

3.4.1. Battery Racks

A 345.6 kWh nickel metal hydride (NiMH) battery is installed inside of two shipping containers underneath the carport structure. It consists of six individual battery racks with a capacity of 57.6 kWh each. The installed model is the *Nilar* ECI-576V-57 rack [54], some of its specifications are shown in table 3.4 and the battery racks inside of the container are seen in figure 3.6.

Figure 3.5: Installed battery inverter in container

Figure 3.6: Installed NiMH battery racks in container

Two of the battery racks are installed in series and three in parallel. Each series connected rack pair is connected to an SunSys PCS^2 SUN-ES100ET30IS inverter manufactured by *Socomec* [55], which is located in a second container next to the battery. Some of the inverter specifications are summarized in table 3.3. Each of the inverters has a rated power of 100 kW, resulting in a total inverter capacity of 300 kW. The installed inverters can be seen in figure 3.5.

Table 3.3: Socomec SunSys PCS^2 SUN-ES100ET30IS inverter specifications [55]

Parameter	Value
Rated Power	100 kW
Max power	110 kW
Battery voltage	450 - 850 VDC
Max (dis)charge current	240 A
Rated output current	144 A_{rms}
Max output current	159 A_{rms}
Max efficiency	96.4 %

Table 3.4: Nilar NIMH battery ECI-576V-57,6kWh specifications for one rack [54]

Parameter	Value
Rated capacity	80 Ah / 57.6 kWh
Pack voltage	144 V
System voltage	576 V
Typical C-rates charging	0.3C
Typical C-rates discharging	0.2C

The chemistry of a NiMH battery is briefly explained below. The electrolyte of the battery is potassium hydroxide (KOH), nickel hydroxide ($Ni(OH)_2$) is the positive electrode and a metal alloy (M) is the negative electrode during charging. The positive electrode releases hydroxide (OH^-) and becomes $NiOOH$ during the charge reaction. The OH^- is taken up by the negative electrode, which forms a metal hydride, MH. This process is driven by electrons flowing through an external electric circuit forcing the negatively charged OH^- to move to the increasingly positively charged $Ni(OH)_2$ electrode. The overall charge reaction of NiMH batteries can be seen in equation 3.1 [56]. During discharge, this process is reversed and electricity produced.

$$M + Ni(OH)_2 \leftrightarrow MH + NiOOH \qquad E_0 = 1.3V \tag{3.1}$$

3.4.2. Battery Management System

The operation of the BESS is controlled by the BMS which has several functions:

- **Monitoring** the state of the battery by measuring voltage, temperature, current and other battery parameters.
- **Computation** of parameters such as battery SoC, state of health, max (dis-) charge current, based on above mentioned measured variables.
- **Protection** of the battery by ensuring operation within a favorable range, regarding SoC, current, voltage, temperature, etc.
- **Control** of power im- and exports to the municipality building and electricity grid. When electricity prices drop below a certain threshold value, power is imported and when a certain threshold value is exceeded, power is exported to the grid for a favorable economic operation of the system. The BMS also controls whether power is supplied to the EVs or not.
- **Communication** of battery state and power measurements to external platforms and receiving data about electricity market prices.

Each battery rack is equipped with its own BMS installed by the manufacturer of the battery. Additionally, there are three BMSs of the type PetaBox (version 3) by PetaWatts [57] installed, which manage two of the six racks each. Two of the PetaBoxes are installed in the battery container under the PV roof and one is installed in a technical room on the alley way between the municipality building and the De Redepassage.

3.4.3. LCA Emissions NiMH Battery

Similarly to the PV system, the BESS does not emit GHGs during its operation. However, during its life cycle, the batteries do cause GHG emissions. To the knowledge of the author only limited literature concerning LCA studies on large-scale NiMH batteries exists [58–60] and the manufacturer of the installed batteries also does not disclose the carbon footprint of the product.

Majeau-Bettez et al. [58] find that one kilogram of NiMH battery emits 20 kg CO_2eq in their cradle-to-gate analysis using the European grid mix for accounting emissions of electricity consumption during production. Silvestri et al. [60] investigate the effect of material recycling on LCA results of NiMH batteries using the German electricity mix. The resulting GWP of their cradle-to-gate analysis is 22.3 kg CO_2eq per kg of battery using virgin materials and 17.9 + 9.43 CO_2eq/kg (27.3 CO_2eq/kg) using recycled materials (additional end of life treatments of recycled materials). Here, it is assumed that virgin materials were used for the production on the NiMh batteries, hence the value of 22.3 kg CO_2eq/kg battery is applied. In another LCA analysis, Wang et al. [59] find an environmental impact between 6.65, 8.8 and 9.45 kg CO_2eq/kg NiMH battery for a reuse & recycling, no recycling and recycling scenario under Japanese production conditions.

The Nilar batteries are produced in Sweden, hence the results attained in [58] and [60], assuming European and German grid mixes respectively, are expected to yield the most accurate GWP estimation. The weight of each battery rack is 1610 kg, accordingly six NiMH battery racks are estimated to emit 193.2 - 215.4 tons CO_2eq, as summarized in table 3.5. Life cycle emissions from the BESS are referred to as C_{BESS} in the following.

Parameter	Value
Amount installed	6 battery racks
Weight per unit	1610 kg
Carbon emissions per unit	20 - 22.3 kg CO_2eq [58, 60]
Total emissions	193.2 - 215.4 tons CO_2eq

Table 3.5: Overview LCA emissions from BESS

3.5. EV Charge Points

The three public charging stations are located to the side of the BESS container and the one reserved for the municipality is located at the end of the second row. The charging stations are the newly developed Quattro 4XL by *Alfen* [61], some of its specifications can be found in table 3.6 and a picture of an installed

charging station is presented in figure 3.7. The available charging power is 22 kW at a max current of 32 A per charging station. The connector type is 2, in accordance with European Commission guideline IEC 62196-2 for charging standards.

Table 3.6: Alfen Quattro 4XL charging station specifications [55]

Parameter	Value
Number of charge points	4
Connector type	IEC62196-2
Nominal output voltage	230 V
Max total current	80 A (all 4 charge points)
Max power charging station	44 kW
Max power per charge point	22 kW

Figure 3.7: Installed EV charging station

The charging stations have the capability of bidirectional charging, which could be employed in the future. Today, the smart charging capability is limited to unidirectional controlled charging where the rate of charging can be controlled by the charging infrastructure or the EV, depending on its technical ability.

3.6. Carport Structure

The deployed carport structure is a double T-frame duo pitch design as shown schematically in figure 3.8 and the installed structure in figure 3.9. The structure makes use of supporting columns in the middle and, due to a strong foundation in the ground, does not require columns on the edges of the roof. An advantage of this design is the ease of parking as no supporting roof structures are blocking the parking space [62]. However, the design requires a higher amount of material, steel in this case, increasing the cost of the design. The duo-pitch roof is east-west facing and has a slope of 10°. The electricity yield of the duo-pitch PV system is almost independent of orientation and expected to generate 92.5 % of the annual yield of a south facing mono-pitch system [62]. The system makes use of PV glazing technology and replaces a conventional roof structure with partially transparent solar PV modules. This allows for the PV modules to produce electricity from the irradiation received on the top but also the ground and structure reflected, the sky diffuse and some direct irradiation reaching its back. This can, rather easily, be implemented into a passivated emitter and rear cell (PERC) technology and increases the cells overall efficiency [63].

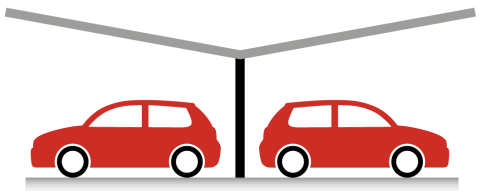

Figure 3.8: T-frame carport structure [62]

Figure 3.9: T-frame carport structure at the car park in Dronten, Source: Fotostudio Wierd

3.6.1. LCA Emissions Carport Structure

Building the carport structure in Dronten required the use of 58 tons of steel and roughly 5.6 tons of aluminium profile (based on personal correspondence with site developer). According to the World Steel Association [64], the production of one ton of crude steel cast releases 1.83 tonnes of CO_2eq. Hence, 106.14 tonnes CO_2eq are attributed to the steel structure.

The emissions occurring during aluminium production differ significantly depending on where production takes place. Here, it is assumed that European aluminium is used which, according to the European Aluminium Association [65], releases 6.7 tonnes CO_2eq for every ton of product. Accordingly, production of aluminium profiles is allocated 37.52 tonnes of CO_2eq emissions. The emissions caused by all components of the solar system, including its structure are summarized in table 3.7.

Parameter	PV modules	Steel	Aluminium
Amount installed	1056 modules	58 ton	5.6 ton
Carbon emissions per unit	238.68 kgCO_2eq/module	1.83 tons CO_2/ton	6.7 tons CO_2/ton
Total emissions	252.05 tons CO_2eq	106.14 tons CO_2eq	37.52 tons CO_2eq
Total emissions PV system	395.7 tons CO_2eq		

Table 3.7: Overview LCA emissions from PV system including the structure

3.7. Utility Grid Electricity Emission Factor Data

This section describes the used data for current MEFs and HEFs in sections 3.7.1 and 3.7.2, respectively.

3.7.1. Marginal Emission Factor

Based on the extensive literature review presented in chapter 2.2, it is established that the use of MEFs is conceptually the most accurate approach in assessing offset carbon emissions. For the current (2019) emissions assessment it is chosen to use MEF from *Tomorrow* [66]. This application programming interface (API) provides real time MEFs that are estimated from a large data collection of observed power system behaviour through machine learning techniques. The underlying model detects any change in generation (dX in the equation in figure 3.10) and classifies it as either due to demand changes, $g(z)$, or independent of demand, $f(z)$, e.g. variation in renewable generation due to weather changes. This separation solves the problem of non-causal generation attribution of the regression models, as seen in [30, 33, 34].

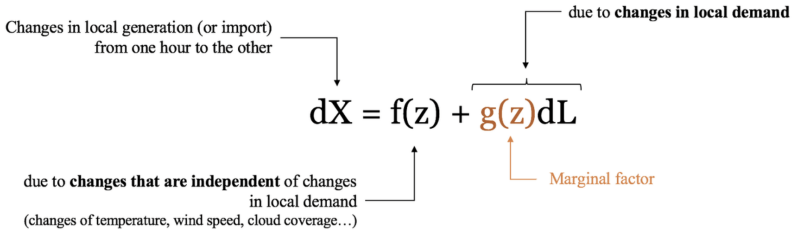

Figure 3.10: Formula used to allocate changes in generation volume to independent of demand and dependent on demand changes [67]

Once the cause of the generation change is identified as a change in demand, the marginal generator is traced back to the location of generation through solving the flow conservation equation of electricity imports and exports for every region. The type of marginal plant is then estimated by disaggregating generation data into generation from each generator and determining which generator increases production [67]. The data is available in real-time for every hour for the Netherlands and recorded historic data is available as well. All previous studies that have been found using MEFs are either based on a merit order model or a regression model (see table 2.6). No study was found that uses observed power plant dispatch MEFs which presents the novelty of the emissions assessment approach in this analysis. Using *Tomorrow's* MEFs solves the concerns about high inaccuracy of MEF estimation raised by Jochem et al. [44]. Additionally, the availability of such database addresses the problem of high modelling effort mentioned by Ghotge et al. [28]. The advantage over a merit order model are that power system dynamics and international trade is accounted for. To conclude, use of observed MEFs is expected to yield the most accurate estimate for marginal emission factors compared to all other reviewed approaches.

It is chosen to simulate the system using MEFs from the year 2019, to exclude the possibility of including unwanted effects of the COVID-19 pandemic in the emissions data of the year 2020. The energy system has not seen significant changes between 2019 and 2020/21 that could lead to any significant deviations between the years 2019 and 2021. Evidently, a full data set for 2021 is not available yet and the conducted emissions analysis is expected to exhibit high seasonal variations, thus simulation of a full year is favorable. Consequently, it is rejected to use the emissions data of only half of 2021 and conduct the analysis solely for 2019.

Access to the historic MEF data requires a license and was made available by Tomorrow [66] in Excel timestamp format. Real-time MEFs can accessed by running the following HTTP (Hypertext Transfer Protocol) request:

```
GET https://api.co2signal.com/v1/latest?countryCode=NL
```

together with an unique authentication token (access also requires a license) which sends a query to *Tomorrow's* server which responds with the current carbon intensity of Dutch grid electricity in g CO_2eq/kWh (see [68] for full documentation).

3.7.2. Hourly Average Emission Factor

MEFs from observed power plant dispatch is naturally not available for the future, as discussed in section 2.2.4. A merit order or regression model introduces high uncertainties to MEFs and, therefore, are not used for the future system model. Instead, HEFs are used for the future system model and also for the conducting the accounting approach on the current emissions assessment. As mentioned in section 2.2.2, HEFs are found by averaging the total emissions of all operational power plants in one hour over the total electricity generation in that hour. This requires a comprehensive model of the energy system, which is described in section 4.3.2 for the future system model.

For conducting the accounting approach in the current emissions assessment, HEFs from the *Tomorrow* database [66] are used. HEF are calculated from observed power plant dispatch, as reported from generation facilities, and technology specific carbon emissions. The methodology is based on a flow-tracing technique, and follows the approach laid out in [15]. This approach identifies zonal (in this case the Netherlands) electricity mixes by tracing the origin of generation of electricity (consumption-based approach). Once the origin is determined, the power generation is broken down by type and power plant specific carbon emission factors (as seen in table A.3 in appendix A.2.4) are used to find overall carbon emissions.

HEFs are accessed from Tomorrow in the same way as MEFs, see section 3.7.1, however, accessing the real-time HEFs data does not require a license.

4

Methodology

This chapter lays out the developed methodology to estimate the carbon emission offset achieved through the PowerParking system. This methodology can be generalised to any system containing local energy generation, time-variable loads and energy storage. An adapted version of the presented methodology can easily be applied to any system containing only one or two of these components.

The simulation scope of this study, including a description of the various simulation scenarios, is given in section 4.1. Section 4.2 defines the methodology for allocation of carbon emissions for the carbon offset and accounting approach and explains the method of determining energy flows within the system. The methodology for the system simulation and its fours sub-models is explained in section 4.3.

4.1. Simulation Scope

The simulation scope of this emissions study is twofold. First, a current emissions assessment using observed power plant dispatch data together with modeled system behaviour is conducted for the year 2019. Second, a future system simulation for the year 2030 is developed. The scope of both emission assessment approaches is defined in this section.

4.1.1. Current Carbon Emissions Assessment

The current emissions assessment of the PowerParking system is aimed at calculating the offset carbon emissions for 2019 and is computed on an hourly timestep. The model is based on simulated system behaviour together with observed consumption based emission factors from the Dutch electricity grid (from [66], as explained in section 3.7.1). A full annual MEF (and HEF) data set exists only for 2019 without effects of the COVID-19 pandemic, which is why it was chosen to simulate the year 2019. The inputs to the current emissions assessment are summarized in table 4.1.

Input	Model or Source	Time-resolution / data points
Power generation PV system	System Advisory Model (NREL)	Hourly / 8670
Power demand EV chargers	EV demand model	Hourly / 8670
Power (dis-) charged from battery	Kinetic Battery Model	Hourly / 8670
MEFs & HEFs of utility grid electricity	Tomorrow [66]	Hourly / 8670

Table 4.1: Required models and sources for current carbon emissions assessment

The first three data inputs are simulated by using different sub-models for each of the variables and will be explained in section 4.3. The fourth variable is based on observed power plant dispatch MEFs, as explained in section 3.7.1.

The 2019 assessment is primarily focused on estimating current offset emissions using MEFs. The offset calculation is repeated using HEFs to derive implications of the use of HEFs instead of MEFs in the future system model.

4.1.2. Future System Model

To estimate emissions from the system in the future, a detailed model of the energy system and carport system in 2030 is developed. It is chosen to model the year 2030, as the Netherlands Environmental Assessment Agency (PBL) has published the Climate and Energy Outlook [69] on the predicted Dutch grid mix in 2030 based on adapted and proposed policy scenarios. Therefore, it is expected that simulation of the year 2030 yields accurate insight into the emissions based on the availability of a realistic description of the energy system in that year. Furthermore, modelling further into the future would inevitable lead to increased inaccuracy and decrease the validity of results. The essential variables to be simulated on an hourly basis in 2030 are summarized in table 4.2.

Input	Model	Time-resolution / data points
Power generation PV system	System Advisory Model (NREL)	Hourly / 8670
Power demand EV chargers	EV demand model	Hourly / 8670
Power (dis-) charged from battery	Kinetic Battery Model	Hourly / 8670
MEFs & HEFs of utility grid electricity	Energy Transition Model & power plant CIs	Hourly / 8670

Table 4.2: Required models and sources for future carbon emissions assessment

Both simulations (2019 & 2030) require the same four inputs in order to determine the system's emissions. One difference is that the 2019 assessment uses the observed MEFs and HEFs while the future EF is modelled using an energy system model. Another difference is the EV demand profile, which is higher in 2030 compared to 2019, as EV adaptation is expected to increase. The PV generation profile is identical for both simulation years, as solar irradiation is not expected to show significant change between 2019 and 2030. The applied battery model is also kept the same in both simulations. The presented carbon offset and accounting methodology is applied to both the 2019 and 2030 simulations of the system.

4.1.3. Simulation Scenarios & Research Questions

In order to answer the four research questions raised in section 1.2, various simulation scenarios of the solar carport are developed. This section first summarizes and describes each of the developed scenarios and, second, lays out which scenarios are required to answer each research question.

All developed scenarios are summarized in table 4.3 with regards to their most important descriptors. The varying parameters across scenarios are the year, the emissions accounting approach, the used EF, inclusion of PV system and BESS and the used EV load profile. Additionally, figure A.1 in appendix A.2.1 gives a visual representation of the various scenarios.

Table 4.3: Summary of the developed scenarios. O means offset approach and A means accounting approach. Y stands for inclusion of system component, and N for exclusion of system component.

Year	Name		Approach	EF	PV	BESS	Annual EV load
2019	Base scenario	B19 MEF	O	MEF	Y	Y	35 MWh
	Base scenario - HEF	B19 HEF	O/A	HEF	Y	Y	
	Base scenario - AEF	B19 AEF	O/A	AEF	Y	Y	
	No BESS	NoB 19	O/A	MEF	Y	N	
	No BESS & no PV	NoB/PV 19	A	HEF	N	N	
	Only PV	PV19	O	MEF	Y	N	No EV charging
2030	Base scenario - HEF	B30 HEF	O/A	HEF	Y	Y	137 MWh
	Base scenario - AEF	B30 AEF	O/A	AEF	Y	Y	
	Base scenario - 24/32 chargers	B30 24 & B30 32	O/A	HEF	Y	Y	206 & 274 MWh
	No BESS	NoB 30	O/A		Y	N	137 MWh
	No BESS & no PV	NoB/PV 30	A		N	N	
	Only PV	PV30	O		Y	N	No EV charging

Offset Carbon Emissions in 2019

In order to answer research questions I:

"*What is the recommended approach and emission factor selection to measure carbon emission offsets? And what is the annual cradle-to-grave carbon emission offset of the solar carport in Dronten?*"

the base scenario for 2019 (B19 MEF) is developed. This scenario entails the 2019 emissions assessment (as described in section 4.1.1) using observed MEFs. The B19 MEF scenario is based on simulated behaviour of the carport system, observed MEF data and LCA emissions of all large system components. Additionally, the offset methodology is compared to the carbon accounting methodology and repeated using different EFs (B19 HEF and B19 AEF), in order to quantify the consequences of choosing a different approach to emissions assessments. The motivation for this scenario is to accurately quantify the carbon emission offset achieved by the solar carport system and be able to evaluate the consequences of selection of accounting methodology and emission factors.

Offset Carbon Emission Potential of BESS in 2019 and 2030 (research question II)
The second research question of:

"*What is the cradle-to-grave carbon emission offset potential of the battery system currently and with a higher share of RES in 2030?*"

aims to quantify the potential of the battery system to offset carbon emissions now and in the future. This requires the development and modelling of several scenarios. First, a scenario which does not include the BESS is developed for 2019 (NoB 19) to find the carbon offset potential of the BESS in 2019. The offset emissions achieved in the scenario without the BESS can then be compared with the base scenario in order to evaluate the difference in offset emissions between the two scenarios. Second, to estimate the emission offset potential of the battery in the future, the system is modeled without including the BESS in 2030 (NoB 30). To be able to evaluate the impact of the BESS, modelling of the base scenario for the future (B30 HEF) is required. Since, MEFs are not available for the future scenario, it is necessary to conduct the base case in 2019 using HEFs (B19 MEF) and determine the consequences of using HEFs instead of MEFs. The motivation for this research question is to provide insights into the impact of, specifically, the battery system in terms of offsetting carbon emissions over the next decade.

Carbon Emissions from EVs Without Solar Carport in 2019 and 2030 (research question A)
The first additional research question A is:

"How much carbon emissions occur by charging EVs directly from the grid, without installing a PV system and BESS, currently and 2030?"

Therefore, two scenarios are developed, which both exclude the BESS and the PV system in 2019 and 2030, NoB/PV 19 and NoB/PV 30 respectively. These scenarios are aimed at quantifying the carbon footprint of EV charging today and in the future and the potential of the solar carport to reduce these carbon emissions.

Effect of Higher EV Demand on Offset Emissions in 2030 (research question B)
EV adoption will increase in the future [70] and, hence, it is interesting to assess the emissions impact of including more EV charge points in the PowerParking system. For this reason, the effect of higher EV charging demand, i.e. more charging stations, on offset carbon emissions in 2030 is investigated in the additional research question B:

"How is the system's carbon emission offset potential and total carbon emissions affected by installing a larger amount of EV charge points by 2030?"

In order to answer this question, scenarios B30 24 and B30 32 are developed in which all system parameters are kept as in the base case, and more charging stations, a total of 24 and 32 respectively, are simulated by increasing the EV demand. This scenario is then compared to the base scenario in 2030 to quantify the difference in offset emissions. The motivation for this research question is to evaluate the emissions reduction impact of adding further charging stations to the system and provide accurate emissions estimates to decision-makers.

4.2. Carbon Emissions Assessment Methodology

There are two approaches in allocating carbon emissions to a project investigated in this study; the carbon offset and the carbon accounting approach, as mentioned in chapter 2.2. This section explains the differences in the approaches and defines both for the solar car park in Dronten.

The sign convention for energy flows in the PowerParking system, as described in section 3.1, used in the methodology presented below is as follows:

- Components *supplying* energy to the system, energy sources, are positive
- Components *extracting* energy from the system, energy sinks, are negative.

4.2.1. Calculation of Carbon Offset

The main focus of this study is to estimate offset carbon emissions. The offset approach quantifies all emissions that are mitigated or occur as a consequence of installing and operating the investigated system. The aim of the offset approach is to investigate the overall impact and change in emissions caused by an emission mitigation project, as defined in section 2.1.2.

Figure 4.1 shows a simplified overview of the possible energy pathways in the car park system. In the following, energy flows and carbon emissions are allocated to each of these pathways for the offset approach.

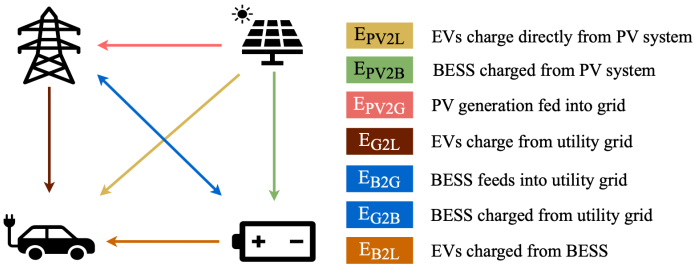

Figure 4.1: Schematic diagram of energy pathways in the system

The first pathway, following the order in figure 4.1, of charging EVs directly from the PV system, E_t^{PV2L}, does not cause emissions. During operation, the PV system does not emit GHGs, however, life cycle emissions need to be accounted for, as described in section 3.3.1. Additionally, there are offset emissions allocated to this pathway as energy charged directly from PV is reducing the load on the grid, allowing the marginal generator to reduce generation. Hence, the offset emissions is the MEF multiplied by the volume of energy charged by the EVs.

The BESS charging directly from the PV system, E_t^{PV2B}, does not lead to emissions nor offset emissions. Both the PV system and BESS are defined as new system components and energy going from one to the other components does not have ramifications in the consequential approach. The offsetting effect of the BESS is accounted for when discharging the solar energy to EVs or the grid.

The PV generation directly fed into the grid, E_t^{PV2G}, replaces generation of the marginal plant and, therefore, this energy pathways offsets marginal grid emissions.

EVs charging from the utility grid, E_t^{G2L}, is not allocated any (offset) emissions as the EV demand would have been supplied by the grid in the reference case of no PV or BESS.

Discharging the BESS, E_t^{B2G}, offsets emissions of the marginal power plant at the time of discharging. When the BESS is charged from the grid, E_t^{G2B}, there are no offset emissions, however the caused marginal emissions of the imported energy are allocated to this pathway. Similarly to the PV system the BESS does not emit GHGs during operation, however, the emissions from production, installation and maintenance of the BESS need to be accounted for, as explained in section 3.4.3.

Finally, EVs charging from the battery system offsets emissions of the marginal plant, as the grid would have supplied the energy used to charge the EVs if the BESS did not exist. Table 4.4 summarizes the specific meaning of the offset and accounting approaches for the system investigated in this study.

Based on the allocation of carbon emissions outlaid above, the equation for calculating the offset carbon emissions used for the carbon offset calculation is defined below. C_{offset}, given in $kgCO_2eq$, are the offset carbon emissions by the system over the period T = [1,...t,...T], as defined in equation 4.1.

$$C_{offset} = \sum_{t=1}^{T=8760} \left(EF_t \cdot \left(E_t^{PV2G} + E_t^{PV2L} + E_t^{B2L} + E_t^{B2G} - E_t^{G2B}\right)\right) - C_{PV} - C_{BESS} \tag{4.1}$$

where t is each minute within the year,
$EF_t \left[\frac{kgCO_2eq}{kWh}\right]$ is the grid emission factor in hour $t, \forall\, t \in [1,...T]$,
E_t^{PV2G} $[kWh]$ is the PV generation exported to the grid in each hour, t,
E_t^{PV2L} $[kWh]$ is the PV generation directly supplied to the EV load in each hour, t,
E_t^{B2L} $[kWh]$ is the energy supplied to the EVs from the battery in each hour, t,
E_t^{B2G} $[kWh]$ is the energy discharged from the BESS and exported to the grid in each hour, t,
E_t^{G2B} $[kWh]$ is the energy imported from the grid to charge the BESS in each hour, t,

C_{PV} $[tCO_2eq]$ are the life cycle emissions cause by the PV system,
C_{BESS} $[tCO_2eq]$ are the life cycle emissions cause by the BESS,

The first term in equation 4.1 is a summation of the total volume of energy going through pathways E_t^{PV2L}, E_t^{PV2G}, E_t^{B2L} and E_t^{B2G} (positive) and pathway E_t^{G2B} (negative) multiplied by the grid EF to allocate all avoided and occurred emissions. As mentioned, the offset emissions originate from exporting PV generation to the grid, E_t^{PV2G}, directly charging EVs from the PV system, E_t^{PV2L}, charging EVs from the BESS, E_t^{B2L}, and exporting energy to the grid from the BESS, E_t^{B2G}. The negative term, E_t^{G2B}, accounts for the occurring emissions from importing energy from the grid to charge the BESS. The energy flows in every hour, t, are summed over the time period $T = 8760$ to calculate the offset emissions over the entire year.

The life cycle emissions of the PV system, C_{PV}, and BESS, C_{BESS}, are added as one at the start of time period T. This method is chosen because it is expected to yield higher accuracy compared to accounting emissions for each unit of electricity produced by the respective components. Sections 3.3.1 and 3.4.3 describe the life cycle emissions for PV and BESS, respectively.

4.2.2. Carbon Emission Accounting

An additional research question in this study is how the offset emissions compare to the emissions actually caused by the system, which are found through the accounting approach. This approach estimates the total GHG emissions attributed to the system, following the attributional approach, as explained in section 2.1.1. Emissions saved through the system are not taken into account. Here, the aim is not to quantify a change in emissions but the total annual GHG emission caused by the system.

The accounting approach accounts for all emissions caused by the system, but excludes the avoided emissions. Consequently, the emissions allocated to the individual pathways for the accounting approach are identical to the occurred emissions of the offset approach. The only difference is that the emissions occurring through importing electricity from the grid to charge EVs will be allocated grid emissions. This is summarized in table 4.4.

Following the accounting approach the emissions caused by the system, denoted by $C_{account}$ $[kgCO_2eq]$, that occur over the period T = [1,...t,...T] are defined by equation 4.2.

$$C_{account} = \sum_{t=1}^{T=8760} \left(EF_t \cdot \left(E_t^{G2L} + E_t^{G2B}\right)\right) + C_{PV} + C_{BESS} \tag{4.2}$$

where t is each hour within the year, t, and E_t^{G2B} $[kWh]$ is the energy imported from the grid to charge the BESS in each hour, t.

Equation 4.2 consists of three terms. The first term is the sum of the energy imported from the grid in every hour t which is multiplied with the EF in that hour (EF_t) and then summed over period T. The second and third term are bulk LCA emissions from the PV system and BESS.

The similarities and differences in the two described approaches can be seen in table 4.4.

Table 4.4: Comparison of the offset and accounting approach, based on energy pathways as defined in figure 4.1.

Name	Offset approach		Accounting approach
	Positive (offset)	Negative (emissions)	
E^{PV2L}	EF of energy charged by EV	-	
E^{PV2B}	-	-	
E^{PV2G}	EF of energy fed into grid	-	
E^{G2L}	-	-	EF of imported energy
E^{G2B}	-	Grid EF of imported energy	
E^{B2G}	EF of energy fed into grid	-	
E^{B2L}	EF of energy discharged from battery	-	
C_{PV}	-	LCA emissions PV system	
C_{BESS}	-	LCA emissions BESS	

4.2.3. Determination of Energy Flows

For the application of the offset emission methodology presented in section 4.2.1, the energy flows within the carpark system need to be established. As mentioned, the input variables within the system are the energy generation of the PV system, E^{PV}, the energy consumed by EVs, E^{EV}, and the energy exchanged with the battery, E^{B} (see section 4.1). These variables are simulated and each of the energy flows as presented in figure 4.1 are derived from them.

The solar energy that is directly supplied to the EVs (the laod), E_t^{PV2L}, for every hour, t, is found through equation 4.3.

$$E_t^{PV2L} = min\left(E_t^{PV}, E_t^{EV}\right) \tag{4.3}$$

According to equation 4.3, the minimum value of EV demand and PV generation is determined to be the amount of energy that is supplied directly to the vehicles from the PV system. The charging EVs have the highest (consumer) priority in the system and, therefore, all EV demand will be satisfied by solar generation if available. If PV generation exceeds EV demand E_t^{PV2L} is the total EV demand and in the opposite case it is limited by the solar generation.

The energy flow from PV to the BESS, E_t^{PV2B}, for every hour, t, is defined by equation 4.4. Energy flows from PV to the BESS in the case of the PV generation being higher than EV demand (as EV has the highest priority) and the BESS charging, i.e. having a negative sign. The magnitude of E_t^{PV2B} is determined by the smaller value of the sum of PV generation and EV demand and the energy available to charge the battery.

$$E_t^{PV2B} = \begin{cases} min\left(\left(E_t^{PV} + E_t^{EV}\right),\ \left|E_t^{B}\right|\right), & \text{if } E_t^{PV} \geq E_t^{EV} \ \wedge \ E_t^{B} < 0 \\ 0 & \text{else} \end{cases} \tag{4.4}$$

Equation 4.5 determines the energy of the PV system delivered to the grid, E_t^{PV2G}, for every hour, t. All of the grid exports, $E_t^{G_{ex}}$, are allocated to the PV exporting energy in the case that PV generation exceeds EV demand and the battery is charging, hence is negative. In the case the battery is discharging, the solar energy export is found to be all PV generation less the EV demand in that hour, t.

$$E_t^{PV2G} = \begin{cases} E_t^{G_{ex}} & \text{if } E_T^{PV} \geq \left|E_t^{EV}\right| \ \wedge \ E_t^{B} < 0 \ \wedge \ (E_t^{PV} + |E_t^{EV}|) > |E_t^{B}| \\ 0 & \text{if } E_t^{PV} \geq \left|E_t^{EV}\right| \ \wedge \ E_t^{B} < 0 \ \wedge \ (E_t^{PV} + |E_t^{EV}|) \leq |E_t^{B}| \\ E_t^{PV} - \left|E_t^{EV}\right| & \text{if } E_t^{PV} \geq \left|E_t^{EV}\right| \ \wedge \ E_t^{B} \geq 0 \\ 0 & \text{if } E_t^{PV} < \left|E_t^{EV}\right| \\ 0 & \text{else} \end{cases} \tag{4.5}$$

The energy delivered from the BESS to the load, E_t^{B2L}, is determined through equation 4.6. In the case that the battery is discharging, i.e. has a positive sign, and the energy consumed by the EVs cannot be fully satisfied by the PV generation, the smaller value of either the unsatisfied EV demand or the discharged energy from the battery is allocated to this pathway.

$$E_t^{B2L} = \begin{cases} \min\left(\left(\left|E_t^{EV}\right| - E_t^{PV2L}\right), \left|E_t^{B}\right|\right) & \text{if } E_t^{B} \geq 0 \ \wedge \ \ \left|E_t^{EV}\right| > E_t^{PV2L} \\ 0 & \text{if } \ E_t^{B} < 0 \\ 0 & \text{if } \ \left|E_t^{EV}\right| \leq E_t^{PV2L} \\ 0 & \text{else} \end{cases} \tag{4.6}$$

The energy injected into the grid from the BESS, E_t^{B2G}, for every hour, t, is found through 4.7. The BESS is exporting energy to the grid in the case that the overall system is exporting energy, the battery is discharging and the discharge of the battery is larger than what its already supplying to the EVs. When these three conditions are fulfilled, E_t^{B2G} is the BESS discharge remaining after supplying the EV demand.

$$E_t^{B2G} = \begin{cases} \left|E_t^{B}\right| - E_t^{B2L} & \text{if } E_t^{G} \leq 0 \ \wedge \ E_t^{B} > 0 \ \wedge \ \left|E_t^{B}\right| > E_t^{B2L} \\ 0 & \text{if } \ E_t^{G} \geq 0 \\ 0 & \text{if } \ E_t^{B} \leq 0 \\ 0 & \text{if } \ \left|E_t^{B}\right| \leq E_t^{B2L} \\ 0 & \text{else} \end{cases} \tag{4.7}$$

Equation 4.8 describes how the energy imported from the grid to charge the BESS is determined. The BESS charges directly from the grid if the total grid connection is positive, i.e. importing, the battery is charging (negative sign) and the total energy charged by the BESS is larger than the energy supplied to the battery from the PV system. This is technically possible for the solar carport system, however, not included in the system simulation. In reality, the BESS imports energy from the grid when electricity prices fall below a certain threshold price, determined by an intelligent BMS. Modelling of market prices is out of the scope of this work and, therefore, excluded.

$$E_t^{G2B} = \begin{cases} \left|E_t^B\right| - E_t^{PV2B} & \text{if } E_t^G \geq 0 \wedge \text{if } E_t^B < 0 \wedge \left|E_t^B\right| > E_t^{PV2B} \\ 0 & \text{if } E_t^G < 0 \\ 0 & \text{if } E_t^B \geq 0 \\ 0 & \text{if } \left|E_t^B\right| \leq E_t^{PV2B} \\ 0 & \text{else} \end{cases} \tag{4.8}$$

The energy imported from the grid to charge the EVs, E_t^{G2L}, is established through equation 4.9. Energy imports are allocated to this pathway if there are grid imports, the BESS is not charging and the EV demand is not covered by PV generation and BESS together. Then, the remaining unsatisfied EV demand is supplied by grid electricity.

$$E_t^{G2L} = \begin{cases} \left|E_t^{EV}\right| - E_t^{PV2L} - E_t^{B2L} & \text{if } E_t^G \geq 0 \wedge E_t^B \geq 0 \wedge \left|E_t^{EV}\right| > \left(E_t^{PV2L} + E_t^{B2L}\right) \\ 0 & \text{else} \end{cases} \tag{4.9}$$

The above explained determination of energy flows within the system in specific to the system in Dronten and is applied in both the current assessment and the future system assessment.

4.3. Solar Carport System Model

This section presents the several sub-models of the carport system model that simulate the behaviour of various components of the carport system. Section 4.3.1 presents the PV generation model. The future energy system model and determination of HEFs in 2030 is explained in section 4.3.2. The model used to estimate the EV demand profile is described in section 4.3.3. Finally, the battery model is explained in section 4.3.4. With the exception of the future energy system model, all three sub-models are used for the current emissions assessment and the future system model.

4.3.1. PV Generation Model and Profile

The operation of the PV system is modelled using the System Advisor Model (SAM), version 2020.2.29, by the National Renewable Energy Laboratory (NREL) [71]. The sub-model used to model the hourly DC power output is the California Energy Commission (CEC) Performance Model with user entered specifications, as described in detail by De Soto et al. [72]. The inputs to the model are the PV module parameters, system design and inverter specifications as described in section 3.3. The orientation of the modules is east-west facing, corresponding to an Azimuth angle of 90°and 270°, respectively. The module tilt is 10°. The bifacial capability is modelled based on the Practical Irradiance Model as described by Marion et al. [73]. Required inputs are bifaciality, which is 70% (see section 3.3), and the transmission fraction, *TF*. *TF* is the ratio of the module area blocking light from being transmitted through the glass of the module and is calculated as defined by equation 4.10.

$$TF = \frac{\sum^n A_{cell,n}}{A_{module}} \tag{4.10}$$

This yields a transmission fraction of 0.885 for the Ulica modules.

It was chosen to use meteorological data of a Typical Meteorological Year (TMY) for the project site of Dronten (52°31'N, 5°42'E), sourced from the Photovoltaic Geographical Information System (PVGIS) [74]. The TMY is chosen because it represents an average meteorological year for a given location. The data set is constructed from hourly meteorological data of a time period of 10 years (2007-2016). The total radiation of each month in the data set is calculated, as well as the total radiation of each month summed for all recorded years. The most representative month (closest to the average radiation of the 10-year period) out of the whole period is chosen to represent that month. This way, the weather data still contains variability, e.g. caused by brief cloud covers or high peaks in radiation, but also takes into account annual fluctuation and filters out

abnormalities. Hence, it is a good prediction for modelling PV generation in combination with a BESS for which such temporal variability is crucial. Using TMY data also allows the application of the same solar power generation profile in the 2019 and 2030 simulation, since it is representative for data collected over a decade.

SAM generates a variety of technical and economic outputs of which the hourly AC yield is the variable required for the future system model.

Output PV Generation Model

The total annual energy yield from the carport PV system is expected to be 436,408 kWh for a TMY. The hourly DC power generation by the PV system along with the global horizontal irradiance (GHI) is shown in figure 4.2. The red line marks the installed capacity of the system, 464.64 kWp. The capacity factor is 10.7 %. The main characteristic outputs are summarized in table 4.5.

The monthly energy yield is shown in figure A.2 in appendix A.2.2. Both figures clearly show the seasonality of solar energy generation with up to seven times higher monthly energy yield in the summer compared to winter months.

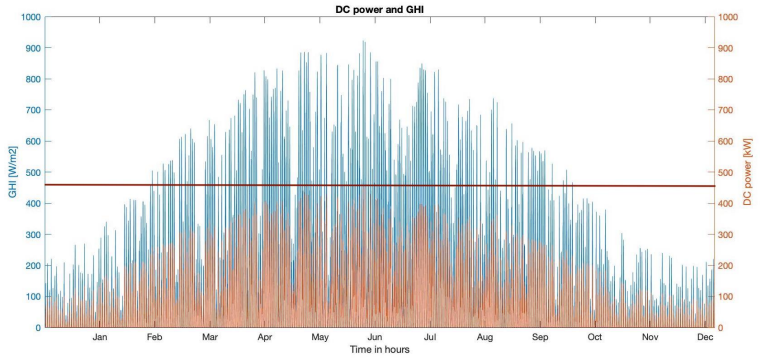

Figure 4.2: Hourly DC power generated by the PV system (orange), GHI (blue) and installed capacity marked in red.

The inter-daily fluctuation of solar power generation is shown in figure 4.3, which plots the DC yield for a week in June. The variability of the TMY weather data can be seen in, for example, the lower generation on Friday and the dips in generation during each day.

Table 4.5: Output of PV generation model

Parameter	Value
Annual energy yield	436.4 MWh
Capacity factor	10.7 %
Time-step	Hourly
Peak power	424.57 kW

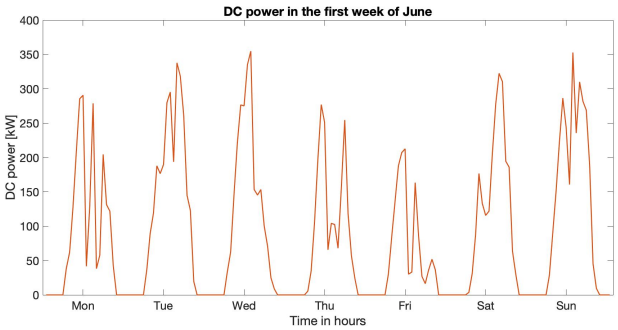

Figure 4.3: Hourly DC power generation by PV system in kW in the first week of June

4.3.2. Electricity System Model and Emission Factor

Current Carbon Emissions Assessment

The 2019 simulation makes use of the observed power plant dispatch EFs presented in sections 3.7.1 & 3.7.2 and, therefore, does not require the use of a model.

Future System Model

The future (2030) HEFs of Dutch utility grid electricity are determined by use of the Energy Transition Model (ETM) [75] and power plant specific carbon emissions. The ETM is a web-based, open-source, interactive tool

for energy modelling and scenario building of sector-coupled energy systems at country, region or city scales. This study models solely the electricity system of the Netherlands and, hence, utilizes only aspects of the ETM. The model determines the energy balance of a specified region from the required demand and available supply. It is demand-driven, meaning that a change in demand is met by adjustment of available controllable energy supply. Further description on how the ETM works, can be found in the online documentation of the tool [75] and the open-source code is shared on Github [76].

The model is based on assumptions about a future scenario and requires detailed inputs for all sectors. The tool has several existing scenarios using well-researched data inputs. However, none of the existing scenarios describe a realistic prediction for 2030 (most are modelled for 2050) and, therefore, a new scenario was developed. Nevertheless, some of the default inputs for 2030 were transferred. The basis for the majority of inputs is the *Klimaat- en Energieverkenning (KEV)* 2020 report [69] with moderate national adapted and proposed policy scenarios. The chosen geographical resolution is the Netherlands, in order to reach results comparable to the real-time HEFs, as described in section 3.7.2. The temporal resolution of the ETM is hourly. The input categories are demand, supply, flexibility and costs, each of them are described in the following. The ETM dashboard showing the electricity supply section, where inputs regarding installed conventional power plant capacity are made, is seen in figure 4.4.

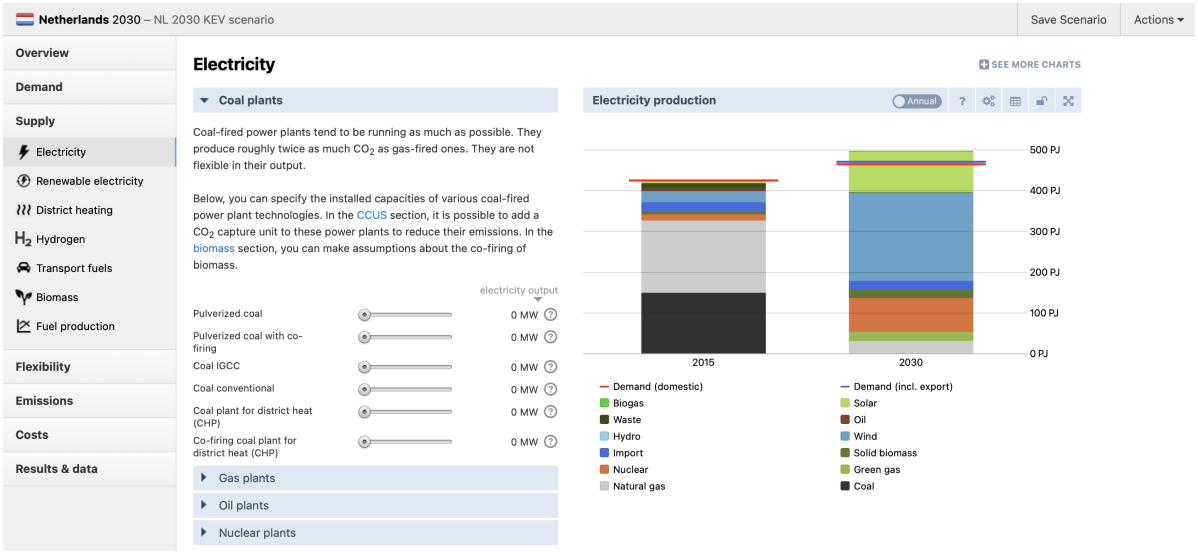

Figure 4.4: Dashboard of ETM showing installed capacity of coal power plants

The energy demand is grouped into households, buildings, transport, industry and agriculture. The biggest consuming sector is the built environment with buildings and households at 200 PJ, followed by industry at 131 PJ, agriculture at 40 PJ and electrified transportation at 20 PJ. Across sectors large-scale electrification of formerly fossil-fuel based processes is predicted, which increases electricity demand. However energy efficiency improvements dampen this increase. Additionally, installed rooftop PV at household decreases demand (and increases generation). Expected population and household increase are summarized in table 4.6, along with some other important inputs to the ETM. A Sankey diagram of the electricity supply and demand is seen in figure A.3 in appendix A.2.3.

Energy supply has various inputs, such as (renewable) electricity, fuels, biomass, carbon capture, utilisation and storage. For the purpose of determining HEFs in 2030, the model is limited to inputs relevant to electricity generation. Hence, the major inputs are the installed capacity of power plants. Over a third of installed capacity is predicted to be solar PV (43.6 %), followed by a quarter of on- and offshore wind (9.5 % and 19.2 % respectively) and less than a quarter of gas power plants (24.2 %). There is little nuclear power capacity installed, making up less than 1 % of the total. The remaining sources are biomass, hydro and waste power plants. Coal is assumed to be phased out by 2030. The installed capacities as predicted by the KEV report are shown in figure 4.5(a) and as modeled with the ETM in figure 4.5(b). The installed capacities are identical in both figures and can be seen in table A.2 in appendix A.2.4.

The flexibility sources of the system consists of grid-connected battery storage and electrolysers, storing inter-daily variability in RES.

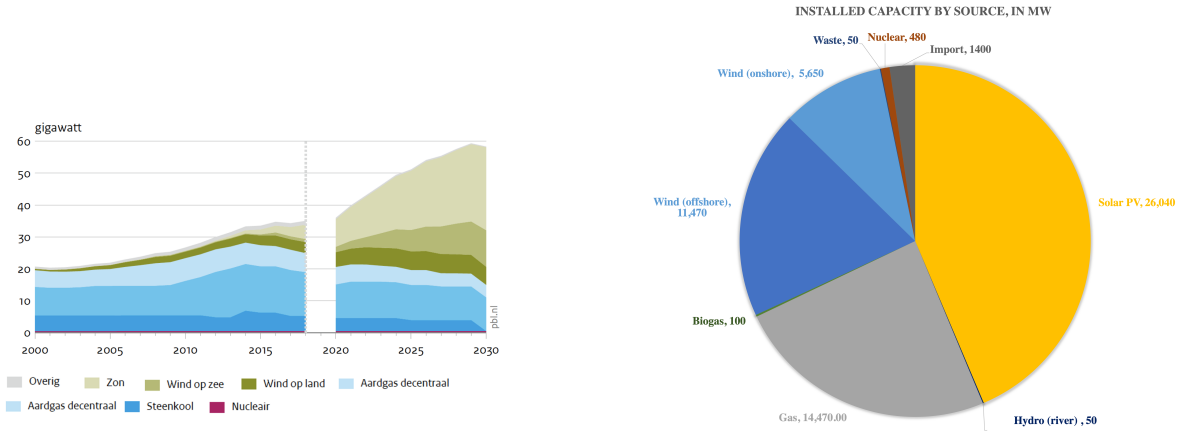

(a) Installed capacities according to KEV 2020 report [69]

(b) Installed capacities by power plant type in 2030

Figure 4.5: Installed capacities according to KEV report (a) and as adapted in ETM (b)

The most crucial costs inputs for modeling power plant dispatch are the marginal costs of power plants, hence fuel prices which are summarized in table 4.6.

Table 4.6: Significant input of ETM based on KEV 2020 [69]

Parameter	Input
Population	18.5 M
Residences	8.7 M
Natural gas price	18 €/MWh
Oil price	45 $/barrel
Coal price	84 $/tonne
Uranium price	69 €/kg

The output of the ETM is the hourly electricity generation by source for the year 2030. To determine HEFs, the emissions of the hourly varying electricity mix and total generation in one hour must be found. In a python script, the emissions for every generation source i for every hour t is found and denoted $F_{t,i}$, as described in equation 4.11.

$$F_{t,i} = \alpha_i E_{t,i} \tag{4.11}$$

Where $E_{t,i}$ is the energy produced in hour t by source i which is multiplied by the technology specific emission factor, α_i. Technology specific emissions are found in table A.3 in appendix A.2.4.

Once the contributions to total hourly emission by every source are found, the HEF for hour t are found by

$$HEF_t = \frac{\sum_{i=1}^{n} F_{t,i}}{\sum_{i=1}^{n} E_{t,i}} \quad . \tag{4.12}$$

Where the numerator is the sum of all emission, $F_{t,i}$, from all sources i in hour t. The denominator is the total electricity generation, $E_{t,i}$, in hour t, found by summing up the generation by n sources for each hour t. The HEF is found by dividing the total emissions from all sources in every hour by the total generation in that hour.

For verification, the AEF is found by

$$AEF = \frac{\sum_{t=1}^{8760} F_t}{\sum_{t=1}^{8760} E_t} \quad . \tag{4.13}$$

4.3.3. Electric Vehicle Load Model

This section explains the model developed to estimate the hourly energy demand from EVs charging at the carport in 2030. The model is based on observed charging behaviour data.

The energy demand caused by EV charging follows characteristic patterns throughout the day and week and can be classified into three locations: public, workplace and private. The Dutch (smart) charging infrastructure knowledge and innovation centre, ElaadNL, has collected data of real charging events for the three locations between 2018 and 2020 and provides various data analytics on charging behaviour for the Netherlands [77]. The relevant charging locations for this study are workplace and public charging, where the four charge points reserved for the municipality are assumed to follow workplace demand while the 12 public chargers follow the public pattern. The model uses three ElaadNL data sets, namely the distribution of arrival time on weekdays (Elaad data set 2), distribution of arrival time on weekends (Elaad data set 3) and the distribution of energy demand per charging event (Elaad data set 5). The data is provided in 15 minute time slots.

Figure 4.6(a) shows the the probability distribution for arrival times on weekdays and figure 4.6(b) displays the distribution of arrival times on weekends. There is no workplace data on weekends, as this is out of regular work hours, and the demand from the municipality charging station is set to zero for weekends.

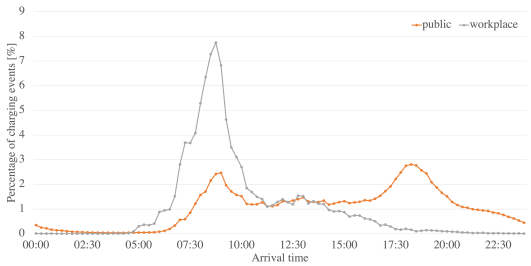

(a) Arrival time distribution on weekdays, data set 2 from [77]

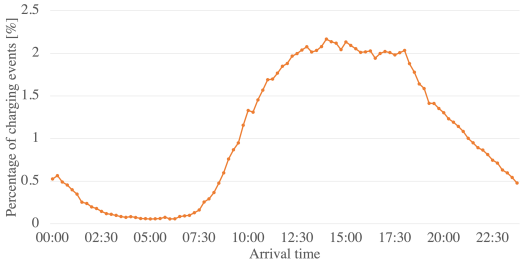

(b) Arrival time distribution on weekends, data set 3 from [77]

Figure 4.6: Arrival times during the week and on weekends

The distribution of energy demand per charging event for both locations can be seen in figure 4.7.

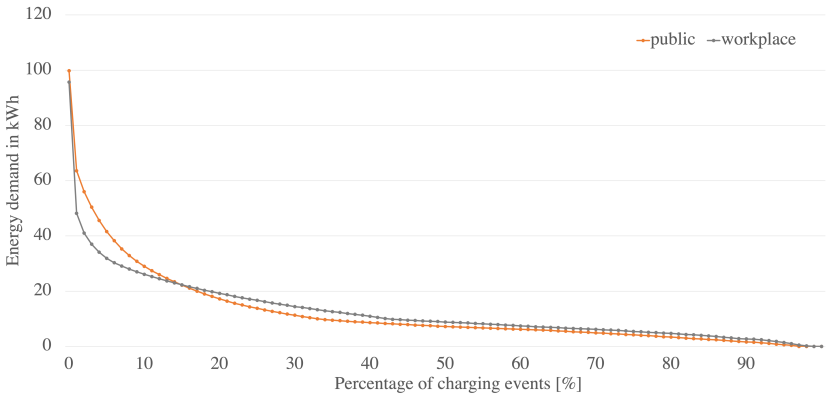

Figure 4.7: Distribution of energy demand, data set 5 from [77]

The model is developed in a python script and the data inputs are the above explained charging statistics. The first step is to create a dataframe with 16 columns, each representing one charge point / parking spot. The model iterates through every time slot, t, and first determines the occupation, O_t, of a parking spot. In order to do this, the probability for arrival, $p_{arrival}$, (data sets shown in figure 4.6) at time t is compared to a randomly drawn integer (0-100), χ_a. If the probability of arrival is higher than χ_a, the occupation is set to 1 (spot is occupied), otherwise occupation is 0 (spot is empty), as follows

$$O_t = \begin{cases} 1 & \text{if } p_{arrival,t} > \chi_a \\ 0 & \text{if } p_{arrival,t} \leq \chi_a \end{cases}. \tag{4.14}$$

Once an EV charges, the energy demand for that charging event at time t is determined using the probability, p_{demand}, for a certain energy demand, $E_{demand,t}$ (data set seen in figure 4.7). The probability is the amount of events observed demanding a certain quantity of energy which is drawn with a random choice out

of the discrete values of E_{demand} with p_{demand}. Next, the duration of the charging event, $t_{charge,t}$, is found by dividing the energy charged by the charging power, P_{charge}, as

$$t_{charge,t} = \frac{E_{demand,t}}{P_{charge}} \tag{4.15}$$

and the amount of time slots the car occupies the charger, denoted by s, is calculated through

$$s = 4 \cdot t_{charge,t} \ . \tag{4.16}$$

In the final step, the next s amount of time slots are set to occupied (1) and the corresponding energy demand, found by

$$E_{demand,s} = \frac{E_{demand,t}}{s} \tag{4.17}$$

is filled into the dataframe, while the last cell is filled with the remainder. Once a charger is freed again, the allocation of cars begins again.

The above described procedure is conducted five times with weekday and seven times with weekend data to create a representative weekly patterns. The left part of the flowchart seen in figure 4.8 portrays the method used to create the daily patterns.

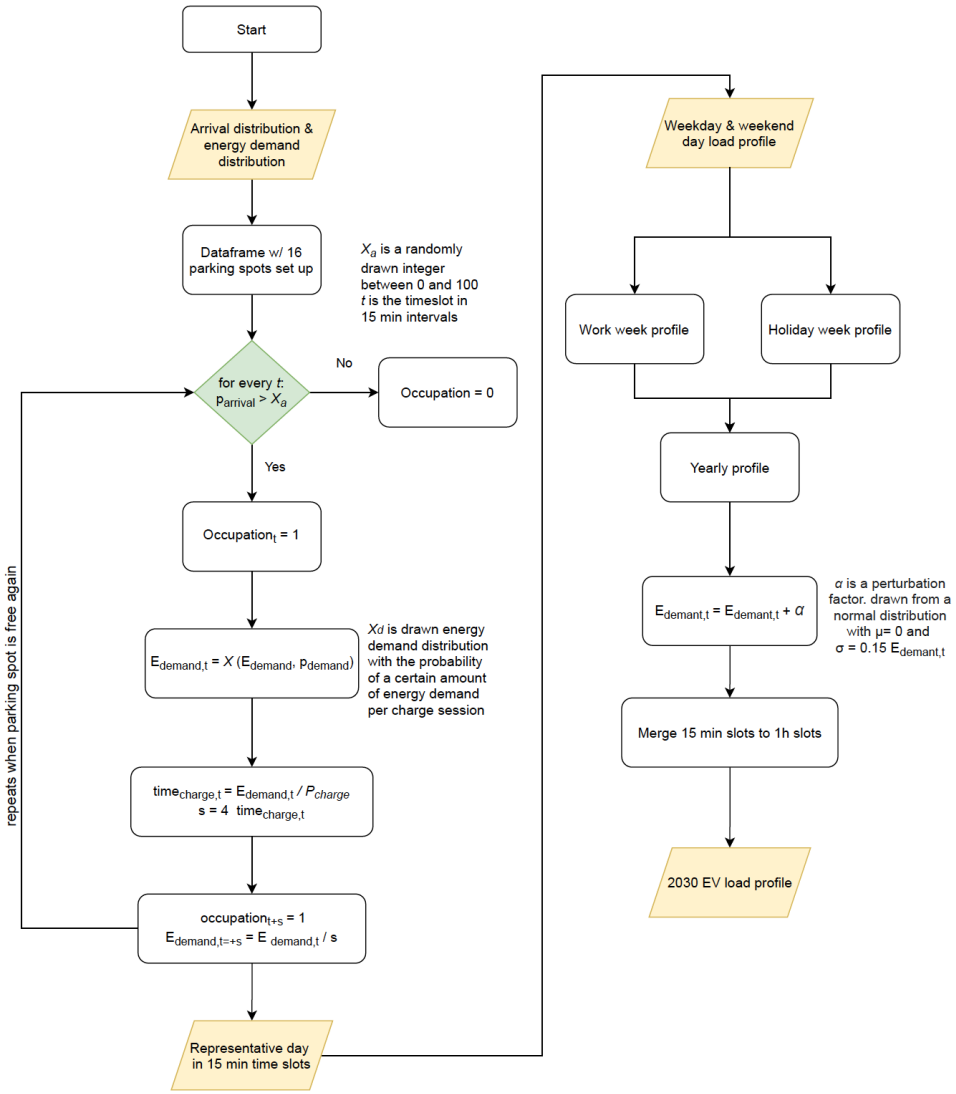

Figure 4.8: Flowchart of EV load model. Decisions shown in green and inputs and outputs shown in yellow.

A weekly pattern is built from the daily patterns. One weekly pattern presents a regular work week and consists of five workdays and two weekend days while the other weekly pattern presents a holiday week consisting of seven weekend days. A yearly profile is created by populating 52 weeks in the year with 48 work weeks and four holidays weeks. To introduce variability into the load profile, a jitter function is applied to each data point:

$$E_{jitter,t} = E_{demand,t} + \alpha \tag{4.18}$$

where α is a perturbation factor that is drawn from a normal distribution with a mean, μ, of 0 and a standard deviation, σ, of $0.15 \cdot E_{demand,t}$. Hence, the jitter function introduces variability with respect to energy demand per 15 minute time slot. To finalise the EV load profile, the 15 min time slots are summed over each hour to create the same hourly time structure as the PV energy generation and the HEFs. The right part of the flowchart in figure 4.8 shows how the annual profile is built from the daily EV demand profiles.

The profile is scaled for the year 2019 and 2030 as the EV adaption is expected to increase in the future. Currently, the project site-developers are expecting an annual EV charging demand of 35 MWh which the EV demand profile is scaled to.

4.3.4. Battery Model

This section explains how the battery model works. First, the kinetic battery model used to model the performance of the battery is described. Second, the logic of the energy management system is laid out.

Kinetic Battery Model

The applied battery model is the Kinetic Battery Model (KiBaM), developed by Manwell and McGowan [78], which allows for detailed modelling of battery voltage, State of Charge (SoC) and capacity (amongst other parameters) over time. The model is based on the chemical kinetic processes in the battery and simplifies them by applying a two-well principle, shown schematically in figure 4.9. The total battery charge is distributed over two wells: the available charge and bound charge well. The available charge supplies the load directly and the bound charge supplies the available charge well. Two valves regulate the charge flow in and out of the two wells, described by constants k and R_0, see figure 4.9. The valve between the available charge well and the load (characterised by R_0) determines the allowed (dis-) charging current, while the valve in between the two wells (characterised by k) determines how much of the total battery charge is available to the load at a moment in time.

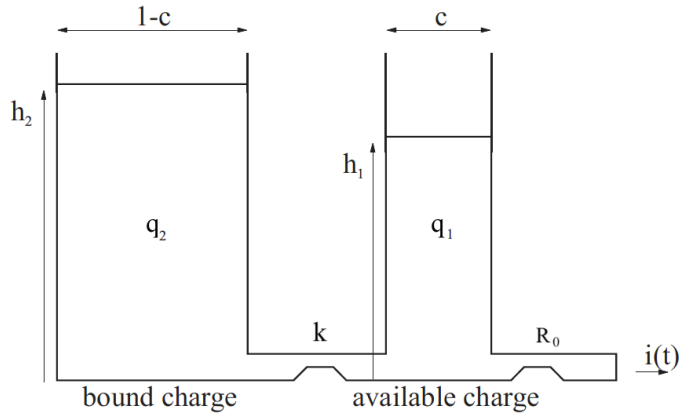

Figure 4.9: Two-well model schematic of the Kinetic Battery Model, figure adapted from [79]

Several parameters serve as inputs to the KiBaM and are determined in a python script based on characteristic parameters from the battery specification sheet [54] and charging and discharging behaviour of the NiMH batteries, as stated in [80]. All characterizing parameters for the battery system, consisting of six individual battery racks (see section 3.4 for battery configuration), are summarized in table 4.7.

The KiBaM calculates the battery voltage as a function of removed or added charge for each time step. Based on the demanded power by the load, P_{load}, the discharge current, I_d, is calculated as in equation 4.19 where V_{nom} is the nominal battery voltage.

Table 4.7: Battery model parameters for Nilar NiMH battery, inputs as required by the KiBaM

Parameter	Variable	Value
Fully charged internal voltage	E_0	645.12 V
Parameter reflecting initial linear variation of voltage and SoC	A	-0.3
Parameter reflecting decrease of battery voltage during progressive discharging	C	-0.9
Maximum discharge capacity	D	600 Ah
Conductance of valve between bound and available charge	k	5
Ratio of maximum capacity that is available for discharge	c	1
Maximum capacity	q_{max}	600 Ah
Internal battery resistance	R_0	0.056 Ω
Time step	t	1 h
Nominal battery voltage	V_{nom}	576 V

$$I_d = \frac{P_{load}}{V_{nom}} \tag{4.19}$$

$$I_c = \frac{P_{avail}}{V_{nom}} \tag{4.20}$$

The maximum allowed charge current, $I_{d,max}$, of the battery is found at the beginning of each time step. The obtained charging current, I_B, is then determined by identifying the limiting discharge current through

$$I_B = \min(I_{inverter}, I_d, I_{d,max}) \tag{4.21}$$

where $I_{inverter}$ is the maximum allowed current of the inverter.

Similarly, the maximum allowed charging current, $I_{c,max}$, is found at the start of each time step, based on the battery's availability to absorb charge. Also, the current available to charge the battery, I_c, based on the available power, P_{avail} is found through equation 4.20. Then, the attained charging current, I_B, is set by identification of the smallest allowed current (absolute value), as follows

$$I_B = \min(|I_{inverter}|, |I_c|, |I_{c,max}|) \ . \tag{4.22}$$

From the charge or discharge current, the battery charge, SoC, change in SoC and battery voltage at the end of each time step are found. These serve as inputs for the next time step, which is done for the whole year to simulate the battery behaviour throughout the year.

The desired output is power in- and output of the BESS, therefore, the battery power is found by multiplication of battery current and voltage, as follows

$$P_B = I_B \cdot V_B. \tag{4.23}$$

Energy Management System

The operation of the battery is dependent on the power generated from the PV system and power demanded by EV charging. In reality the consumption from the municipality building also affects the battery operation, however energy exchange with the municipality building is seen as out of the system boundary and, therefore, seen as grid exports as defined in section 3.1. The application of the battery follows a battery logic that determines the amount of power entering and leaving the BESS and the power exchange with the grid. Depending on whether there is solar power generation and EV charging demand and which is larger, the power charged and discharged from the BESS is found, as presented in the flowchart in figure 4.10. Inputs and outputs are shown in yellow while decisions are shown in green in figure 4.10.

When solar PV generation is positive and EV demand is lower than solar generation the remaining battery capacity at time step t is checked and the remainder of PV power minus EV demand is charged to the battery. If not all remaining power can be added to the battery, e.g. due to inverter limits or insufficient remaining charge capacity, it is exported to the grid. When the EV demand exceeds solar generation and there is remaining charge in the BESS, the demand that is not satisfied by PV generation is met by the battery. If the available battery charge is not sufficient, the remaining EV demand is met by grid imports. When there is no PV generation and no EV charging, the BESS is inactive and no grid exchange is required. When there is EV demand with no or insufficient PV production, the demand is first met by the BESS (as long as there is sufficient charge available) and, if required, by grid imports as a second priority.

The KiBaM and the described logic are implemented in a python script which is simulated for the years 2019 and 2030 (8760 hours each). The output is the energy charged and discharged by the battery, E_t^B, for

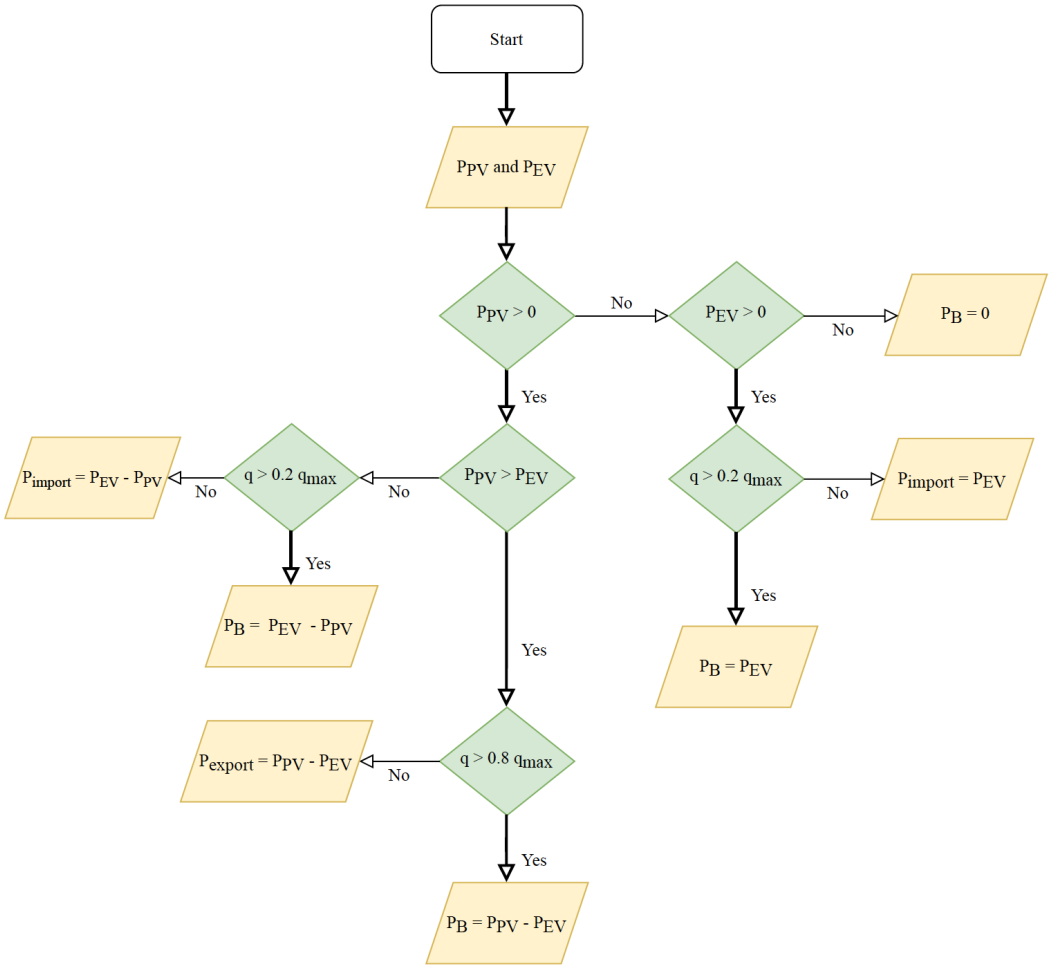

Figure 4.10: Flowchart of battery model logic. Inputs and outputs shown in yellow, decisions shown in green.

each hour, t, of the year. Together with the hourly PV generation and EV load found in sections 4.3.1 and 4.3.3 respectively, the energy flows in the system can be determined in the next step, as explained in section 4.2.3.

5

Results & Discussion

This chapter presents the results of the solar carport system model in section 5.1. The different carbon accounting methods applied in this research along with varying emission factors are compared in section 5.2. Section 5.3 gives answers to all four research questions and summarizes the carbon (offset) emission assessment results for all simulated scenarios. Life cycle emissions of the solar carport are analysed and compared to the achieved carbon offsets in section 5.4. Section 5.5 discusses the limitations of the presented work.

5.1. Solar Carport System Model

This section presents the estimated electricity generation and HEFs in 2030 in section 5.1.1. Section 5.1.2 presents the modeled EV demand pattern for 2019 and 2030 and section 5.1.3 presents the expected battery operation. The outputs of these models serve as the basis to determine the energy flows within the system, which are presented for some representative days in section 5.1.4.

5.1.1. Future System Model and Emission Factor

The total annual electricity generation according to the developed energy system model for 2030 amounts to 136.16 TWh, based on the installed capacities described in figure 4.5, section 4.3.2. For comparison, the Dutch electricity generation in 2019 was 121.35 TWh [81]. As large-scale electrification is a key element of the future system model such a generation increase, due to increase in demand, is expected. The output of the ETM is the hourly electricity generation which can be seen in figure 5.1. The figure shows a lower base

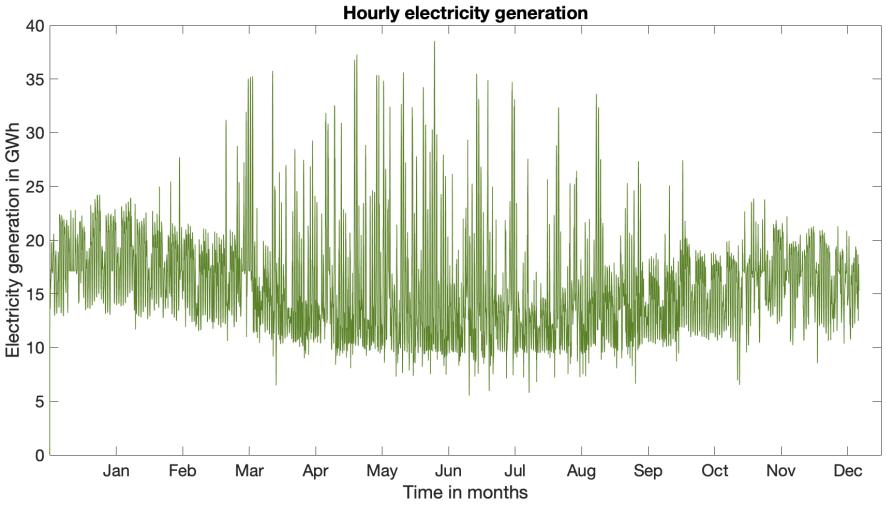

Figure 5.1: Hourly utility grid electricity generation 2030 modeled with ETM

demand over the summer months compared to winter, as heating and lighting demand is lower. At the same

time, it can be seen that there are higher peaks in the summer which is unusual for today's energy system (currently the largest peaks are seen in winter). This is caused by the large amount of solar energy capacity (43.6 % of total installed capacity, see section 4.3.2) that is not controllable and produces large amounts of energy on summer days with high irradiation.

The HEFs found from the hourly electricity generation are shown in figure 5.2 for the year 2030. It can be seen that the HEFs are in a range between 15 g CO_2eq/kWh and 368 g CO_2eq/kWh throughout the year. The HEF is never zero, because all generation technologies have non-zero carbon intensities (see table A.3 in appendix A.2.4) and generation is never zero. The mean value of HEFs is 136.9 gCO_2eq/kWh for the year 2030.

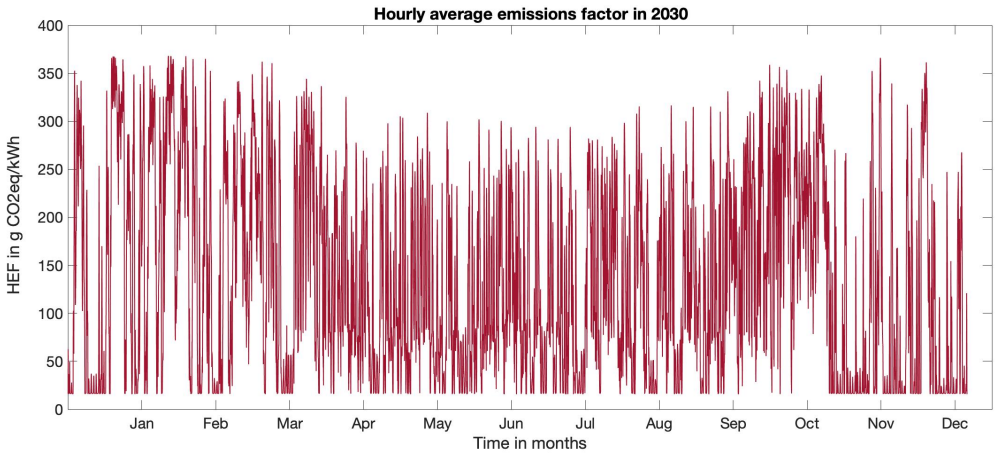

Figure 5.2: Hourly average emission factor in g CO_2eq/kWh in 2030

Figure 5.3 shows the monthly mean of HEFs for 2030. It can be seen that HEFs decrease in the summer (May to September), which is due to increased solar energy generation with low emissions. HEFs are low in November and December, which can be explained by higher wind generation as wind speeds increase in the winter weeks. In the intermediate seasons, spring and autumn, HEFs increase as neither solar nor wind resources are at their peak and gas powered plants cover demand more frequently.

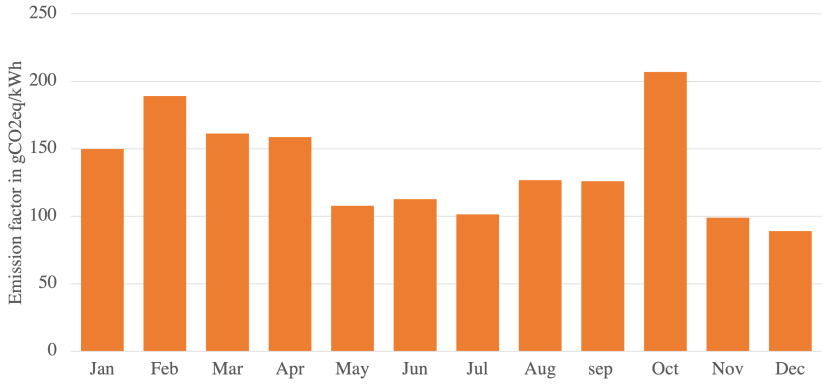

Figure 5.3: Monthly mean of HEFs in 2030

HEFs are shown with a higher temporal resolution in figure 5.4 for the first week of June in 2030. There is a characteristic inter-daily fluctuation seen in HEFs throughout the week. As shown in figure 5.4, emissions drop during night when electricity demand decreases and demand is covered by an increase generation of wind energy as wind speeds usually increase at night. During the day, typically two peaks can be seen, which coincide with increased power demand in the morning (7-11 am) and in the late afternoon/evening (5-9 pm). This increase in HEFs is caused by high-emitting gas power plants covering the peak demand that cannot be satisfied by RES and must-run power plants. Nevertheless, this characteristic pattern is often distorted as a result of the high share of uncontrollable RES and variations in weather conditions.

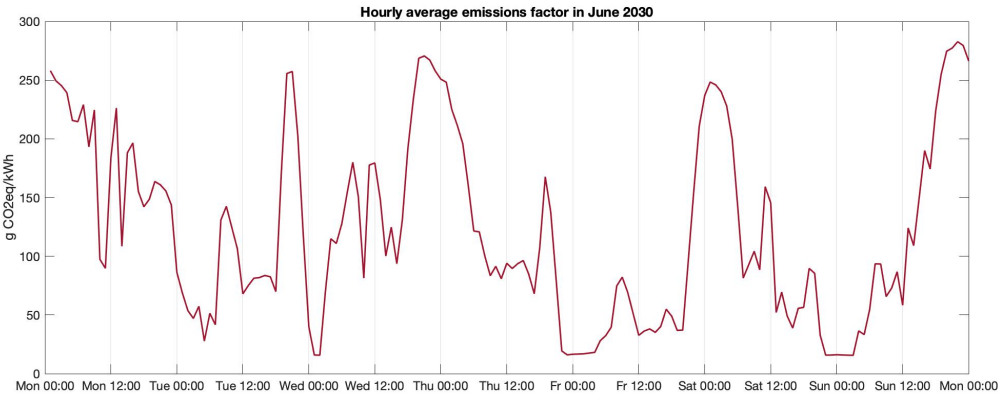

Figure 5.4: Hourly average emission factor during the first week of July in g CO_2eq/kWh in 2030

Figure 5.5 shows HEFs in the first week of December 2030. In winter, HEFs have higher variability than in summer. Due to high wind generation, HEFs are generally low, especially at night. However, at times with lower wind speeds, emissions increase significantly as gas powered plants increase their generation and solar generation is low.

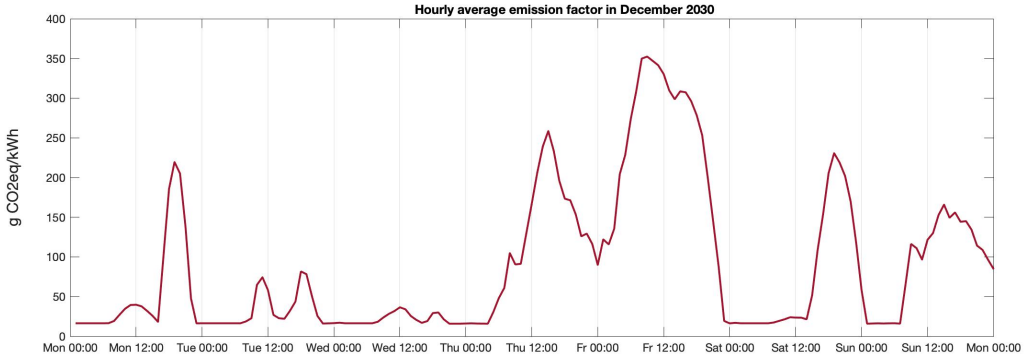

Figure 5.5: Hourly average emission factor during the first week of December in g CO_2eq/kWh in 2030

Verification Future Energy System Model

To verify the output of the future energy system model, the annual emission factor of 136.9 gCO_2eq/kWh found with the developed model is compared to predictions in the KEV report. The AEF stated in the KEV report is 14 % lower, at 120 g CO_2eq/kWh (following the integral method, see pg. 181 in [69]). A slightly increased AEF compared to the KEV value is found to be acceptable because government climate policies have shown to be ambitious and have not always been accomplished in the past. Hence, it is a likely assumption that EFs will be slightly higher in the future.

For further verification, the found emissions factor is compared with a recently published independent research. Hamels [82] develops and applies a detailed unit commitment economic dispatch model for the European electricity system using flow-tracing techniques to determine European emission factors based on power plant dispatch at an hourly timestep. They model the years 2025 and 2040 and find average consumption-based emission factors of 240 gCO_2eq/kWh and 60 gCO_2eq/kWh for the Netherlands for the respective years. Hence, the 2030 AEF will lie in the range of 60 - 240 gCO_2eq/kWh and, assuming a linear decrease, be around 180 gCO_2eq/kWh in 2030. It is concluded that the determined AEF of 136.9 gCO_2eq/kWh lies within an acceptable range of both the estimates in [69] and [82].

5.1.2. Electric Vehicle Demand Profile

The representative pattern for a regular working week as estimated with the developed EV demand model (in section 4.3.3) is shown in figure 5.6 and the representative holiday week is shown in figure 5.7. Figure 5.6 clearly shows the lower energy demand on weekends, due to less employees and visitors at the municipality building. Additionally, it can be seen that demand is low during night and peaks in the mornings as expected following the probability distribution in figure 4.6(a) in section 4.3.3. Often a second peak can be seen in the afternoon, following the underlying probability distribution. The weekly patterns are the same for the simulations in 2019 and 2030, the magnitudes of energy demand are solely scaled to the expected annual charging demand. Figures 5.6 and 5.7 show the magnitudes found for the 2030 demand, the 2019 demand profile is scaled to a total annual demand of 35 MWh.

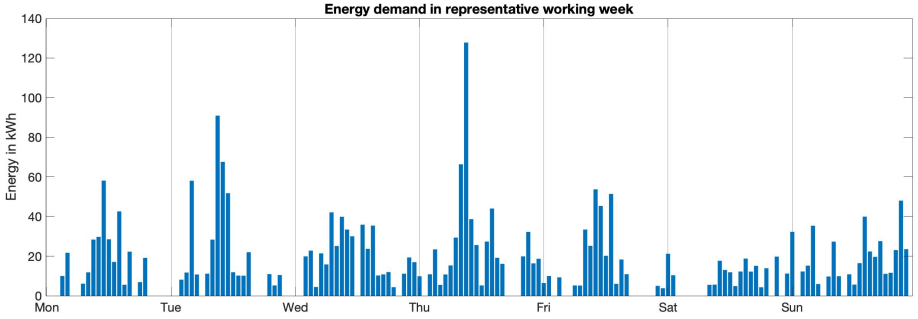

Figure 5.6: Energy demand EVs during representative work week in 2030, ticks and grid lines mark midnight

The peak demand in the holiday week profile (figure 5.7) is shifted further back within the day to about 12 - 6 pm. Generally, there is more variation in the holiday week profile because there is a large range of arrival times with significantly higher, but still low probabilities of arrival. This is also due to the fact that it is more difficult to predict and characterise public charging.

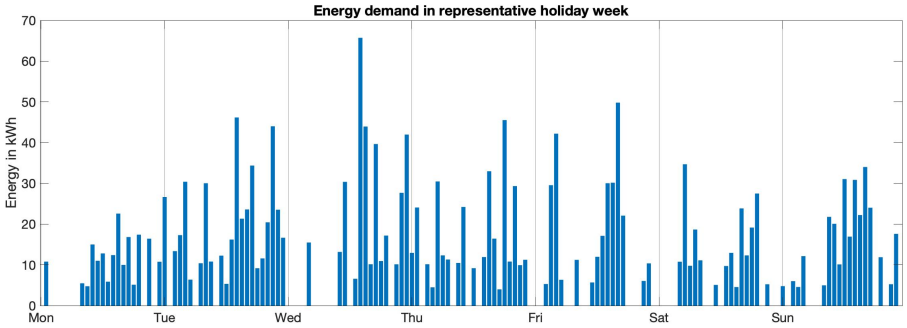

Figure 5.7: Energy demand EVs during holiday week in 2030, ticks and grid lines mark midnight

In 2019, the daily energy demand from EVs is 6 kWh per charge point and 95 kWh for all charge points together. The total annual demand are 35 MWh accumulated for all charging stations. The accumulated average daily energy demand of one EV charging station at the solar carport in 2030 is 23.1 kWh. This amounts to an annual demand of 8.43 MWh for each of the 16 charging points. The total annual energy demand from EVs charging at the 16 charge points is 135 MWh in 2030 and the total average daily demand is 368.5 kWh.

Verification EV Charging Demand

To validate the model results, the output is compared with expert EV demand predictions. The Netherlands Knowledge Platform for Charging Infrastructure (NKL) estimates demand of 9.9 kWh/day for one 11 kW charging station, acknowledging a 50 % growth potential to 15 kWh/day by 2030, in their *Public Charging Benchmark report* [70]. The installed chargers at the solar carport can deliver double the power of the benchmark report of up to 22 kW, depending on how many cars are charging at one charging station. As laid out in section 3.5, the max power for the Alfen charging station is 44 kW and max power for each charge point is 22 kW. Hence, when two cars charge concurrently, both can receive max power. When three or four cars

occupy the charging station, each receives 15 kW or 11 kW respectively. The occupancy of the car park is 2.8 cars on average for the hours in which cars are charging (most night hours are excluded) in 2030. Therefore, the average power can be assumed to be 15 kW. Adjusting for the larger power supply and up to a 50 % growth potential, the daily demand can be expected at about 21 kWh for the charger type used at the solar carport. Figure 5.8 shows the predicted EV demand from the model (in grey) compared to the estimates in NKL report. The blue bar shows the predicted daily demand for an 11 kW station, the orange bar adjusts for a power of 15 kW and the green bar represents the potential 50 % growth. The error bar represent the range of the estimated value based on which assumption is taken. The minimum and maximum of the error entails 50 % growth scenario for 11 kW and 22 kW average power respectively and present a possible EV demand range between 15 to 30 kWh per day.

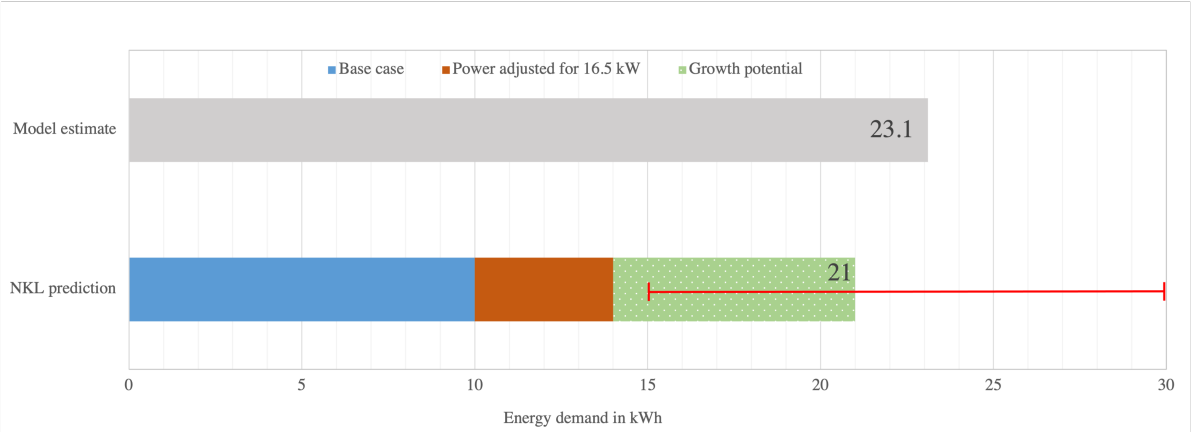

Figure 5.8: Estimated EV demand from EV demand model compared to NKL report predictions for 2030

The energy demand estimated by the model described in section 4.3.3 of 23.1 kWh/day is very close to the adjusted NKL prediction of 21 kWh/day. It lies well in the range of 15 - 30 kWh/day and, hence, it is concluded that the EV load model is a good estimation for demand in 2030. The EV charging demand in 2019 is scaled to estimates of project partners of the PowerParking project and assumed to be accurate. Further future investigations on the system should verify this number with actual recorded charging data.

5.1.3. Battery Operation

The annual profiles for PV generation, hourly EFs and EV demand, described in sections 4.3.1, 5.1.1 and 5.1.2 respectively, are used as the basis for the battery simulation, see methodology in section 4.3.4. A very important parameter in battery operation is the SoC, which is shown for base scenario in 2030 in figure 5.9. The battery SoC limits of 20 - 80 % can clearly be seen, as the SoC never exceeds these limits. Figure 5.9 shows that the battery is rarely discharged to less than 50 % in the months between March to September, but is well utilized in the winter months between October and February. This is caused by the significantly higher PV generation (up to a factor of seven) in the summer. The BESS stores the residual (not consumed by EVs) solar energy in the summer months and is, simultaneously, not required to discharge energy as often because EV demand is covered by PV directly for the majority of the time. Hence, the SoC of the BESS is often high and is never discharged fully. The sizing of the BESS is better adapted for winter months, assuming the goal of the BESS is increasing self-consumption. Here, additional solar energy is actually stored in the BESS during the day and discharged for EV demand in the evening and night hours. This can be seen in figure A.5 in appendix A.3.1 where the BESS SoC is shown for one week in winter and figure A.6 in appendix A.3.1 shows the SoC for one week in the summer.

The SoC for 2019 is shown in figure A.4 in appendix A.3.1. The BESS is used less in 2019 than in 2030 and the SoC rarely drops below 60 % in winter and 70 % in summer. The difference to the year 2030 in terms of battery utilization can be explained by the lower EV demand in 2019. Accordingly, the BESS does not get discharged deeply and is charged again quickly from the large PV system.

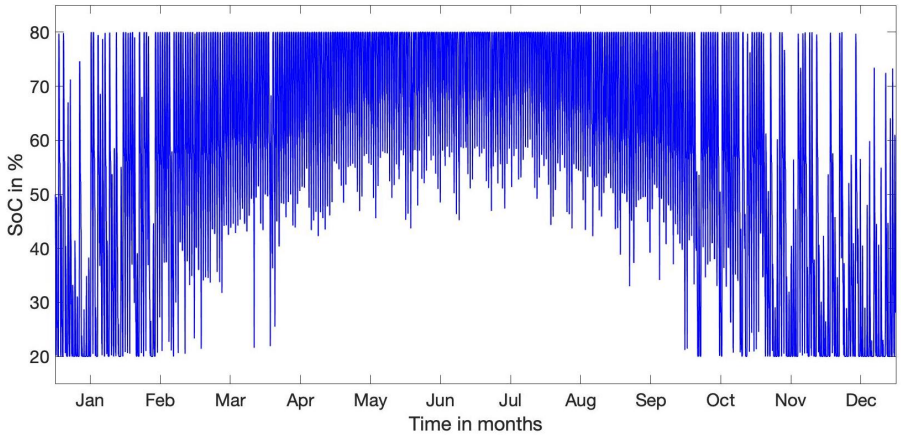

Figure 5.9: SoC of BESS in base scenario in 2030

The result of the BESS often being fully charged in the summer are increased power exports to the electricity grid, as seen in blue in figure 5.10 for 2030. All of the solar energy that cannot be stored, is exported to the grid. The total annual exports to the grid amount to 401 MWh and 309 MWh in 2019 and 2030, respectively. This is over 90 % of total PV generation in 2019 and about 70% of total PV generation in 2030. 3.5 % and 11% of solar generation is stored in the battery in 2019 and 2030. The remaining relief on the grid, i.e. avoided exports, is due to directly charging EVs from PV. This way, the battery system does not alleviate grid capacity constraints significantly for exports. Additionally, large grid exports are unfavorable for increasing self-consumption, however, it can be beneficial when examining offset CO_2 emissions, as all exported electricity substitutes the marginal operating plant and, hence, offsets marginal grid emissions. On the contrary, the system requires some grid imports in the winter months at times when the BESS is fully discharged. However, the annual grid imports are relatively low at 0.2 MWh and 18.4 MWh in the base cases in 2019 and 2030, respectively. This is 0.6 % of total EV demand in 2019 and 13.4 % of demand in 2030.

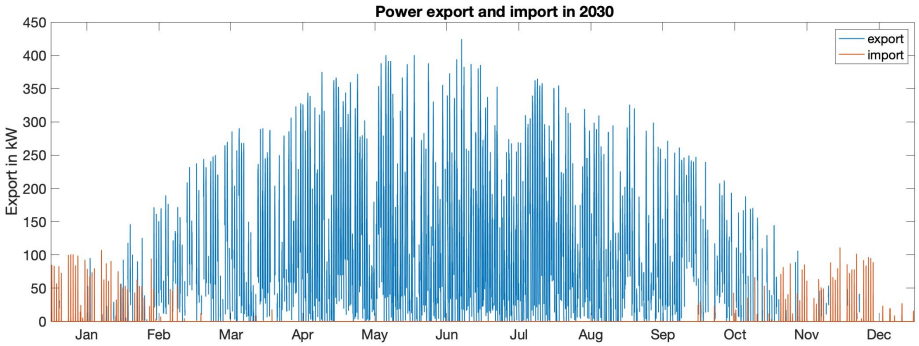

Figure 5.10: Grid exchange of BESS in 2030, exports shown in blue and imports shown in orange

The power flows of the crucial system components are shown for four days across seasons in 2030 in figure 5.11. The PV generation and EV demand are the result of the PV model and EV demand model, while the battery power and grid exchange is the output of the battery model. Negative values show power extraction from the system (consumption & exports) and positive power flows show power injection into the system (generation & imports), see section 4.2 for the definition. The corresponding battery SoC for the same days are shown in figure A.7 in appendix A.3.1.

Each individual figure shows that there is a balance of power flows at all times, i.e. positive and negative power flows balance each other. Hence, a certain EV demand is met by either solar generation, imports or a combination of both. Similarly, solar generation must either be consumed by EVs, charged by the battery or exported to the grid.

Figure 5.11(a) shows a winter day, on which the battery can satisfy EV demand in the early morning hours (without solar generation). Once PV generation increases, the BESS begins to charge and is quickly fully charged (10 am) when solar generation begins to be exported to the grid. The figure also nicely shows how

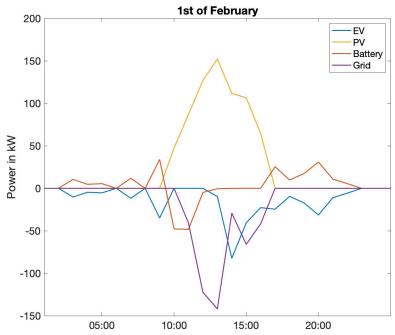

(a) Activities of system components on the 1st of February

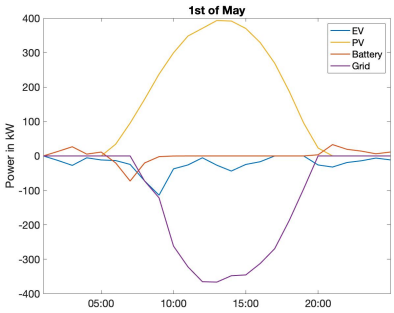

(b) Activities of system components on the 1st of May

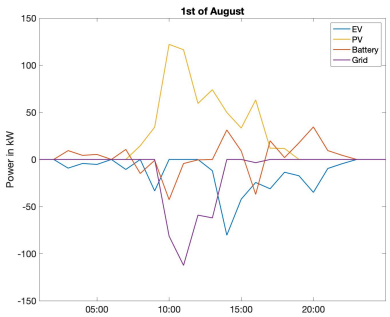

(c) Activities of system components on the 1st of August

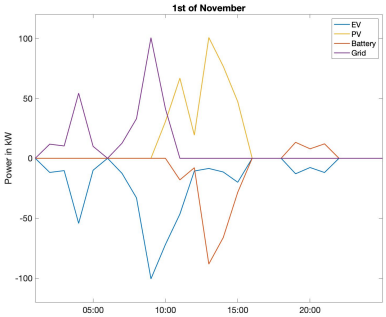

(d) Activities of system components on the 1st of November

Figure 5.11: EV demand, PV generation, battery power and grid exchange on different days throughout the year 2030, in kW

grid imports decrease in the afternoon around 3 pm when EV demand increases and solar generation is used to charge the vehicles directly. As the BESS is fully charged in the evening, EV demand at night is, again, covered by the BESS.

PV generation increases significantly in the spring, as seen in figure 5.11(b) showing the 1st of May. Again, the BESS is fully charged very quickly and the large majority of solar generation is exported to the grid.

A cloudy summer day is shown in figure 5.11(c) where solar generation is relatively low and the BESS can be well utilized to store solar energy and also satisfy EV demand. The battery power is positive in the early morning hours to cover EV demand and used to store solar generation around 10 am. In the afternoon cloud covers and high EV demand coincide and the battery is discharging to cover EV demand. This can also be seen in the oscillations in SoC, see figure A.7(c) in appendix A.3.1. Such high utilization of the BESS increases self-consumption of the system and alleviate grid capacity constraints.

The effect of high EV demand and low solar generation concurring can be examined in figure 5.11(d). EV demand is covered by grid imports during the first half of the day and once the PV system starts generating power, it is stored in the BESS which then supplies EV demand in the evening / night.

5.1.4. Energy Flows & Model Verification

Once the activity of each system component has been established, the energy flows within the system, as required for the emissions assessment is conducted, according to the methodology laid out in section 4.2.3. Figure 5.12(a) and 5.12(b) show the power flows from the PV generation to the load, battery and grid for a winter and a summer day in 2030, respectively. Naturally, all power produced must be delivered to one of the three components and the sum of them always add up to the total solar power. Figure 5.12(a) shows that the solar energy is first used to charge the BESS and once that is fully charged, is exported to the grid and/or used to charge EVs. Figure 5.12(b) shows moments when solar power is supplied to the load, battery and grid at the same time (e.g. 3 pm).

It is seen that the BESS is fully charged after only a few hours of solar generation, both in winter and in summer. Combining this with the characteristic pattern of MEFs and HEFs (seen in figure 5.4 and 5.5), it

is concluded that shifting the charging of the BESS (from the PV system) to hours with a low grid CI would achieve the highest emission mitigation. The solar energy can be exported when the electricity CI is high and mitigate more emissions. Therefore, a BMS with information about the current MEFs (or HEFs) would yield the best results in terms of carbon offsets.

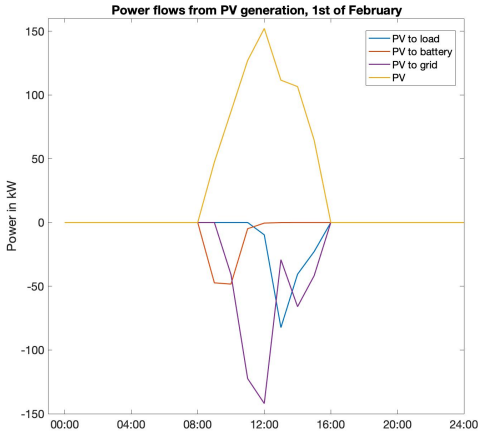

(a) Power flows from PV generation on 1st of February

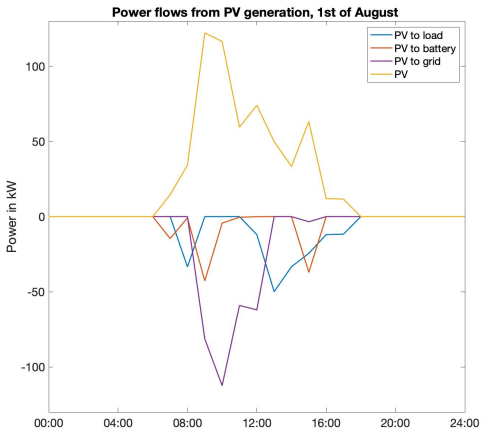

(b) Power flows from PV generation on 1st of August

Figure 5.12: Estimated power flows from PV generation on the 1st of February and the 1st of August 2030

The power flows into and out of the battery are shown in figures 5.13(a) and 5.13(b). Here, the battery power must match either the power flow into the battery (PV generation) when charging or out of the battery (EV demand) when discharging. The sign of the battery in figures 5.13(a) and 5.13(b) is negative for charging and positive when discharging. Accordingly, on the 1st of February, a large peak in power charged from the PV modules is met with a peak of the same magnitude in battery power at 9-10 am.

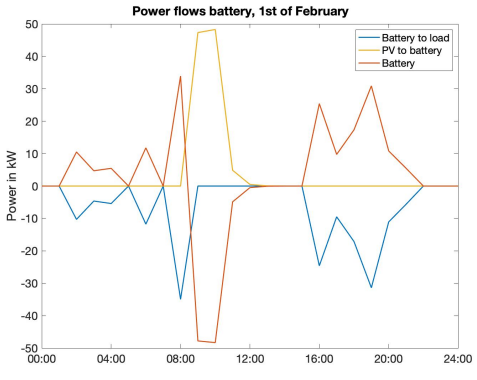

(a) Power flows from battery on 1st of February

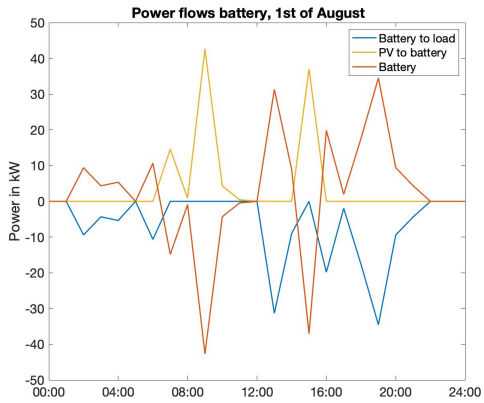

(b) Power flows from battery on 1st of August

Figure 5.13: Estimated power flows in and out of battery on the 1st of February and the 1st of August 2030

Based on the determined power flows for each hour of the years 2019 and 2030, the emissions assessment can be conducted with its results presented in the next section 5.3.

5.2. Carbon Accounting Methodology Comparison

5.2.1. Comparison Between Marginal and Hourly Average Emission Factors

For the year 2019, hourly data for both MEFs and HEFs based on observed power plant dispatch is available. The average value of MEFs in 2019 was 605.58 gCO_2eq/kWh, compared to an average HEF (i.e. AEF) of 465.13 gCO_2eq/kWh. Thus, MEFs are generally higher than HEFs which is caused by the nature of the merit order of

power plants. Low-carbon technologies, i.e. renewables, have the lowest marginal costs and are the first to be dispatched. However, because installed RES (and nuclear) capacities are not sufficient to satisfy demand in 2019, coal and gas plants are usually the marginal operating plant and, therefore, determine the magnitude of MEFs. An exemplary merit order curve is seen in figure A.8 in appendix A.3.2 which visualizes this. Additionally, must-run power plants often do not have ramping ability which particularly gas power plants can offer, making them suitable to satisfy marginal demand. Due to the fact that marginal emissions of gas (and coal) plants are higher (see table A.3 in appendix A.2.4), MEFs are on average 30.2 % higher than HEFs. Evidently, the contribution of low-emission technologies, especially RES, to HEFs reduces their magnitude.

MEFs have relatively little variation in 2019 and stay within a narrow range between 555.2 - 690.3 gCO_2eq/kWh. While HEFs have larger variety between 256.0 - 618.6 gCO_2eq/kWh. This is because HEFs are strongly dependent on the amount of RES generating electricity at a certain moment in time, which is combined with considerable variability in RES, causing this large fluctuation in HEFs. Low-emission technologies are never on the margin in 2019. The maximum share of RES during the whole year is 74.3 % and the average share is 22.5 % in 2019. When there are high volumes of RES, the supply curve shifts to the right and, hence, shifts the marginal plant technology between various coal and natural gas plants. These plants may vary in their efficiencies and specific technology and thereby cause the small variations in MEFs.

The average of HEFs in 2030, i.e. the AEF, is 136.9 gCO_2eq/kWh, with a range between 15 - 368 gCO_2eq/kWh, as mentioned in section 5.1.1 and seen in figure 5.2. Average HEFs show a decrease of roughly 70 % in 2030 compared to 2019. This is as expected due to the higher share in RES in 2030. The large variation in HEFs seen in the 2019 data can also be seen in the modeled HEFs in 2030, see figure 5.14. Again, this is due to the strong dependence of HEFs on RES shares combined with high variability in renewable electricity generation.

Seasonal and Hourly Variability

As part of the conclusion of the literature review, it is expected that electricity emission factors display temporal variability. To investigate whether this assumption is correct for the data applied in the simulations, the observed EF data from 2019 is analysed.

Figure 5.14 shows the annual profiles of both EFs in 2019. To compare seasonal deviations, the monthly averages are compared. In January, the monthly average of HEFs is 519.4 gCO_2eq/kWh, while the average in August is 414.7 gCO_2eq/kWh. These are the two most extreme months in terms of monthly average HEF. The seasonal change in average monthly HEFs between winter (Dec-Feb) and summer (Jun-Aug) is a 14.3 % decrease in summer compared to winter. Therefore, it can be concluded that there is considerable seasonal variability in HEFs and including information on such variability in emissions accounting enhances the accuracy of its results. The seasonal variability in MEF is insignificant, which can be seen in the orange line in the graph in figure 5.14 staying rather constant at around 600 gCO_2eq/kWh. This is expected to be similar in comparable climates, but cannot be generalized for countries in different climates.

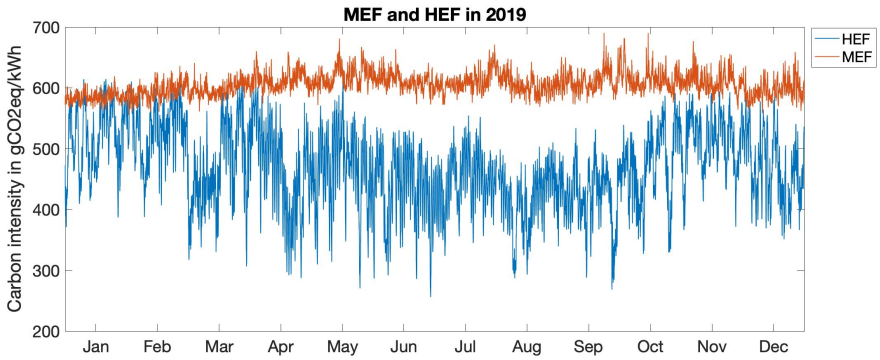

Figure 5.14: Annual profile of MEF and HEF in 2019 based on observed power dispatch data (data source: [66])

The hourly variability is very significant in HEFs. Changes of up to 362.6 gCO_2eq/kWh are observed, hence HEFs can be more than doubled, or halved, in consecutive hours of the day. The deviation from the AEF can be a decrease of up to 45% and an increase of up to 33 %. Undoubtedly, this has large consequences on the results of emissions calculations and should, therefore, be considered instead of an AEF.

Even though seasonal variability is low for MEFs in the Netherlands, their hourly change is up to 24.3 %, i.e. they can change by up to 135.1 gCO_2eq/kWh.

From this, valuable consequences can be drawn, not only for more accurate emissions accounting, but also for emissions mitigation efforts when scheduling flexible loads. Recognizing inter-daily patterns and developing algorithms and control strategies based on time-dependent MEFs or HEFs is expected to lead to increased mitigation of carbon emissions. To conclude, due to the observed hourly variability in carbon intensities it is more accurate to apply hourly data in carbon emissions assessments, confirming the conclusions of the literature review.

Implications of using HEFs instead of MEFs

The future system model does not predict MEFs in 2030 due to potentially high inaccuracies, as laid out in section 2.2.4. However, it is seen as conceptually more accurate to use MEFs for carbon offset calculations and, hence, it is necessary to evaluate the deviation between MEFs and HEFs.

Based on the relationship of MEF and HEF in 2019 (MEF 30.2 % higher than HEF), the average value of MEFs in 2030 can be expected at 180.71 gCO_2/kWh. However, there is uncertainty in assuming that the relationship of HEF and MEF is the same in 2030 as 2019. In order to validate this relationship, the merit order curve in 2030 together with the load factor of certain power plants is examined. The load factor (or capacity factor) is the actual power output in a year divided by the theoretical maximum output in a year of a power plant. Figure 5.15 shows the underlying merit order of installed capacities in 2030 as modelled using the ETM.

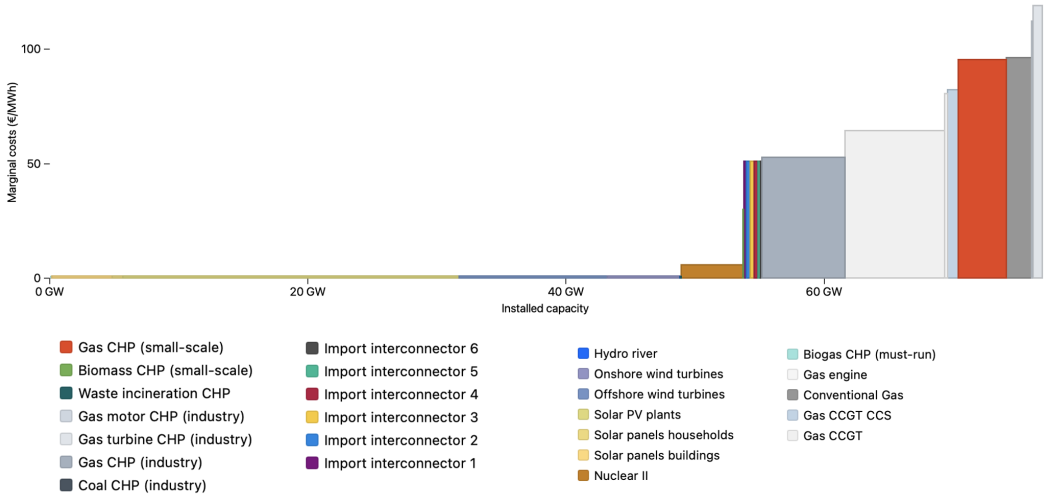

Figure 5.15: Merit order or installed capacities in 2030 from ETM

Gas CHP plants (dark grey) have a load factor of 28.3 % and gas CCGT (light grey) 6.2 %. The remaining plants to right of gas CCGT CCS plants each have load factors below 1 % and are, therefore, not expected to be on the margin for a significant amount of time. Therefore, the marginal plant is expected to be a combination of renewables, nuclear, interconnector capacity, gas CHP and gas CCGT at different moments in time. Dividing the load factor of each technology by the technology specific CI gives an average MEF of 198.7 gCO_2/kWh. This value is relatively close to the prediction of average MEF based on the 2019 relationship. It is concluded that the average MEF in 2030 will be 30 - 45 % higher than average HEFs. This means that the carbon offset estimation in 2030 is also roughly underestimated by 30 - 45 %. Average MEF and HEF values for 2019 and 2030 are summarized in table 5.1.

So far only the averaged MEF and HEF values have been compared to indicate the trend of MEFs in relation to HEFs. However, these averaged values lack the crucial temporal variability mentioned in section 2.2. Therefore, it is important to assess the outcome in calculated carbon offset when applying HEFs instead of MEFs in the base scenario (B19 MEF and B19 HEF). The carbon offset is 30.8 % lower when applying HEFs compared to MEFs, which is almost identical to the 30.2 % difference in average MEF and HEF data. Consequently, it can be concluded, that the trend in average EF data strongly follows the outcome of a carbon offset emission study.

	2019 (observed power plant dispatch data)	2030 (model based)
Mean MEF	605.58	180.71 - 198.7 (assumption)
Mean HEF	465.13	136.9

Table 5.1: Mean of MEFs and HEFs in 2019 and 2030 in gCO_2/kWh

5.2.2. Comparison Carbon Offset and Accounting Approach with Varying EFs

Carbon Offset Versus Accounting Approach

The accounting and offset approaches differ fundamentally and cannot be directly compared. The approaches indicate different measures. Carbon accounting studies give a static carbon footprint of a project or action while carbon offset queries yield insight into changes in emission caused by a project, based on the attributional-consequential distinction explained in section 2.1.1.

Application of Different Emissions Factors in Emissions Accounting

Most emissions accounting approaches apply annual or hourly average EFs, as identified in the literature review in section 2.2. To assess whether there is a significant change when using MEFs instead of an AEF or HEFs, the offset of the solar carport is simulated using the three different EFs. The annual average carbon intensity is constant for every hour for the Dutch grid and was 464 gCO_2/kWh in 2019, as mentioned section 5.2.1. The total offset carbon emissions using MEFs are 265.25 ton CO_2eq, 183.43 ton CO_2eq using HEF and 202.62 ton CO_2eq applying an AEF, as summarized in figure 5.16. The total offset using HEFs compared of MEFs is 30.8 % lower and using an AEF the offset is underestimated by 23.6 %. Comparing offsets between applying HEFs and an AEF in 2019 results in an increase of 10.5 % for using an AEF compared to HEFs. This emphasizes the need to accurately assess the aim of an emissions study and select corresponding CI data accordingly. Additionally, this complies with the findings of the previous studies of Ryan et al. [3] and Schram et al. [25] of significantly varying emissions outcomes when using MEFs compared to HEFs or an AEF.

The carbon offset in 2030 is 22.8 % percent higher when using an AEF instead of HEF. Applying HEFs, the offset is 59.01 tons CO_2eq and using an AEF 48.04 tons CO_2eq are mitigated. Based on the variation in using HEFs instead of MEFs in 2019 of 30 - 45 %, as analysed in section 5.2.1, carbon offsets in 2030 can be expected at 62.45 - 69.66 tons CO_2eq in 2030.

Table 5.2: Carbon offset and emissions using different accounting methodologies and EFs in 2019 and 2030 in tons CO_2eq

	Carbon offset	Carbon emissions
2019		
MEF	265.25	-
HEF	183.43	0.10
AEF	202.62	0.01
2030		
MEF	62.45 - 69.66	-
HEF	48.04	1.80
AEF	59.01	2.20

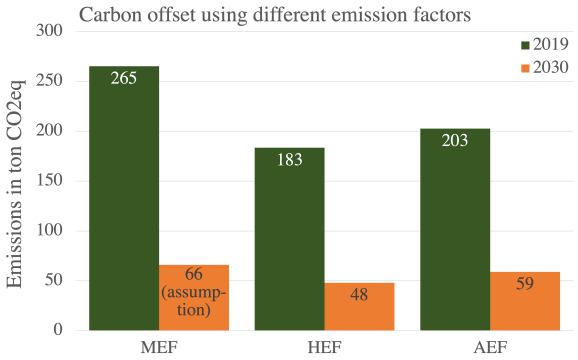

Figure 5.16: Carbon offset using MEFs, HEFs and AEF in 2019 and 2030

Calculating emissions based on the accounting approach in 2019 results in 97.76 $kgCO_2$eq applying an AEF and 100.37 $kgCO_2$eq using HEFs. Hence, emissions are slightly underestimated by 2.6 % when using the annual average. In 2030, the carbon emissions are 2200 $kgCO_2$eq using the AEF and 1800 $kgCO_2$eq when applying HEFs, hence overestimated by 22.2 % when using the AEF. The results between applying the varying methods are summarized in figure 5.16.

The table shows that carbon emissions are higher in 2030 compared to 2019. This is due to the fact that total annual imports are about 90 times higher in 2030 (18.4 MWh) compared to now (0.2 MWh), see table A.5 in appendix A.3.4. These imports are a consequence of the higher EV charging demand in 2030. Nevertheless, carbon emissions do not increase at the same rate as imports, because HEFs are lower in 2030. Hence, carbon emissions are 18 times higher in 2030 compared to 2019.

5.3. Carbon Offset & Emissions in Various Simulation Scenarios

This section presents the results of the various system simulation scenarios with regards to carbon offset and emission calculation results. This includes the relevant results for answering to the four research questions raised in this work.

5.3.1. Offset Carbon Emissions in 2019

A major focus of this work was to develop an accurate method to calculate carbon offset emissions. The chosen method is the carbon offset approach applying observed MEFs. Applying this carbon offset methodology to the PowerParking system in Dronten results in an annual carbon offset of 265.25 tons CO_2eq in the year 2019. Figure 5.17 shows the cumulative carbon offset in 2019, starting at the total life-cycle emissions of the solar carport system (600 tons CO_2eq). After the first year of operation 44.2 % of life-cycle emissions caused by the solar carport are offset by the system.

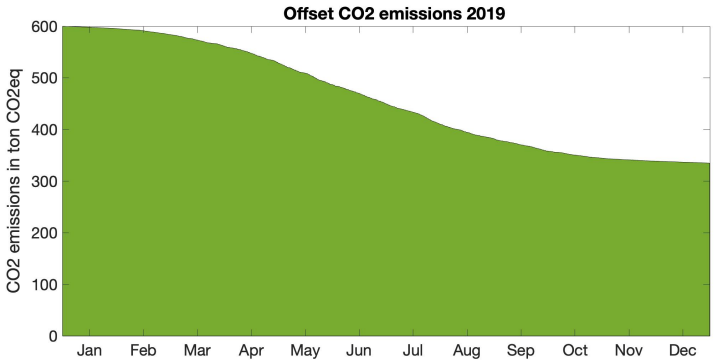

Figure 5.17: Cumulative carbon offset in 2019 in ton CO_2eq. The total offset in 2019 is 265.25 tons CO_2eq.

5.3.2. Offset Carbon Emission Potential in 2019 and 2030

Solar Carport and PV System

The carbon offset achieved by the PV system alone (scenario PV19 and PV30) are 265 tons CO_2eq and 47 (65 adjusted for MEFs) tons CO_2eq in 2019 and 2030, respectively. This corresponds to a contribution of 99.96% and 97.59% to the total carbon offset for the respective years. Evidently, this is the largest contribution to offsets within the system.

Overall carbon offset decreases by around 75 % between 2019 and 2030, corresponding to about 199 tons CO_2eq in absolute terms. This is caused by the grid mix being cleaner in the future, as seen in the 70 % decrease in emission factors by 2030. To illustrate this, the average share of RES in 2019 was 22.5 % while it is 75 % in the future energy system scenario.

Battery Energy Storage System

In order to evaluate the carbon offset potential of the BESS in 2019 and 2030, the scenario of not including the BESS is compared to the base scenario of including the BESS for the two years (B19 MEF & NoB 19 and B20 HEF & NoB 30). In 2019, the additional offset achieved by having the BESS are 98.7 kg CO_2eq, corresponding to less than 0.1 % of the total carbon offset. In 2030, the difference in offset between the base scenario and no BESS scenario are 1.16 tons CO_2eq. When adjusting for MEFs, as explained section 5.2.1, the additional offset is 1.5 - 1.7 tons CO_2eq in 2030. This result is unexpected because it was predicted that the emissions mitigating impact of the BESS is higher today with a more polluting grid mix and lower in the future with a cleaner grid mix. Meaning, the BESS was expected to have a lower impact when the energy imported from the grid is almost as clean as the solar energy produced on-site. However, the low impact of the battery in 2019 can be explained by the fact that it is not utilized well in 2019. The total energy cycled through the BESS are 29 MWh, corresponding to 140 full cycles (based on SoC limits of 20 - 80%), which is seen in figure 5.9 in section 5.1.3. In 2030, the utilization of the BESS increases to 227 cycles, however the impact on carbon offsets is still relatively low at less than 3% of the total carbon offset in 2030. To summarize, the contribution of the BESS to the total carbon offset achieved by the carport system is low today and in 2030.

5.3.3. Carbon Emissions from EVs Without Solar Carport in 2019 and 2030

Charging EVs in 2019 without implementation of the PV system nor the BESS (scenario NoB/PV 19) causes 16.4 tons of CO_2eq emissions. The total annual emissions caused by charging EVs in 2030 (NoB/PV 30) is 18.5 tons CO_2eq. These are emissions according to the accounting approach using HEFs, and since this scenario excludes the PV system and battery there are no offset emissions. The total EV demand is 75 % higher in 2030 (35 MWh in 2019 and 137 MWh in 2030), simply due to higher adoption of EVs. Regardless, the emissions from EV charging in both years is almost the same because the carbon intensity of utility grid electricity is 74 % lower for average HEFs in 2030. Accordingly, charging vehicles from the grid in the future will emit roughy 75 % less carbon than today. Emissions from EV charging are summarized in figure 5.18(b).

Cumulative EV charging emissions for 2030 are shown in figure 5.18(a). The figure shows that emissions increase at a rather constant rate throughout the year, without large seasonal effects. Therefore, it is a fair approximation to calculate average emissions per kilometer driven for EVs charging from the Dutch utility grid. The average Dutch EV driver consumes 20.2 kWh/100km driven [83]. In 2019, the average emissions caused by driving one kilometer after charging from the utility grid are 93.96 gCO_2eq/km (based on the average value of HEFs of 465.13 gCO_2eq/kWh). Assuming the same vehicle efficiency in 2030 of 20.2 kWh/100km, the EV emissions for vehicles charging from the Dutch grid are 30.39 gCO_2eq/km driven. To put this into perspective, new petrol vehicles in 2019 emit roughly 163 gCO_2eq/km [83]. Accordingly, the use phase emissions of EVs are 42 % and 80 % lower than new (and efficient) petrol vehicles (from 2019) in 2019 and 2030, respectively. To conclude, emissions from driving EVs will decrease by 68 % due to a cleaner grid mix and the climate change mitigation impact of EV driving will intensify in the future.

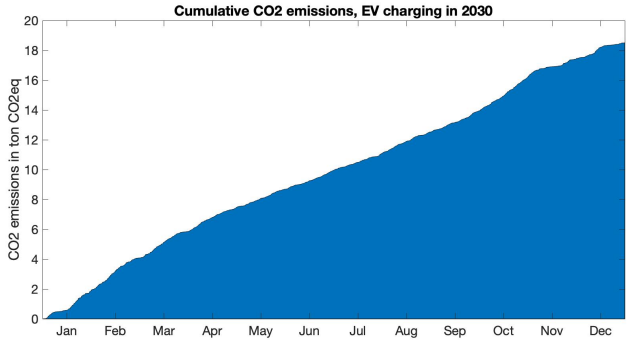

(a) Cumulative GHG emissions from directly charging EVs from the utility grid in 2030

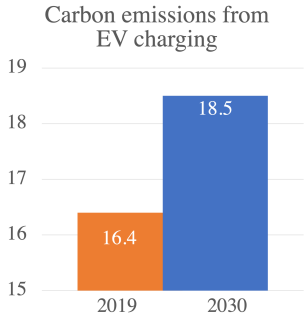

(b) Emissions caused by EV charging at 16 charge points in 2019 (35 MWh total) and 2030 (137 MWh total)

Figure 5.18: Cumulative annual carbon emissions from EV charging in 2030 (a); and total carbon emissions caused by charging EVs in 2019 and 2030 (b).

5.3.4. Effect of Higher EV Demand on Carbon Offset in 2030

The carbon offset is similar for the system containing 16, 24 and 32 charge points. The change in offset when adding 8 charge points is an increase of roughly 0.6 %, or 304 kg CO_2eq. When adding 16 charge points the offset increases by 1.2 %, or 564 kg CO_2eq. Examining the accounted carbon emissions from importing additional energy from the grid shows an increase of 208 % in emissions (3.8 tons CO_2eq) for 24 instead of 16 charge points. Installing 32 charger leads to six times the carbon emissions, hence an additional 9 tons of CO_2eq emissions. This is as expected, because as more vehicles charge at the solar carport, additional grid imports are necessary which increase carbon emissions. The cumulative emissions in each of the scenarios are shown in figure 5.19.

The large discrepancy of offset and accounted emissions within the three scenarios is due to the exclusion of accounting for emissions caused by grid imports directly to EVs, E_{G2L}, in the offset methodology and inclusion in the accounting methodology. These emissions do not occur as a consequence of the PowerParking system and should, therefore, not be included in the consequential carbon offset calculation. Accordingly, carbon offsets are primarily caused by the solar system and are not very sensitive to changing EV demand. Carbon emissions, however, are sensitive to EV demand as they directly affect grid imports which increase emissions.

Based on the additional, roughly 1 %, carbon offset achieved when including further charge points, no strong recommendation for including more charging stations can be drawn from an emissions perspective. At the same time, there is no objection to adding further charge points, since the offset does increase.

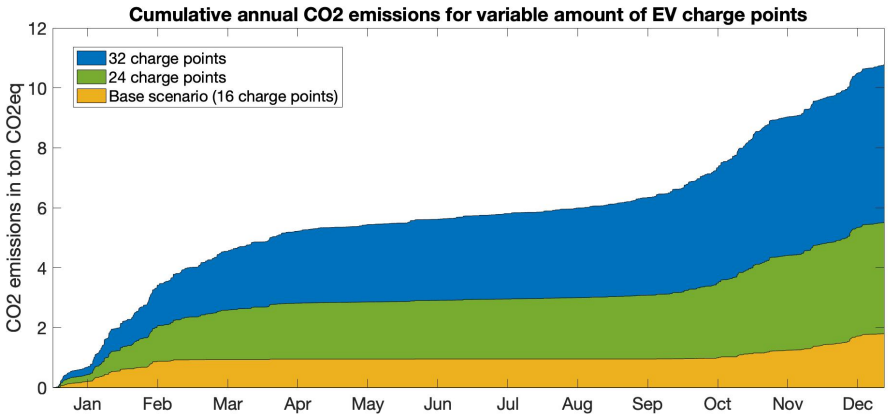

Figure 5.19: Cumulative CO_2eq emissions for variable amount of EV charge points in 2030. Total annual emissions are 1.8, 5.6 and 10.9 tons CO_2eq for 16, 24 and 32 charge points respectively.

Figure 5.20 shows the carbon emissions occurring when including 16, 24 and 32 charge points for the PowerParking system as installed and for only charging EVs from the grid, hence, for the PowerParking system not existing. Carbon emissions are 10 times higher without including the carport system with 16 charge points because 86.5 % of the EV demand is covered by the solar carport (directly from PV or through the BESS). When adding 8 charge points (24 in total), emissions caused with all system components included are only 22% of emissions occurring when EV demand is satisfied exclusively from the utility grid, totalling to 26.4 tons CO_2eq. The EV demand covered by the solar carport is 78.1 %. Adding two further Quattro charging stations (8 charge points) leads to 35.2 tons CO_2eq emissions by only charging from the grid which is reduced by 69 % through implementation of the carport, because 69.4 % of EV demand is satisfied by the carport system. Assessing the absolute reduction in accounted emissions gives 16.7, 20.8 and 24.3 tons CO_2eq for 16, 24 and 32 charge points, respectively.

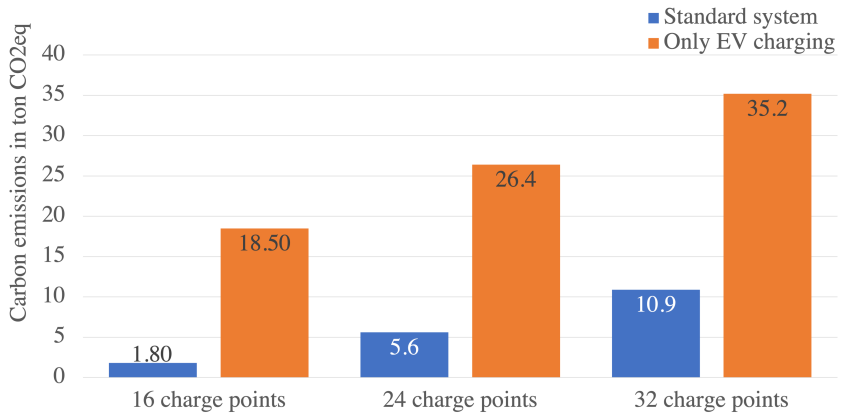

Figure 5.20: Carbon emissions when including 16, 24 and 32 charge points for the standard carport system and for only EV charging

To conclude, there is no direct recommendation nor objection to implement further charging stations based on the small additional carbon offsets. However, examining the discrepancy in carbon emissions from EV charging in combination with the solar carport and without the carport shows that occurring carbon emissions can be reduced by 90 %, 78 % and 69 % for 16, 24 and 32 charge points, respectively. While the percentage decrease reduces with more charge points, the absolute decrease in accounted emissions are 16.7, 20.8 and 24.3 tons CO_2eq for 16, 24 and 32 charge points. Hence, based on 31 % decrease in accounted carbon emissions, it is recommended to install four further Quattro charging stations (16 charge points).

5.3.5. Summary

Table 5.3 summarizes the carbon offset and carbon emissions for all simulation scenarios in 2019 and 2030. The default EF in carbon offset calculations are MEFs for 2019 and HEFs in 2030, unless otherwise indicated

by the scenario name. The default EF used for carbon accounting are HEFs, unless otherwise indicated and as defined in section 4.1.3. A more detailed version of this table can be seen in table A.5 in appendix A.3.4.

Table 5.3: Summary of carbon offset and emissions of all simulated scenarios.* means adjusted for MEF. The values include operational emissions and offset and do not include the fixed LCA emissions of the system.

Scenario		Year	Offset emissions [kg CO2eq]	Accounting emissions [kg CO2eq]
B19 MEF	Base scenario - MEF	2019	265254.93	-
B19 HEF	Base scenario - HEF		183425.81	100.37
B19 AEF	Base scenario - AEF		202623.34	96.76
No B19	No BESS		265156.23	6829.54
No B/PV19	No BESS & no PV		-	16433.32
PV19	Only PV		265156.23	-
B30 HEF	Base scenario - HEF	2030	48035.035 (62445.5 - 69650.8 *)	1803.195
B30 AEF	Base scenario - AEF		59010.00	2200.00
B30 24	24 EV chargers		48339.14	5559.87
B30 32	32 EV chargers		48598.96	10858.25
No B30	No BESS		46875.04	9233.74
No B/PV30	No BESS & no PV		-	18502.503
PV30	Only PV		46875.04	-

5.4. LCA Emissions Solar Carport

The total cradle-to-grave life cycle emissions of the four major components of the solar carport total to 600 tons CO_2eq. Figure 5.21 shows the emissions contribution of each component. The majority (76 %) of the total LCA emissions are caused by the BESS and the PV modules. The remainder stems from the carport structure, made up of steel and aluminium.

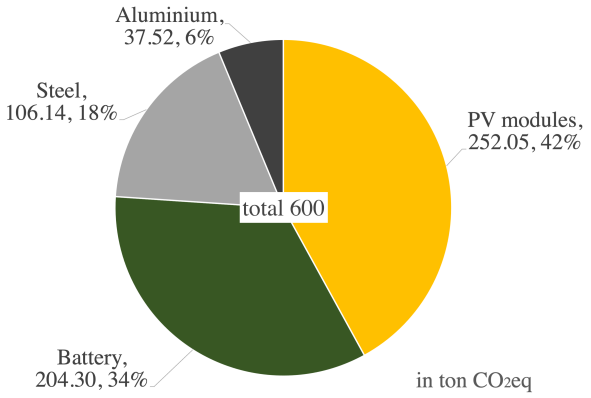

Figure 5.21: LCA emissions of all major solar carport components and their percentage contribution to the total, all in tons CO_2eq.

5.4.1. Carbon Emission Investment versus Carbon Offset

In the first year of operation, the solar carport achieves a carbon offset of 265 tons CO_2eq, as established in section 5.3.1. In 2030, the annual carbon offset is roughly 66 tons CO_2eq, as discussed in section 5.3.2. The total life cycle emissions of the major components of the solar carport are roughly 600 tons CO_2eq. Therefore, the emissions caused by implementing the system are mitigated elsewhere in the system after operation for 2 years and 3 months by displacing grid electricity. This assumes that the operation of the system and MEFs do not vary significant in the second and third year of operation. A greener grid mix (hence, lower MEFs) in the second and third year would most likely decrease the carbon offset and the mitigation of LCA emissions would take longer. Figure 5.22 shows the LCA emissions by major system component and the achieved mitigation in 2019 and 2030.

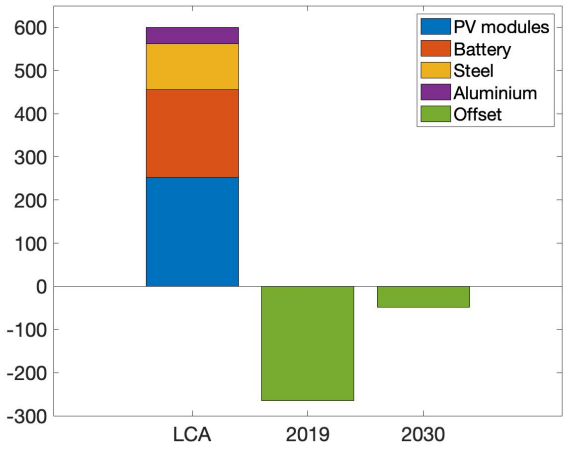

Figure 5.22: Life cycle emissions of all major system components by source and carbon offset in 2019 and 2030

5.4.2. PV system emission offset versus life cycle emissions

The carbon offset achieved through the PV system alone (scenario PV19) are 265.16 tons CO_2eq in 2019, which is 99.96% of the total offset. The total LCA emissions from the PV system are 396 tons CO_2eq. In the scenario of only installing the PV system, 67% of total LCA emissions (PV modules, steel, aluminium) are mitigated after the first year of operation through carbon offsets. Assuming similar operation and grid mix in the first year, the LCA emissions would be mitigated after 1 and a half years. LCA emissions from the PV modules alone are mitigated after less than a year.

5.4.3. BESS emission offset versus life cycle emissions

The contribution to the carbon offset by the BESS are 98.7 kg CO_2eq in 2019 and 1.5 - 1.7 tons CO_2eq in 2030, as analysed in section 5.3.2. Assuming a battery life time of 20 years, and using the higher carbon offset of 2030, the contribution to carbon offsets after 20 years would amount to 30 - 34 tons CO_2eq. For comparison, the LCA emissions from only the BESS are 204 tons CO_2eq, hence, only about 16 % of the emissions caused by the BESS are mitigated at the end of its life time. To conclude, a net emission increase is created when installing a BESS for a pure solar carport system, considering the emission investment in production and the offset achieved during its operation.

5.5. Limitations

This section describes the limitations of the presented research. The presented assessment makes use of models that predict current and future behaviour of the solar carport and, therefore, it is naturally based on assumptions and simplifications which bring limitations with them. The limitations of the future system model, the conducted simulations and the scope of this research are discussed in the following.

5.5.1. Limitations of System Model

Future Energy System Model

The model of the future energy system is mainly based on policy scenarios from one report. The report provides a moderate future scenario, as opposed to a best or worst case scenario, leading to a likely scenario. Developing multiple energy system scenarios is out of scope of this research. Regardless, the future electricity mix can not be predicted with certainty and depends on political developments in the coming years. Therefore, this study can only present an assumed future scenario. The actual installed capacities of RES in the future will evidently affect grid CIs and, thereby, the outcome of emissions assessments.

EV Demand Profile

The EV demand profile is based on statistics of observed EV charging data, however, the charging schedule is not validated. The daily amount of energy charged was successfully validated, however, its distribution over the day and week was not. The hourly variability of loads has a significant impact on carbon emission calculations and deviations from the developed charging profile can effect the study results. Hence, the more accurately the temporal distribution of loads can be predicted, the more precise the outcome of the emissions study. Application of recorded charging data would increase the accuracy of the study and can be used to verify the developed EV charging schedule.

Battery Model & Energy Management System

The applied Kinetic Battery Model and underlying control, hence energy management system, provide a simplified approximation of the battery operation. Some of the limitations that can influence the emissions study are:

- During one time step (one hour) only charging or discharging of the BESS is possible. In reality, the battery can switch between charging and discharging many times during one hour.
- During one time step (one hour) only import or export from and to the grid is possible. While, in reality, it is also possible for the carport system to facilitate both ex- and imports within one hour.
- Exclusion of the connection to municipality building which is also supplied by the BESS.
- Improvements in battery technology in the future, yielding performance and production improvements. The most crucial consequences in the context of this work would be efficiency improvements during the operation of the BESS and a decrease in emissions caused during the production of batteries. As batteries will be produced using a cleaner grid mix, its LCA emissions will decrease.

5.5.2. Limitations of Simulation

Unavailability of MEFs in 2030

One important contribution of this work is the application of observed MEF data in the 2019 simulation. Therefore, it is a limitation that such data or accurate prediction can not be generated for simulating the year 2030. Additionally, the assumption that the proportion of MEFs and HEFs is proportionate in 2019 and 2030 can not be validated. Evidently, this directly impacts the result of the emissions assessment and achieved carbon offset.

Exclusion of Intermediate Years

The simulation has been conducted for 2019 and 2030 and not the intermediate years. While the solar generation profile is representative for multiple years due to application of TMY data, the grid EFs and EV demand are potentially not representative for other years. Especially the 2019 grid EFs can show variation due to extremes in renewable energy generation, potential unavailability of major power plants or other irregularities. Hence, there is only limited transferability of conclusions drawn for the investigated years onto the intermediate years.

5.5.3. Research Scope

The use of the solar carport and its BESS have several advantages. The present research has only investigated the consequences of the system on emissions. Hence, conclusions drawn within this paper can only refer to carbon emissions.

The scope of this work is limited to the PowerParking project and does not consider changes to the energy system as a whole. For instance, a large quantity of batteries providing frequency control services to the grid could potentially replace the need for one gas power plant (for some time during the year) which mostly provide such services today. Hence, changing the structure of the merit order and significantly reducing carbon emissions. This requires very detailed modelling of the energy system which is out of scope of this research but could impact decision making on installations of battery systems.

6

Conclusions & Recommendations

This chapter presents the conclusions drawn from the presented research in section 6.1 with answers to all research questions. Topics for future work emerging from the present research are given in section 6.2 and recommendations for project stakeholders, policy-makers and solar carport designers are given in section 6.3.

This paper presents a methodology developed to accurately calculate the carbon emission offset of a solar carport system with energy storage and EV charging and applies it to the PowerParking system in Dronten. A computer model, including various sub-models, was developed to simulate the system behaviour in various current and future scenarios and implement the developed carbon offset assessment methodology in order to answer the following research questions:

- **Research question I:** What is the recommended approach and emission factor selection to measure carbon emission offsets? And what is the annual cradle-to-grave carbon emission offset of the solar carport in Dronten?
- **Research question II:** What is the cradle-to-grave carbon emission offset potential of the battery system currently and with a higher share of RES in 2030?

With the following additional research questions:

- **Additional research question A:** How much carbon emissions occur by charging EVs directly from the grid, without installing a PV system and BESS, currently and 2030?
- **Additional research question B:** How is the system's carbon emission offset potential and total carbon emissions affected by installing a larger amount of EV charge points by 2030?

These questions have been answered by the investigations in this work and are concluded in the following.

6.1. Conclusions

Within the presented study a carbon offset assessment methodology was successfully developed and applied to the solar carport at the municipality building in Dronten, the Netherlands (52°31' N, 5°42'E). The system consists of a 464 kWp solar system with bifacial PV modules, a 345 kWh NiMH battery system and has 16 EV charge points. A computer simulation was conducted for 13 different system scenarios, varying in applied carbon assessment methodology, system configuration, year and EV demand. Several sub-models, including a PV generation model, an energy system model, an EV load model and a battery model, serve as the basis for the computer simulation. Use of observed power plant dispatch marginal and hourly average emission factors provide high level accuracy of the present emissions study.

6.1.1. Carbon Offset Methodology using Marginal Emission Factors Most Accurate

A carbon offset assessment methodology was developed in response to research question I. The methodology follows the concept of a consequential assessment and applies a consumption based approach to carbon

accounting. Based on an in-depth literature review of carbon emissions accounting literature, it was established that the use of marginal emission factor data is the most accurate parameter to describe the time variable carbon intensity of utility grid electricity. Hence, MEFs should be applied to determine carbon offsets in grid-connected energy systems, such as the investigated solar carport. The developed methodology exhibits high temporal granularity and evaluates the energy flows within the system separately, increasing the accuracy of results. Additionally, the novelty of the proposed methodology consists of observed MEFs data from real power plant dispatch instead of a regression or merit order model, further increasing the approach's accuracy. The carbon offset methodology was applied to the solar carport in Dronten and it was found that the PowerParking system is able to achieve a carbon offset of 265 tons CO_2eq in 2019 and 66 tons CO_2eq in 2030.

To compare the developed approach to other emissions assessment methods, the offset method was repeated using HEFs and an AEF. Additionally, an accounting methodology was developed and applied to the same system using HEFs and an AEF. MEF and HEF data has shown significant deviations with HEFs being 30% lower on average than MEFs. This led to a proportional deviation in calculated carbon offset of a 30% decrease when using HEFs instead of MEFs in 2019. As a result, carbon offsets are significantly underestimated when applying HEFs instead of conceptually more accurate MEFs. Figure 6.1 shows the significance of the emission factor selection on the outcome of the carbon emission assessment study and summarizes the most important findings in this study.

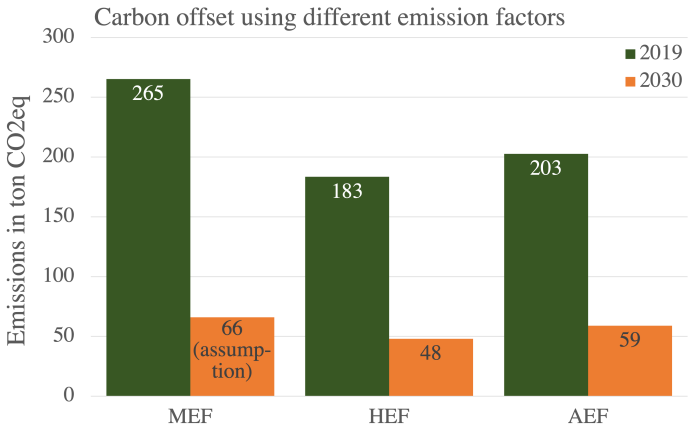

Figure 6.1: Carbon offset for different emission factors in 2019 and 2030

6.1.2. Carbon Offset Potential 2019 and 2030

Lower Carbon Offset in Future

The carbon offset potential of the carport system decreases by 75 % between 2019 and 2030. This is a consequence of a grid emission factors being roughly 70 % lower in 2030 than 2019 as shares in RES increase. The greener the grid becomes, the more the carbon offset of the solar carport will decrease. Therefore, it is concluded that early adoptions of solar carports can achieve the highest carbon offset throughout their system lifetime. Installation of RES will, evidently, continue to be essential in achieving a low-to-zero emission electricity system and combating the climate crisis.

Installation of Battery System at Solar Carport results in Net Emission Increase

The estimated carbon offset achieved by the BESS in 2019 compared to 2030 shows the opposite trend compared to the overall carport system. Answering research question II, the offset attributed to the battery is low, at around 100 kgs CO_2eq annually, in 2019 and increases to roughly 1.5 - 1.7 tons CO_2eq in 2030.

Assuming the operation of the system as purely a solar carport system, the carbon offset achieved by the battery does not mitigate the 204 tons of CO2eq cradle-to-grave carbon emissions caused by the BESS. It mitigates about 1 % of its LCA emissions in the year 2030. Roughly a sixth of life cycle emissions are mitigated by the battery system after 20 years, which evidently is not favorable from an emissions point of view. Additionally, the BESS does not significantly contribute to alleviation of grid capacity constraints. Therefore, it is not recommended to include the (NiMH) battery system in solar carport applications.

6.1.3. Emissions from EV Charging Decrease in Future

Investigation of additional research question A has shown that EV charging at 16 charge points from the Dutch utility grid in 2019 causes 16.4 tons CO_2eq. The average for driving EVs when charging the 2019 Dutch grid mix is 93.96 gCO_2eq/km driven. The total emissions caused by charging at the 16 chargers in 2030 are 18.5 tons CO2eq, and the average emissions for driving one kilometer are 30.39 gCO_2eq. Even though, EV demand roughly quadruples between 2019 and 2030, the total emissions only increase by about 13 %. To conclude, emissions from driving EVs will decrease by 68 % due to a cleaner grid mix and the climate change mitigation impact of EV driving will increase in the future. Already today, the average use phase emissions of EVs are 42 % lower than those of new ICE vehicles. It is important to note that this is only considering use phase emissions and not manufacturing and end-of-life emissions of EVs.

6.1.4. Installation of Additional EV Chargers Mitigate Emissions

In response to additional research question B, it has been found that the additional carbon offset by installing further EV chargers is relatively low. However, the decrease in carbon emissions achieved through the solar carport is 20.8 and 24.3 tons CO_2eq annually for 8 and 16 additional charging points, respectively. This is not a carbon offset, as the emissions caused by EV charging from the grid are not consequential from the solar carport, instead, it is a decrease in carbon footprint of EV charging when combining it with a solar carport. To conclude, emissions from charging EVs are significantly decreased by combining EV chargers with a solar carport system today and in the future.

6.1.5. Emission Mitigation of Life-cycle Carbon Emissions Through Solar Carport

The carbon emissions investment for building the PowerParking system are roughly 600 tons CO_2eq for its major components. It takes about 2 years and 3 months to mitigate the LCA emissions of the solar carport. When excluding the BESS, the LCA emissions are already mitigated after 1.5 years of operation. Also, the emissions caused by the steel and aluminium structure to build the car park only contribute to 24 % of total life cycle emissions of the system and when excluding the battery, they make up 36 %. This emissions investment is evaluated as justifiable, as locations like car parks could not generate renewable electricity without such structure. The life cycle emissions of only the PV modules are mitigated within a year.

6.2. Future Work

6.2.1. Investigation of Battery Emission Reduction Potential Using Collected Carport Data

An earlier version of the methodology laid out in this work included the development of a real-time system monitoring & emissions assessment tool. Due to delays in data monitoring and sharing from the physical system, it was not possible to realize this within the present study. The insights that can be gained by assessing carbon offset and emissions using measured system data is, however, expected to be very valuable in order to validate the results presented in this study. The necessary variables for the emissions assessment will all be measured in real time at the solar carport and Dutch MEFs are also available in real time from the *Tomorrow* API. This research presents the methodology and, hence, the data and background needed for such a live monitoring system are given. A test-run has already been developed for a solar carport system at the GreenVillage at TU Delft.

The carbon offset should be evaluated again after collecting data on the operation of the PowerParking system for at least a year. Applying the developed carbon offset methodology and using observed MEFs will lead to the most accurate evaluation of achieved carbon offset through the system. This way, uncertainties about battery operation, EV load and scheduling and potential variations in solar irradiation will be eliminated.

6.2.2. Application of Carbon Offset Methodology to Other Systems

The developed carbon offset methodology was created with the goal of a wide applicability within the domain of energy systems. It is expected that the method can be easily adapted for other systems, that offer similar features to the PowerParking system. Application in systems that contain a time-shifting energy storage component, such as a battery or an electrolyser / fuel cell system, benefit most from the developed methodology. The method can also be applied to systems containing only local generation and demand, however, the carbon emission and carbon offset calculation here is rather straight forward. Successful application of the developed carbon offset methodology will validate this research and pave the path for a wider application.

6.3. Recommendations

6.3.1. Recommendations for PowerParking Project Stakeholders

Utilization of battery storage for other purposes

It has been established that implementation of the BESS causes more emissions than it has capacity to offset emissions over its lifetime for the sole application within the carport system. A promising use case could be offering frequency control services to the utility grid. Frequency control, or primary control, services are a high value ancillary grid services which provide flexibility to the grid in the case of an imbalance of demand and supply within a few seconds for short amounts of time (up to 15 min). Today, most of the frequency control is carried out using fossil fuel powered plants due to their fast response. However, energy storage systems, such as batteries, provide the same benefits and are becoming more popular as a low-emission alternative. With higher shares of RES in the grid and less thermal power plants, frequency control will become more difficult and thus more important. This application is seen as a favorable option for the BESS at the PowerParking system and is recommended to be explored.

6.3.2. Recommendations for Policy Makers

Standardized Methodology for Carbon Offset Assessments

This research, amongst others, has criticized the current standards for emissions accounting. It was found that the approach of an emissions assessment has significant consequences on its results and that there is a fundamental distinction between carbon offsets and carbon emissions or footprints. Despite the importance for distinguishing these two methodologies, the used emissions data has significant influence on the study outcome as well. Therefore, it is recommended to incorporate specific data requirements on which type of EF should be used for the specific question to be answered. Currently, frameworks such as United Nations Framework Convention on Climate Change (UNFCCC) [8] make the EF choice dependent on data availability, leading to inaccuracies.

Data Availability of Utility Grid Electricity Carbon Intensities

A major obstacle in applying MEFs is the unavailability of such data. Currently, only Tomorrow [66] provides observed MEF data with high temporal resolution, to the knowledge of the author. However, access requires a subscription. To facility wide application of MEFs a central and open-source data sharing platform for MEFs (and HEFs) should be established.

6.3.3. Recommendations for Solar Carport Designers

Solar Carports Offset Several Times the Amount of Emissions Caused to Manufacture Them

The carbon offset that can be achieved by solar carports outweighs the emissions investment of the raw materials and PV module production needed to build them. Without a battery system, the solar carport investigated in this study is expected to mitigate its LCA emissions after 1.5 years of operation. Hence, based on the emissions balance of a solar carport system, it is recommended to roll-out a large-scale implementation of solar carports. Potential application areas are street-parking locations, private carports and large-scale carports at public or company parking lots. The central business district land area of 44 of some of the biggest cities in the world are 31 % covered by street parking spaces [84]. These are areas that are not otherwise utilized and provide a prime application for solar carports. Many homeowners construct carports for their vehicles anyways and exchanging a conventional roof by (bifacial) PV modules can be rather easily implemented. The existing benefits of a conventional carport remain and additional ones are created, including green electricity for EV charging, feed-in of electricity to the utility grid or storage for self-consumption. Large-scale public and company car parks offer a great location for big solar carports. The added benefits exceed generation of electricity by EV charging opportunities, shaded parking, protection from weather or other harsh elements, better security and other factors.

Inclusion of Battery System Creates More Emissions than it Offsets

This study has shown that it is not beneficial today, from an emissions perspective, to include a battery system at a solar carport without additional use applications beyond the daily time shift considered in this study. Therefore, it is recommended to design solar carports without battery storage unless a higher utilization can be ensured or a different use case is deployed.

Bibliography

[1] UNFCC. *The Paris Agreement*. Tech. rep. United Nations, 2015.

[2] European Environment Agency. *EEA greenhouse gases - data viewer*. 2021. URL: https://www.eea.europa.eu/data-and-maps/data/data-viewers/greenhouse-gases-viewer.

[3] N. A. Ryan, J. X. Johnson, and G. A. Keoleian. "Comparative Assessment of Models and Methods to Calculate Grid Electricity Emissions". In: *Environmental Science and Technology* 50.17 (2016), pp. 8937–8953. ISSN: 15205851. DOI: 10.1021/acs.est.5b05216.

[4] M. Brander, M. Gillenwater, and F. Ascui. "Creative accounting: A critical perspective on the market-based method for reporting purchased electricity (scope 2) emissions". In: *Energy Policy* 112 (2018), pp. 29–33. ISSN: 03014215. DOI: 10.1016/j.enpol.2017.09.051.

[5] S. Schaltegger, D. Zvezdov Igor Alvarez Etxeberria, and M. Csutora Edeltraud Günther Editors. *Corporate Carbon and Climate Accounting*. Tech. rep. Springer, 2015.

[6] L. Schneider, A. Kollmuss, and M. Lazarus. "Addressing the risk of double counting emission reductions under the UNFCCC". In: *Climatic Change* 131.4 (2015), pp. 473–486. ISSN: 01650009. DOI: 10.1007/s10584-015-1398-y.

[7] United Nations Environment Programme. *The emissions gap report 2020*. 2020, p. 101. ISBN: 9789280738124.

[8] United Nations Framework Convention on Climate Change (UNFCCC). *Tool to calculate the emission factor for an electricity system*. Tech. rep. 2018. URL: https://cdm.unfccc.int/methodologies/PAmethodologies/tools/am-tool-07-v7.0.pdf.

[9] IEA. *World electricity final consumption by sector*. URL: https://www.iea.org/data-and-statistics/charts/world-electricity-final-consumption-by-sector-1974-2018.

[10] A. Moro and L. Lonza. "Electricity carbon intensity in European Member States: Impacts on GHG emissions of electric vehicles". In: *Transportation Research Part D: Transport and Environment* 64 (2018), pp. 5–14. ISSN: 13619209. DOI: 10.1016/j.trd.2017.07.012.

[11] G. P. Peters. "From production-based to consumption-based national emission inventories". In: *Ecological Economics* 65.1 (2008), pp. 13–23. ISSN: 09218009. DOI: 10.1016/j.ecolecon.2007.10.014.

[12] M. Lenzen, J. Murray, F. Sack, and T. Wiedmann. "Shared producer and consumer responsibility - Theory and practice". In: *Ecological Economics* 61.1 (2007), pp. 27–42. ISSN: 09218009. DOI: 10.1016/j.ecolecon.2006.05.018.

[13] Intergovernmental Panel on Climate Change (IPCC). *IPCC Emissions Factor Database*. 2021. URL: https://www.ipcc-nggip.iges.or.jp/EFDB/main.php.

[14] H. N. Larsen and E. G. Hertwich. "The case for consumption-based accounting of greenhouse gas emissions to promote local climate action". In: *Environmental Science and Policy* 12.7 (2009), pp. 791–798. ISSN: 14629011. DOI: 10.1016/j.envsci.2009.07.010.

[15] B. Tranberg, O. Corradi, B. Lajoie, T. Gibon, I. Staffell, and G. B. Andresen. "Real-time carbon accounting method for the European electricity markets". In: *Energy Strategy Reviews* 26 (2019). ISSN: 2211467X. DOI: 10.1016/j.esr.2019.100367.

[16] T. Ekvall and A. S. Andræ. "Attributional and consequential environmental assessment of the shift to lead-free solders". In: *International Journal of Life Cycle Assessment* 11.5 (2006), pp. 344–353. ISSN: 09483349. DOI: 10.1065/lca2005.05.208.

[17] G. Finnveden, M. Z. Hauschild, T. Ekvall, J. Guinée, R. Heijungs, S. Hellweg, A. Koehler, D. Pennington, and S. Suh. *Recent developments in Life Cycle Assessment*. 2009. DOI: 10.1016/j.jenvman.2009.06.018.

[18] R. J. Plevin, M. A. Delucchi, and F. Creutzig. "Using Attributional Life Cycle Assessment to Estimate Climate-Change Mitigation Benefits Misleads Policy Makers". In: *Journal of Industrial Ecology* 18.1 (2014), pp. 73–83. ISSN: 15309290. DOI: 10.1111/jiec.12074.

[19] J. Goodward and A. Kelly. “The Bottom Line on Offsets”. In: *World Resources Institute* (2010).

[20] World Resources Institute. *The Greenhouse Gas Protocol - A Corporation Accounting and Reporting Standard*. Tech. rep. 2004.

[21] P. Bhatia, C. Cummis, A. Brown, D. Rich, L. Draucker, and H. Lahd. *Corporate Value Chain (Scope 3) Accounting and Reporting Standard*. Tech. rep. Greenhouse Gas Protocol, 2011. URL: https://www.wri.org/research/greenhouse-gas-protocol-corporate-value-chain-scope-3-accounting-and-reporting-standard.

[22] G. Myhre et al. “Anthropogenic and Natural Radiative Forcing”. In: *Climate Change 2013: The Physical Science Basis. Contribution of Working Group I to the Fifth Assessment Report of the Intergovernmental Panel on Climate Change* (2013). URL: www.ipcc.ch.

[23] T. R. Hawkins, B. Singh, G. Majeau-Bettez, and A. H. Strømman. “Comparative Environmental Life Cycle Assessment of Conventional and Electric Vehicles”. In: *Journal of Industrial Ecology* 17.1 (2013), pp. 53–64. ISSN: 15309290. DOI: 10.1111/j.1530-9290.2012.00532.x.

[24] R. Nealer, D. Reichmuth, and D. Anair. *Cleaner Cars from Cradle to Grave How Electric Cars Beat Gasoline Cars on Lifetime Global Warming Emissions*. Tech. rep. 2015. URL: www.ucsusa.org.

[25] W. Schram, A. Louwen, I. Lampropoulos, and W. Van Sark. “Comparison of the greenhouse gas emission reduction potential of energy communities”. In: *Energies* 12.23 (2019). ISSN: 19961073. DOI: 10.3390/en12234440.

[26] I. Khan, M. W. Jack, and J. Stephenson. “Analysis of greenhouse gas emissions in electricity systems using time-varying carbon intensity”. In: *Journal of Cleaner Production* 184 (2018), pp. 1091–1101. ISSN: 09596526. DOI: 10.1016/j.jclepro.2018.02.309.

[27] I. Khan. “Importance of GHG emissions assessment in the electricity grid expansion towards a low-carbon future: A time-varying carbon intensity approach”. In: *Journal of Cleaner Production* 196 (2018), pp. 1587–1599. ISSN: 09596526. DOI: 10.1016/j.jclepro.2018.06.162.

[28] R. Ghotge, M. Paanakker, A. Van Wijk, B. Baeten, and Z. Lukszo. “The effect of price-optimized charging on electric vehicle fleet emissions”. In: IEEE PES Innovative Smart Grid Technologies Europe, 2020. ISBN: 9781728170992.

[29] N. Baumgärtner, R. Delorme, M. Hennen, and A. Bardow. “Design of low-carbon utility systems: Exploiting time-dependent grid emissions for climate-friendly demand-side management”. In: *Applied Energy* 247 (2019), pp. 755–765. ISSN: 03062619. DOI: 10.1016/j.apenergy.2019.04.029.

[30] A. D. Hawkes. “Estimating marginal CO2 emissions rates for national electricity systems”. In: *Energy Policy* 38.10 (2010), pp. 5977–5987. ISSN: 03014215. DOI: 10.1016/j.enpol.2010.05.053.

[31] A. D. Hawkes. “Long-run marginal CO2 emissions factors in national electricity systems”. en. In: *Applied Energy* 125 (2014), pp. 197–205. ISSN: 0306-2619. DOI: 10.1016/j.apenergy.2014.03.060. URL: http://www.sciencedirect.com/science/article/pii/S0306261914003006.

[32] R. Loulou, U. Remne, A. Kanudia, A. Lehtila, and G. Goldstein. *The Integrated MARKAL-EFOM System (TIMES) Model*. 2005. URL: https://www.iea-etsap.org/index.php/etsap-tools/model-generators/times.

[33] J. S. Graff Zivin, M. J. Kotchen, and E. T. Mansur. “Spatial and temporal heterogeneity of marginal emissions: Implications for electric cars and other electricity-shifting policies”. In: *Journal of Economic Behavior and Organization* 107.PA (2014), pp. 248–268. ISSN: 01672681. DOI: 10.1016/j.jebo.2014.03.010.

[34] M. A. M. Tamayao, J. J. Michalek, C. Hendrickson, and I. M. Azevedo. “Regional variability and uncertainty of electric vehicle life cycle CO2 emissions across the United States”. In: *Environmental Science and Technology* 49.14 (2015), pp. 8844–8855. ISSN: 15205851. DOI: 10.1021/acs.est.5b00815.

[35] S. W. Hadley and A. A. Tsvetkova. “Potential Impacts of Plug-in Hybrid Electric Vehicles on Regional Power Generation”. In: *Electricity Journal* 22.10 (2009), pp. 56–68. ISSN: 10406190. DOI: 10.1016/j.tej.2009.10.011.

[36] C. E. Thomas. “US marginal electricity grid mixes and EV greenhouse gas emissions”. In: *International Journal of Hydrogen Energy* 37.24 (2012), pp. 19231–19240. ISSN: 03603199. DOI: 10.1016/j.ijhydene.2012.09.146.

[37] R. McCarthy and C. Yang. “Determining marginal electricity for near-term plug-in and fuel cell vehicle demands in California: Impacts on vehicle greenhouse gas emissions”. In: *Journal of Power Sources* 195.7 (2009), pp. 2099–2109. ISSN: 03787753. DOI: 10.1016/j.jpowsour.2009.10.024.

[38] R. A. Verzijlbergh and Z. Lukszo. “System impacts of electric vehicle charging in an evolving market environment”. In: *2011 International Conference on Networking, Sensing and Control, ICNSC 2011*. 2011, pp. 20–25. ISBN: 9781424495702. DOI: 10.1109/ICNSC.2011.5874924.

[39] R. Harmsen and W. Graus. “How much CO2 emissions do we reduce by saving electricity? A focus on methods”. In: *Energy Policy* 60 (2013), pp. 803–812. ISSN: 03014215. DOI: 10.1016/j.enpol.2013.05.059.

[40] W. Schram, I. Lampropoulos, T. Alskaif, and W. Van Sark. “On the Use of Average versus Marginal Emission Factors”. In: *Proceedings of the 8th International Conference on Smart Cities and Green ICT (SMARTGREENS 2019)*. 2019, pp. 187–193. ISBN: 978-989-758-373-5. URL: https://orcid.org/0000-0002-1780-4553.

[41] W. L. Schram, T. Alskaif, I. Lampropoulos, S. Henein, and W. G. Van Sark. “On the Trade-Off between Environmental and Economic Objectives in Community Energy Storage Operational Optimization”. In: *IEEE Transactions on Sustainable Energy* 11.4 (2020), pp. 2653–2661. ISSN: 19493037. DOI: 10.1109/TSTE.2020.2969292.

[42] K. Siler-Evans, I. L. Azevedo, and M. G. Morgan. “Marginal emissions factors for the U.S. electricity system”. In: *Environmental Science and Technology* 46.9 (2012), pp. 4742–4748. ISSN: 0013936X. DOI: 10.1021/es300145v.

[43] F. Hacker, R. Harthan, F. Matthes, and W. Zimmer. *Environmental impacts and impact on the electricity market of a large scale introduction of electric cars in Europe-Critical Review of Literature*. Tech. rep. ETC/ACC Technical Paper, 2009.

[44] P. Jochem, S. Babrowski, and W. Fichtner. “Assessing CO2 emissions of electric vehicles in Germany in 2030”. In: *Transportation Research Part A: Policy and Practice* 78 (2015), pp. 68–83. ISSN: 09658564. DOI: 10.1016/j.tra.2015.05.007.

[45] Ulica solar. *Mono half-cut bifacial UL-430*.

[46] Huawei. *SUN2000-69KTL-M0 Smart String Inverter*.

[47] NREL. *Life Cycle Greenhouse Gas Emissions from Solar Photovoltaics Fact Sheet*. 2012. DOI: NREL/FS-6A20-56487.

[48] D. D. Hsu, P. O’Donoughue, V. Fthenakis, G. A. Heath, H. C. Kim, P. Sawyer, J. K. Choi, and D. E. Turney. “Life Cycle Greenhouse Gas Emissions of Crystalline Silicon Photovoltaic Electricity Generation: Systematic Review and Harmonization”. In: *Journal of Industrial Ecology* 16.SUPPL.1 (2012). ISSN: 10881980. DOI: 10.1111/j.1530-9290.2011.00439.

[49] X. Jia, C. Zhou, Y. Tang, and W. Wang. “Life cycle assessment on PERC solar modules”. In: *Solar Energy Materials and Solar Cells* 227 (2021). ISSN: 09270248. DOI: 10.1016/j.solmat.2021.111112.

[50] M. M. Lunardi, J. P. Alvarez-Gaitan, N. L. Chang, and R. Corkish. “Life cycle assessment on PERC solar modules”. In: *Solar Energy Materials and Solar Cells* 187 (2018), pp. 154–159. ISSN: 09270248. DOI: 10.1016/j.solmat.2018.08.004.

[51] W. Luo, Y. S. Khoo, A. Kumar, J. S. C. Low, Y. Li, Y. S. Tan, Y. Wang, A. G. Aberle, and S. Ramakrishna. “A comparative life-cycle assessment of photovoltaic electricity generation in Singapore by multicrystalline silicon technologies”. In: *Solar Energy Materials and Solar Cells* 174 (2018), pp. 157–162. ISSN: 09270248. DOI: 10.1016/j.solmat.2017.08.040.

[52] M. De Wild-Scholten and T. Huld. *Solar Resources and Carbon Footprint of Photovoltaic Power in Different Regions In Europe*. Tech. rep. Smartgreenscans, 2014. URL: http://re.jrc.ec.europa.eu/pvgis/download/Yearly-.

[53] A. Louwen, W. G. Van Sark, A. P. Faaij, and R. E. Schropp. “Re-assessment of net energy production and greenhouse gas emissions avoidance after 40 years of photovoltaics development”. In: *Nature Communications* 7 (2016). ISSN: 20411723. DOI: 10.1038/ncomms13728.

[54] Nilar. *EC Racks - ECI-576V-57,6kWh*.

[55] Socomec. *SUNSYS PCS 2 Inverter: SUN-ES100TR20CE*.

[56] K. Young, C. Wang, L. Y. Wang, and K. Strunz. "Electric Vehicle Battery Technologies". In: *Electric Vehicle Integration into Modern Power Systems*. Springer, 2013. DOI: 10.1007/978-1-4614-0134-6.

[57] PetaWatts. *PetaBox*. URL: https://petawatts.nl/petabox/.

[58] G. Majeau-Bettez, T. R. Hawkins, and A. H. StrØmman. "Life cycle environmental assessment of lithium-ion and nickel metal hydride batteries for plug-in hybrid and battery electric vehicles". In: *Environmental Science and Technology* 45.10 (2011), pp. 4548–4554. ISSN: 15205851. DOI: 10.1021/es103607c.

[59] S. Wang, J. Yu, and K. Okubo. "Life cycle assessment on the reuse and recycling of the nickel-metal hydride battery: Fleet-based study on hybrid vehicle batteries from Japan". In: *Journal of Industrial Ecology* (2021). ISSN: 15309290. DOI: 10.1111/jiec.13126.

[60] L. Silvestri, A. Forcina, G. Arcese, and G. Bella. "Recycling technologies of nickel–metal hydride batteries: An LCA based analysis". In: *Journal of Cleaner Production* 273 (2020). ISSN: 09596526. DOI: 10.1016/j.jclepro.2020.123083.

[61] Alfen. *Quattro 4XL*.

[62] C. Jackson. *Solar car parks A guide for owners and developers*. Tech. rep. BRE National Solar Centre, 2016. URL: www.bre.co.uk/nsc.

[63] C. W. Hansen, J. S. Stein, C. Deline, S. MacAlpine, B. Marion, A. Asgharzadeh, and F. Toor. "Analysis of irradiance models for bifacial PV modules". In: *2016 IEEE 43rd Photovoltaic Specialists Conference (PVSC)*. IEEE, 2016. ISBN: 978-1-5090-2724-8. DOI: 10.1109/PVSC.2016.7749564.

[64] World Steel Association. *Sustainability Indicators 2020 Report*. Tech. rep. 2020.

[65] European Aluminium Association. *Environmental Profile Report*. Tech. rep. 2018. URL: https://european-aluminium.eu/media/2052/european-aluminium-environmental-profile-report-2018-executive-summary.pdf.

[66] Tomorrow. *electricityMap*. URL: https://www.electricitymap.org/map.

[67] O. Corradi. *Estimating the marginal carbon intensity of electricity with machine learning*. 2018. URL: https://www.tmrow.com/blog/marginal-carbon-intensity-of-electricity-with-machine-learning/.

[68] ElectricityMap API. *Live Carbon Intensity*. URL: http://static.electricitymap.org/api/docs/index.html#live-carbon-intensity.

[69] Planbureau voor de Leefomgeving (PBL). *Klimaat- en Energieverkenning 2020*. Tech. rep. 2020. URL: www.pbl.nl/kev.

[70] The Netherlands Knowledge Platform for Charging Infrastructure. *NKL EV Public Charging Benchmark Repor*. Tech. rep. 2018.

[71] N. Blair, N. Diorio, J. Freeman, P. Gilman, S. Janzou, T. Neises, and M. Wagner. *System Advisor Model (SAM) General Description*. Tech. rep. National Renewable Energy Laboratory, 2018. URL: www.nrel.gov/publications..

[72] W. De Soto, S. A. Klein, and W. A. Beckman. "Improvement and validation of a model for photovoltaic array performance". In: *Solar Energy* 80.1 (2006), pp. 78–88. ISSN: 0038092X. DOI: 10.1016/j.solener.2005.06.010.

[73] B. Marion, S. Macalpine, C. Deline, A. Asgharzadeh, F. Toor, D. Riley, J. Stein, and C. Hansen. "A Practical Irradiance Model for Bifacial PV Modules Preprint A Practical Irradiance Model for Bifacial PV Modules". In: *2017 IEEE 44th Photovoltaic Specialists Conference*. 2017. URL: http:/www.osti.gov/scitech.

[74] European Commission. *Photovoltaic Geographical Information System*. URL: https://re.jrc.ec.europa.eu/pvg_tools/en/.

[75] Quintel Intelligence. *Energy Transition Model*. URL: https://pro.energytransitionmodel.com.

[76] Quintel. *Quintel Intelligence - ETM*. URL: https://github.com/quintel.

[77] ElaadNL. *Open Datasets for Electric Mobility Research*. 2020. URL: https://platform.elaad.io/analyses/ElaadNL_opendata.php.

[78] J. F. Manwell and J. G. McGowan. *Extension of the Kinetic Battery Model for Wind/Hybrid Power Systems*. Tech. rep. 1994. URL: https://www.researchgate.net/publication/246153107.

[79] M. R. Jongerden and B. R. Haverkort. "Which battery model to use?" In: *IET Software* 3 (2009), pp. 445–457.

[80] Nilar. *Product catalogue Nilar EC*. URL: https://www.nilar.com/wp-content/uploads/2020/03/Product-Catalogue-Nilar-EC-Series-EN-v3.1.pdf.

[81] International Energy Agency. *The Netherlands: Electricity generation by source, 2019*. 2021. URL: https://www.iea.org/countries/the-netherlands.

[82] S. Hamels. "CO2 intensities and primary energy factors in the future european electricity system". In: *Energies* 14.8 (2021). ISSN: 19961073. DOI: 10.3390/en14082165.

[83] René van Gijlswijk, Mieke Paalvast, Norbert Ligterink, and S. Richard. *Real-world fuel consumption of passenger cars and light commercial vehicles*. Tech. rep. 2020. URL: www.tno.nl.

[84] M. Manville and D. Shoup. "Parking, People, and Cities". In: *Journal of Urban Planninng and Development* 131.(4) (2005), pp. 233–245. DOI: 10.1061/ASCE0733-94882005131:4233.

[85] IPCC Working Group III. *Mitigation of Climate Change, Annex III Technology-specific Cost and Performance Parameters - Table A.III.2 (Emissions of selected electricity supply technologies)*. 2014. URL: https://www.ipcc.ch/site/assets/uploads/2018/02/ipcc_wg3_ar5_annex-iii.pdf#page=7.

[86] L. Pereira, R. Kantamaneni, J. Wachsmuth, and S. Lehmann. *Draft Methodology for Calculation of GHG emission avoidance First Call for proposals under the Innovation Fund*. Tech. rep. European Commission, 2020. URL: https://ec.europa.eu/clima/sites/clima/files/innovation-fund/20200205_ghg_en.pdf.

[87] Next Kraftwerke. *What is the merit order curve in the power system?* URL: https://www.next-kraftwerke.be/en/knowledge-hub/merit-order-curve/.

A

Appendix

A.1. Theory

A.1.1. Global Warming Potential of Greenhouse Gases

Table A.1 summarizes the global warming potential of the major greenhouse gases based on a 100-year time horizon. Information on all GHGs can be found in [22].

Table A.1: Global Warming Potential of major greenhouse gases [22].

Gas	Chemical formula	GWP (100-year horizon)
Carbon dioxide	CO_2	1
Methane	CH_4	28
Nitrous oxide	N_2O	265
Chlorofluorocarbon-12 (CFC-12)	CCl_2F_2	10,200
Hydrofluorocarbon-23 (HFC-23)	CHF3	12,400
Sulfur hexafluoride	SF6	23,500
Nitrogen Trifluoride	NF_3	16,100

A.2. Methodology

A.2.1. Simulation Scenarios in 2019 and 2030

The various simulation scenarios employed in this study are visualized in figure A.1.

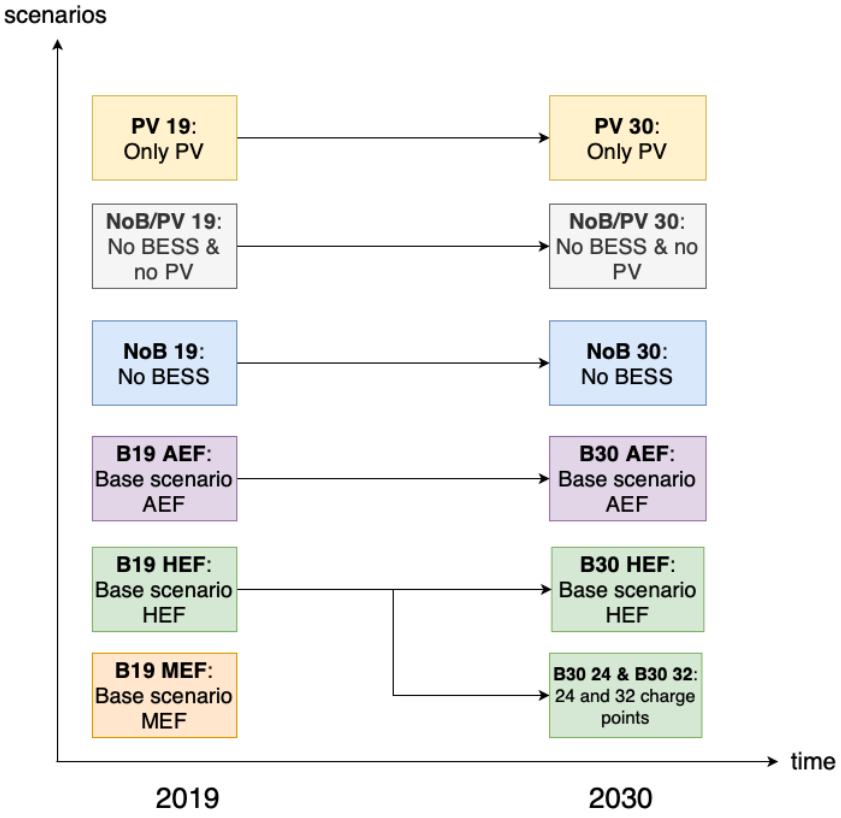

Figure A.1: Overview of all scenarios simulated in 2019 and 2030

A.2.2. PV Generation Monthly Yield

The monthly energy yield from the PV system, as modeled using SAM, are given in figure A.2.

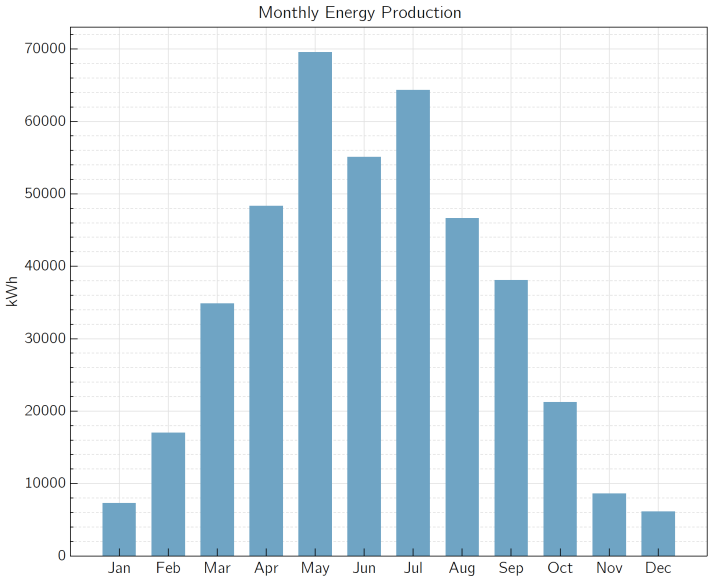

Figure A.2: Monthly energy yield from the PV system

A.2.3. Electricity System Model

Figure A.3 shows a Sankey diagram of the inputs and outputs of electricity generation by source in the energy system model for 2030.

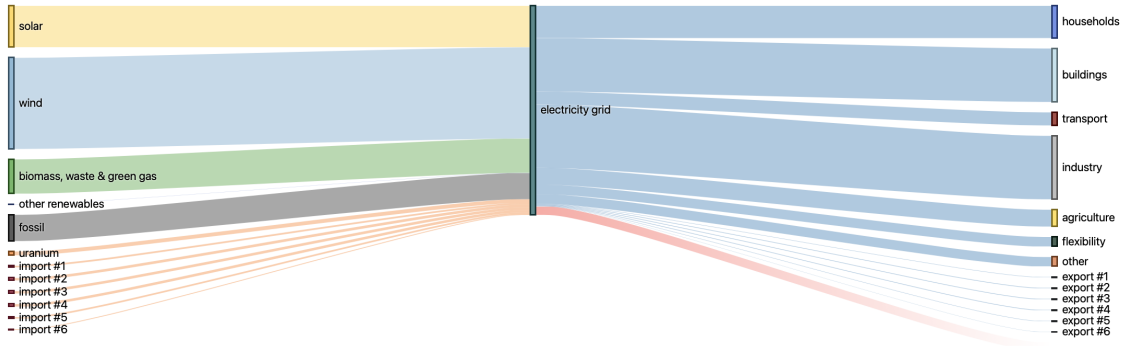

Figure A.3: Sankey diagram of energy inputs and outputs, electricity only

Installed capacities 2030

The installed capacities by power plant type as predicted by the Climate and Energy Outlook 2020 (KEV report) and adapted in the ETM model are summarized in table A.2. A visual representation of the installed capacities can be seen in figure 4.5 in section 4.3.2.

Technology	Installed capacity in MW
Solar PV	26,040
Gas	14,470
Wind (offshore)	11,470
Wind (onshore)	5,650
Nuclear	480
Biogas	100
Hydro (river)	50
Waste	50

Table A.2: Installed capacities by power plant in 2030

A.2.4. Technology Specific Emission Factors

Technology specific emissions are the emissions occurring due to generation of one unit of electricity for a certain power plant technology. Most of the technology specific CIs are adapted from Tranberg et al. [15] and used for 2019 and 2030 for better comparability. Technology specific emissions are summarized for the year 2019 and 2030 in tables A.3 and A.4, respectively.

Table A.3: Technology specific emissions in 2019, source specified per data point

Technology	CO_2eq emissions in $\frac{gCO2eq}{kWh}$	Source
Must-run CHP	450	[15]
Solar	109	[15]
Wind (offshore)	16.3	[15]
Hydro reservoir	14.7	[15]
Nuclear (2nd Gen)	12	[15]
Biomass CHP (small-scale)	53.8	[15]
Industry gas CHP (CCGT)	465	[15]
Gas CCGT	465	[15]
Coal	1030	[15]
Coal	1020	[15]
Average Imports	426	[15]

Table A.4: Technology specific emissions in 2030, source specified per data point

Technology	CO_2eq emissions in $\frac{gCO2eq}{kWh}$	Source
Must-run CHP	450	[15]
Solar	109	[15]
Wind (offshore)	16.3	[15]
Hydro reservoir	14.7	[15]
Waste Chp	230	[85]
Nuclear (2nd Gen)	12	[15]
Biomass CHP (small-scale)	53.8	[15]
Industry gas CHP (CCGT)	465	[15]
Gas CCGT	465	[15]
Industry gas CHP (turbine)	490	[85]
Import	150	[86]

A.3. Results

A.3.1. Battery Model

The SoC of the BESS in 2019 is shown in figure A.4. The battery system is not being utilized much in 2019, and cycles are usually only in a range between 70 and 80 % SoC.

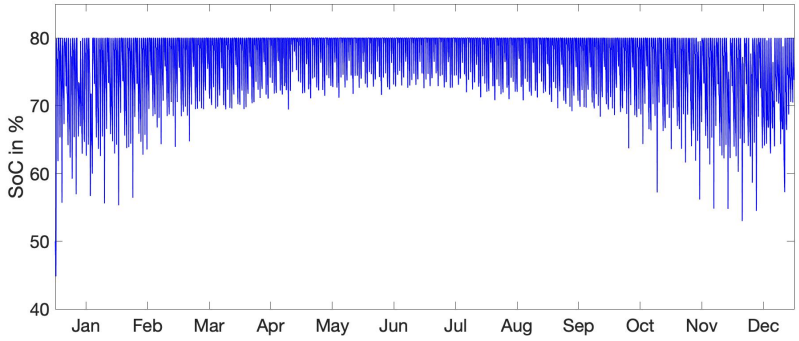

Figure A.4: SoC of BESS in base scenario in 2019

A weekly profile of the operation of the BESS, characterized by its SoC, is shown in figure A.5 for a winter week and in figure A.6 for a summer week.

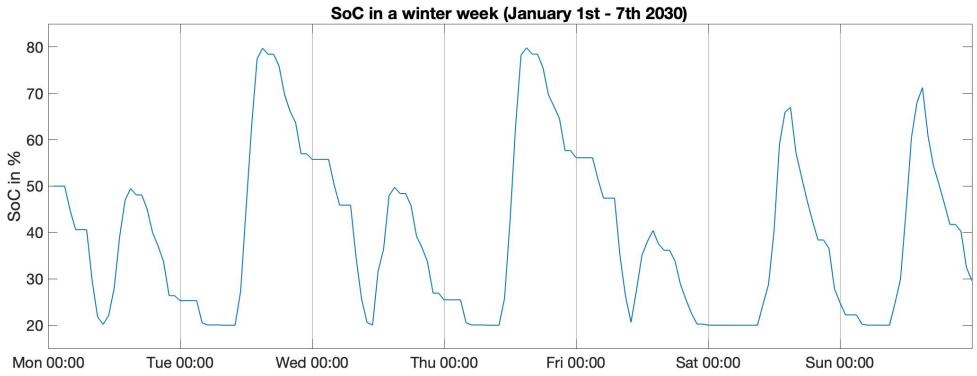

Figure A.5: SoC in the first week on January 2030

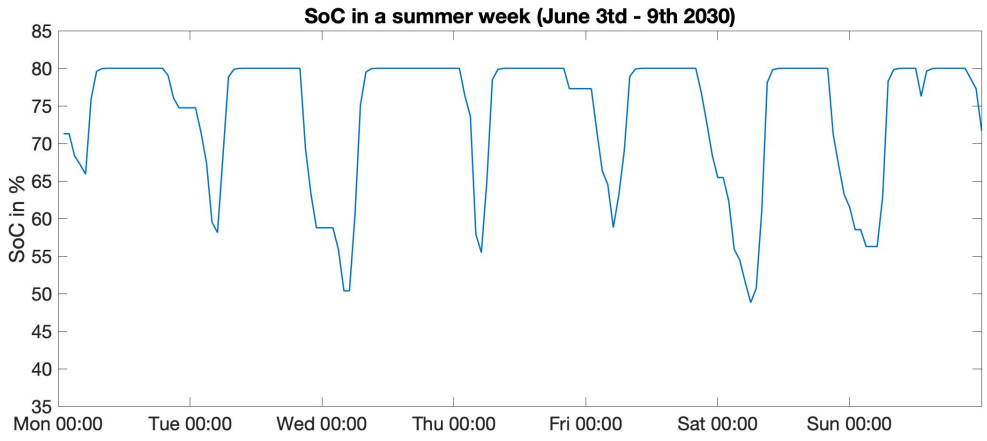

Figure A.6: SoC in the first week on June 2030

The SoC during four different days, corresponding to the four seasons, in 2030 is shown in figure A.7.

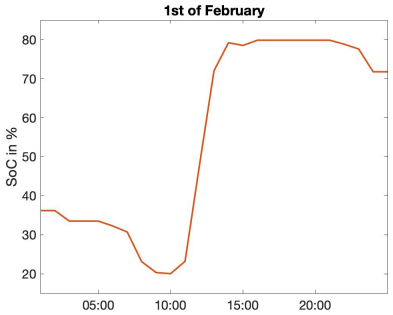

(a) SoC of BESS on the 1st of February

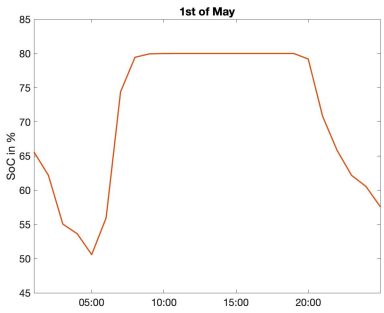

(b) SoC of BESS on the 1st of May

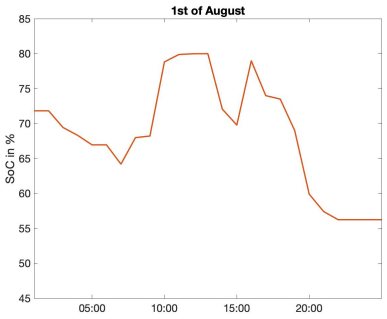

(c) SoC of BESS on the 1st of August

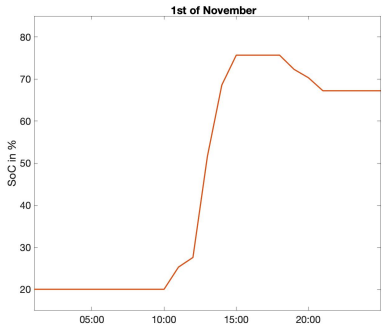

(d) SoC of BESS on the 1st of November

Figure A.7: State of charge of the BESS on different days throughout the year 2030, corresponding to figure 5.11 (section 5.1.3)

A.3.2. Comparison MEF and HEF

An exemplary merit order curve is shown in A.8.

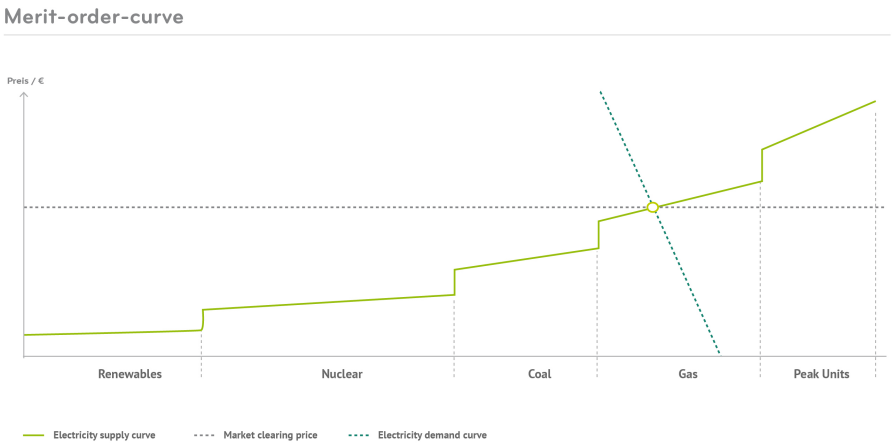

Figure A.8: Exemplary merit order curve [87]

A.3.3. Carbon Offset PV System

The carbon offset achieved by the PV system alone applying HEFs is shown in figure A.9, starting at the emission balance expected at the start of 2030.

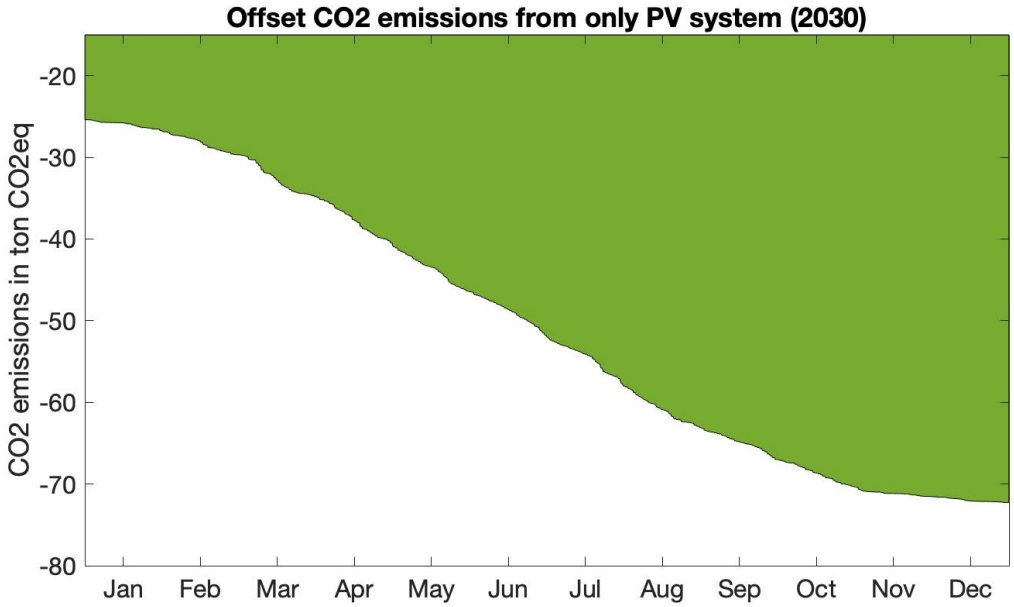

Figure A.9: Offset carbon emissions by only the PV system in 2030, total annual offset is 46.9 ton CO_2eq

A.3.4. Summary Simulation Scenarios

Table A.5 summarizes the various simulation scenario outcomes and its descriptors.

Table A.5: Overview of scenario results and most important descriptors, emissions in kg CO_2eq.

Scenario		Year	Offset	Accounting	EV demand [MWh]	Export [kWh)]	Import [kWh]	Energy cycled battery [MWh]	Total cycles
B19 MEF	Base scenario	2019	265254.93	100.37	35	400504.32	208.47	14.5	70.05
B19 HEF	Base scenario - HEF		183425.81	100.37	35	400504.32	208.47	14.5	70.05
B19 AEF	Base scenario - AEF		202623.34	96.76	35	400504.32	208.47	14.5	70.05
NoB 19	No BESS		265156.23	6829.54	35	414479.64	0 (13881.86 to EVs)	-	-
NoB/PV 19	No BESS & no PV		-	16433.32	35	-	35800	-	-
PV 19	Only PV		265156.23	0.00	no EV	436408.44	-	-	-
B30 HEF	Base scenario - HEF	2030	48035.04	1803.19	137	309360.55	18373.66	47.00	227.05
B30 AEF	Base scenario - AEF		48339.14	5559.87	137	271517.68	44958.79	57.00	275.36
B30 24	24 chargers		48339.14	5559.87	205.76	271517.68	44958.79	57.00	275.36
B30 32	32 chargers		48598.96	10858.25	274.34	240928.40	84081.97	60.00	289.85
NoB 30	No BESS		46875.04	9233.74	137	357050.97	63893.44	-	-
NoB/PV 30	No BESS & no PV		-	18502.50	137	-	137	-	-
PV 30	Only PV		46875.04	0.00	no EV	436408.44	-	-	-